



**Escola de Camins**

Escola Tècnica Superior d'Enginyeria de Camins, Canals i Ports  
UPC BARCELONATECH

## Design and structural verification of a concrete spar type platform for a 15 MW wind turbine

Treball realitzat per:

**Iago Lorenzo García**

Dirigit per:

**Climent Molins Borrell**

**Pau Trubat Casal**

Màster en:

**Enginyeria de Camins, Canals i Ports**

Barcelona, 26 de juny de 2020

Departament d'Enginyeria Civil i Ambiental

**TREBALL FINAL DE MÀSTER**

## **ACKNOWLEDGEMENTS**

I would like to thank the professor Climent Molins and Pau Trubat for giving me the opportunity to introduce myself and discover the world of off-shore wind turbines.

I would also like to thank them for the constant advice and help received during the development of the project, specially taking into account the conditions of the realization of it, forced by the crisis of the COVID-19.

## **ABSTRACT**

Taking into account the increasing of the demand of renewable energy, one of the solutions which help to cover this demand is the off-shore technology. This is precisely, the object of this thesis, the structural verification and analysis of a floating off-shore wind turbine platform type spar, supporting a 15 MW wind turbine.

It will be used the software OpenFAST to compute motions, stresses and moments of the structure, and then, taking into account that the structure of the spar is made with concrete, it will be defined the post-tensioning steel and the passive steel, according to the Spanish standard for concrete structures EHE-08.

It will be also made the structural analysis during the construction process, when the spar is placed in horizontal position. This will be necessary taking into account the huge dimensions of the structure.

ACKNOWLEDGEMENTS .....	1
ABSTRACT .....	2
INDEX OF FIGURES .....	7
INDEX OF TABLES .....	10
1. INTRODUCTION .....	11
2. STATE OF ART .....	13
2.1. BRIEF HISTORY AND ACTUAL SITUATION.....	13
2.2. TYPES OF FLOATING PLATFORMS.....	15
2.2.1. Spar-Buoys.....	15
2.2.2. Semi-submersible.....	16
2.2.3. Tension Leg Platform (TLP) .....	16
2.3. DEFINITION OF MOTIONS IN A FLOATING STRUCTURE.....	18
2.4. EXTERNAL LOADS IN FLOATING OFFSHORE WIND TURBINES .	19
2.4.1. Hydrostatic pressure .....	19
2.4.2. Archimedes law and buoyancy .....	20
2.4.3. Gravity and inertial loads.....	20
2.4.4. Aerodynamic loads .....	21
2.4.5. Tower interference.....	23
2.4.6. Hydrodynamics .....	24
2.5. WINDCRETE FLOATER DESCRIPTION .....	26
2.6. CONSTRUCTION, TRANSPORT AND INSTALLATION .....	28
2.7. FAST AND OPENFAST SOFTWARE.....	31
2.7.1. Subroutines.....	32
2.8. CODES AND STANDARDS .....	34
2.8.1. DNVGL .....	34
2.8.2. IEC.....	35
2.8.3. EHE-08.....	36
3. DEFINITION OF THE PROBLEM .....	37
3.1. WINDCRETE PROPERTIES.....	37

3.2.	MODAL ANALYSIS OF THE STRUCTURE .....	39
3.3.	ENVIRONMENTAL DATA .....	43
3.3.1.	Wind .....	43
3.3.2.	Waves .....	44
3.4.	LOAD CASES .....	46
3.4.1.	DLC 1.1.....	47
3.4.2.	DLC 1.2.....	47
3.4.3.	DLC 1.3.....	48
3.4.4.	DLC 1.6.....	48
3.4.5.	DLC 6.1.....	48
3.4.6.	DLC 6.2.....	49
3.5.	Design conditions .....	50
4.	ANALYSIS OF THE RESULTS .....	51
4.1.	Motions and accelerations .....	51
4.1.1.	DLC 1.1.....	51
4.1.2.	DLC 1.2.....	51
4.1.3.	DLC 1.3.....	52
4.1.4.	DLC 1.6.....	53
4.1.5.	DLC 6.1. ....	53
4.1.6.	DLC 6.2.....	54
4.2.	Forces .....	55
4.2.1.	DLC 1.1.....	55
4.2.2.	DLC 1.2.....	55
4.2.3.	DLC 1.3.....	55
4.2.4.	DLC 1.6.....	55
4.2.5.	DLC 6.1.....	56
4.2.6.	DLC 6.2.....	56
4.2.7.	Analysis.....	56
5.	STRUCTURAL DESIGN.....	57

5.1.	ANALYSIS OF THE SERVICEABILITY LIMIT STATE (SLS).....	57
5.1.1.	Data provided .....	57
5.1.2.	Materials.....	60
5.1.3.	Post-tensioning design.....	60
5.1.4.	Concrete cover.....	63
5.1.5.	Calculation of the losses .....	64
5.1.6.	SLS Cracking .....	70
5.2.	ANALYSIS OF COMPRESSIVE STRESSES UNDER PERMANENT LOADS .....	72
5.3.	ANALYSIS OF THE ULTIMATE LIMIT STATE (ULS) .....	73
5.3.1.	Bending moment.....	73
5.3.2.	Shear force .....	76
5.3.3.	Torsion.....	78
5.3.4.	Interaction of forces .....	80
5.4.	ANALYSIS OF THE CONSTRUCTION PROCESS .....	82
5.4.1.	Ultimate Limit State (ULS) .....	83
5.4.2.	Serviceability limit state (SLS) .....	87
5.4.3.	Verification of tensions in other sections .....	92
5.5.	SUMMARY OF RESULTS AND BILL OF QUATITIES .....	104
5.5.1.	Summary of the reinforcement.....	104
5.5.2.	Bill of quantities .....	104
6.	CONCLUSIONS .....	106
7.	BIBLIOGRAFY .....	109
	APPENDIX 1. NUMERICAL RESULTS FOR THE LONGITUDINAL STRUCTURE .....	112
1.	Post-tensioning steel area .....	112
2.	Post-tensioning losses .....	113
3.	Verification of cracking.....	114
4.	Verification under permanent loads.....	115
5.	Verification of bending moment in ULS .....	116

6. Verification of shear force in ULS .....	117
7. Verification of torsion in ULS .....	118
8. Interaction of forces .....	119
APPENDIX 2. NUMERICAL RESULTS FOR CIRCUMFERENTIAL STRUCTURE .....	120
1. Post-tensioning steel and losses in the floater .....	120
2. Post-tensioning steel losses in section of 0.3 metres thickness .....	121
3. Post-tensioning steel losses in section of 0.4 metres thickness .....	122
4. Post-tensioning steel losses in section of 0.45 metres thickness.....	123
5. Post-tensioning steel losses in section of 0.5 metres thickness .....	124
6. Post-tensioning steel losses along the transition piece.....	125
APPENDIX 3: DRAWINGS.....	126

## **INDEX OF FIGURES**

Figure 1: Total installed wind power capacity in Europe (Trubat et al. 2019)(Sesto y Lipman 1992).....	13
Figure 2: Annual offshore wind installations by country (left axis) and cumulative capacity (right axis) [GW] (Walsh 2019).....	14
Figure 3: Types of platform for off-shore wind turbine (International Renewable Energy Agency (IRENA) 2016).....	15
Figure 4: Definition of ship motions in six degrees of freedom (Journée y Massie 2001).....	18
Figure 5: Steady-state air flow (Hau 2005).....	21
Figure 6: Vertical wind shear and cross wind (Hau 2005).....	22
Figure 7: Wind turbulence (Hau 2005).....	22
Figure 8: Position of the rotor related to wind direction (Hau 2005).....	23
Figure 9: Flow field due to the tower dama head of a cylindrical tower with diameter D(Hau 2005).....	23
Figure 10: Flow around a circular cylinder in dependence on the Reynolds number (Hau 2005).....	24
Figure 11: Steel crown detail (Molins et al. 2016).....	26
Figure 12: Windcrete overview (Cobra et al. 2019).....	27
Figure 13: Towing of Windcrete.....	28
Figure 14: Erection process (Molins et al. 2016).....	29
Figure 15: Wind Turbine installation (Molins et al. 2016).....	29
Figure 16: Structure emerging (a) and ballasting (b) (Molins et al. 2016).....	30
Figure 17: Degrees of freedom of a floating wind turbine (Jonkman 2013).....	31
Figure 18: FAST control volumes for floating systems (Jonkman y Jonkman 2016).....	32
Figure 19: Windcrete dimensions.....	38
Figure 20: Campbell's diagram (Molins et al. 2016).....	39
Figure 21: 3-D model of the structure made by Robot Structural Analysis.....	41
Figure 22: Modes of vibration 7, 8, 9 and 10 respectively, taken from Robot....	42
Figure 23: Diagram of bending moment due to action of wind and waves for each DLC [kN*m]. .....	58
Figure 24: Diagram of axial forces due to action of wind, waves and self-weight corresponding to DLC 6.2 [kN]. .....	58
Figure 25: scheme of the structure.....	59
Figure 26: Quantity of Steel along the structure.....	63
Figure 27: Limitations of the minimum concrete cover.....	64



Figure 28: Friction losses of pre-stresses force along the structure. ....	65
Figure 29: Wedge set losses along the structure. ....	66
Figure 30: Elastic losses.....	67
Figure 31: Time-dependent losses.....	68
Figure 32: Initial and final post-tensioning forces, and limits along the structure. .....	69
Figure 33: Tension and compression stresses.....	71
Figure 34: Tension and compression stresses.....	72
Figure 35: scheme of forces. ....	73
Figure 36: minimum reinforcement in ‰. ....	75
Figure 37: Scheme of the longitudinal active (red) and passive (black) reinforcement. ....	77
Figure 38: scheme of dimensions of a piece with torsional moment (EHE-08 2008).....	79
Figure 39: Model of the structure made by Robot. ....	82
Figure 40: Bending moment diagram. ....	83
Figure 41: Axial forces.....	83
Figure 42: Shear forces. ....	84
Figure 43: Scheme of equilibrium of forces.....	84
Figure 44: Scheme of the active (red) and passive (black) reinforcement. ....	91
Figure 45: Model of the structure made by Robot.....	92
Figure 46: Tensions in the top of the tower.....	92
Figure 47: Model of the structure made by Robot. ....	93
Figure 48: Tensions in the section.....	93
Figure 49: Model of the structure made by Robot. ....	94
Figure 50: Tensions in the section. ....	94
Figure 51: Scheme of the active (red) and passive (black) reinforcement. ....	95
Figure 52: Model of the structure made by Robot. ....	96
Figure 53: Tensions in the section. ....	96
Figure 54: Scheme of the active (red) and passive (black) reinforcement. ....	97
Figure 55: Model of the structure made by Robot. ....	97
Figure 56: Tensions in the section. ....	98
Figure 57: Scheme of the active (red) and passive (black) reinforcement. ....	98
Figure 58: Model of the structure made by Robot. ....	99
Figure 59: Tensions in the section. ....	99
Figure 60: Scheme of the active (red) and passive (black) reinforcement. ....	100
Figure 61: Model of the structure made by Robot. ....	101

Figure 62: Tensions in the section. ....	101
Figure 63: Scheme of the active (red) and passive (black) reinforcement from the sea level until 3 metres depth. ....	102
Figure 64: Scheme of the active (red) and passive (black) reinforcement from 3 until 7 metres depth. ....	103
Figure 65: Scheme of the active (red) and passive (black) reinforcement from 7 until 10 metres depth. ....	103

## **INDEX OF TABLES**

Table 1: Center of gravity and inertia of the real spar and the model of Robot Structural Analysis (values taken from AutoCad).....	40
Table 2: Frequencies of the rigid body behaviour obtained with Robot (Mahfouz et al. 2020). .....	41
Table 3: Modal analysis results obtained with Robot.....	42
Table 4: Normal wind speed profile (Cobra et al. 2019). .....	43
Table 5: Extreme condition wind speed profile (Tr =50 years) (Cobra et al. 2019). .....	44
Table 6: Wave data for Gran Canaria (Cobra et al. 2019).....	44
Table 7: Wind-Wave scatter diagram (Cobra et al. 2019).....	44
Table 8: Significant wave height-Peak period frequency for Gran Canaria (Cobra et al. 2019). .....	45
Table 9: Design load cases (DNVGL-ST-0437 2016). .....	46
Table 10: Excursion and acceleration limits (Mahfouz et al. 2020).....	50
Table 11: Motions and accelerations for DLC 1.1 given by OpenFAST, underlining the values out of the limits defined by the design bases. ....	51
Table 12: Motions and accelerations for DLC 1.2 given by OpenFAST, underlining the values out of the limits defined by the design bases. ....	51
Table 13: Motions and accelerations for DLC 1.3 given by OpenFAST, underlining the values out of the limits defined by the design bases. ....	52
Table 14: Motions and accelerations for DLC 1.6 given by OpenFAST, underlining the values out of the limits defined by the design bases. ....	53
Table 15: Motions and accelerations for DLC 6.1 given by OpenFAST, underlining the values out of the limits defined by the design bases. ....	53
Table 16: Motions and accelerations for DLC 6.2 given by OpenFAST, underlining the values out of the limits defined by the design bases. ....	54
Table 17: Tension in DLC 1.1, given by OpenFAST. ....	55
Table 18: Tension in DLC 1.2, given by OpenFAST. ....	55
Table 19: Tension in DLC 1.3, given by OpenFAST. ....	55
Table 20: Tension in DLC 1.6, given by OpenFAST. ....	56
Table 21: Tension in DLC 6.1, given by OpenFAST. ....	56
Table 22: Tension in DLC 6.2, given by OpenFAST. ....	56
Table 23: Safety factors imposed by the EHE-08.....	60
Table 24: Tension on the transition piece. ....	102

## **1. INTRODUCTION**

Nowadays, when we read newspapers, it is unusual that the words “global warming” do not appear at some point, since these have become part of our daily routine, as well as the high temperatures that we suffer in months that theoretically, should be cold. On larger scale, our televisions usually appear full of pictures of the earth poles, with dramatic “before and after” of their situation, showing the volume of ice lost in recent decades, caused by high temperatures, affecting the ecosystem, as well as the species that inhabit them.

Due to all these factors, since few years ago, part of our leader’s political campaigns have been based on the environment, either by adopting restrictions or the use of energy sources, such as oil or nuclear power. Or by promising large investments in renewable energies, such as solar or wind. The last one will be the main topic of this thesis.

There are a lot of countries that have set themselves a medium-term objective of supplying 100% of these types of energy. This objective could be considered almost impossible if only on-shore structures were taken into account, since space limitation and visual and acoustic pollution could make difficult for people living in nearby areas to coexist with these infrastructures. For this reason, since a few years ago, investments in off-shore technology have begun to increase, because it allows to build bigger infrastructures, and therefore, to produce greater electricity power. This is possible since being far from the coast, the visual and acoustic pollution is considerably reduced, and the space limitation practically eliminated, being the resistance of the platform materials that support them the main limitation in the infrastructure size.

The objective of this thesis is, precisely, the structural analysis of one of these platforms. Specifically, a floating spar which function is to support a wind turbine capable of generating 15 MW of energy. This turbine will be placed near the coast of Gran Canaria Island, in Spain.

Initially, using the software OpenFAST, the needed simulations will be performed in order to obtain the motions, moments and tensions along the structure for the different load cases defined by the standards (DNVGL-ST-0437 2016).

The Serviceability Limit State analysis of the structure will be carried out to determine the necessary post-tensioning steel needed in order to avoid cracking

under any load case in all the structure. The strength of the structure in the Ultimate Limit State will be verified for the bending moment, shear stress and torsional stress, and the interaction between them. It will be calculated the needed reinforcement to support the ULS actions required by EHE-08.

Considering the size of the structure (which diameter is 18.6 metres in the largest section), and that it will be built in a horizontal position, a structural analysis of it in this position will also be necessary, to also avoid the appearance of cracks during the construction process, placing more reinforcement and post-tensioning steel, if necessary.

Finally, after having carried out the pertinent verifications, the final design of the structure will be presented, together with the quantity of material necessary to carry it out, in order to have an initial idea of the materials cost when constructing it.

## 2. STATE OF ART

### 2.1. BRIEF HISTORY AND ACTUAL SITUATION

Since 1982, when a group of European agricultural machinery manufacturers fly to California to assess the market for producing wind turbines («History of Europe’s Wind Industry» 2020) the wind industry have been developed until the huge wind turbines designed nowadays. It happened because in the recent years the governments have invested a significant percentage of their money in renewable energy in order to try to avoid the climate change and the global warming.

The demand of this kind of energy is increasing nowadays, that is why make investments on renewable energy is very important to satisfy the demand. On-shore wind turbines, built in different landscapes with appropriate wind conditions have some size limitations, like the space needed and also the production of acoustic pollution when is working, and furthermore, as bigger is the turbine, more noise produces. This fact makes necessary the creation of an alternative, which are the off-shore wind turbines.

In 1991 was built in Denmark the first off-shore wind farm, consisting on eleven 450 kW turbines («History of Europe’s Wind Industry» 2020). Since then, the off-shore wind industry have been growing until nowadays, when Europe has the capacity to produce 205 GW of wind energy taking into account onshore and offshore wind turbines (Sesto y Lipman 1992).

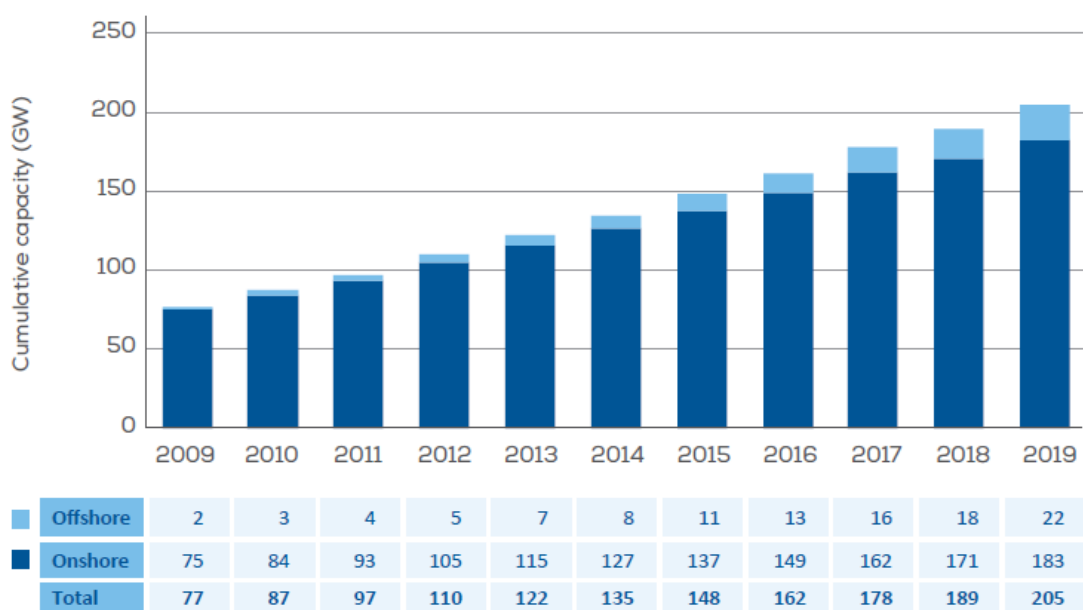


Figure 1: Total installed wind power capacity in Europe (Trubat et al. 2019)(Sesto y Lipman 1992).

As shown in Figure 1, Europe nowadays has a total installed offshore wind capacity of 22,072 MW. This corresponds to 5,047 grid-connected wind turbines across 12 countries (Walsh 2019). Figure 2 shows the amount of capacity of each country, cumulative capacity and annual installed capacity.

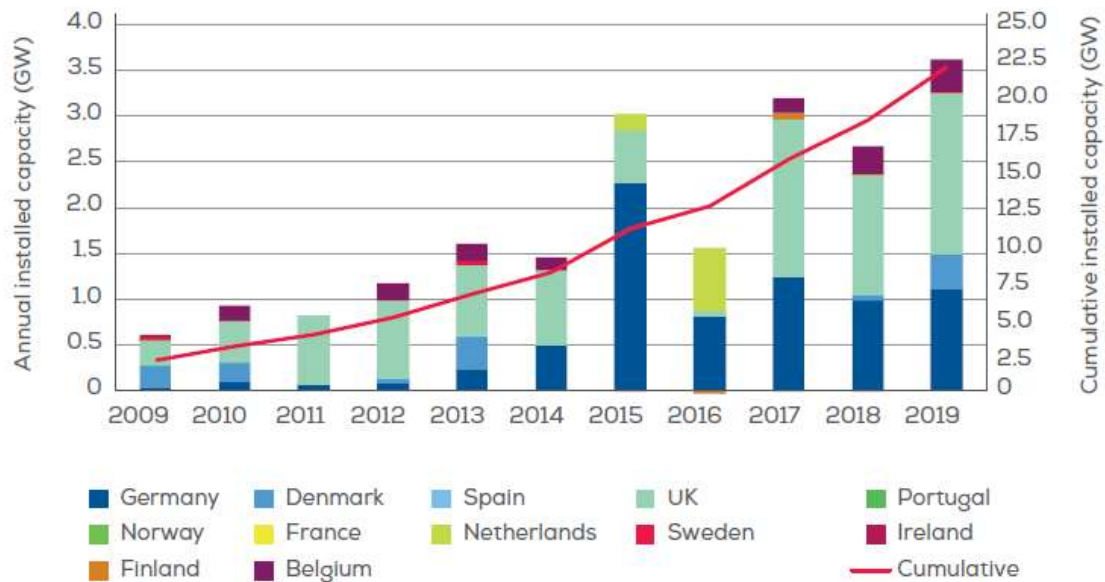


Figure 2: Annual offshore wind installations by country (left axis) and cumulative capacity (right axis) [GW] (Walsh 2019).

As shown in Figure 1 and Figure 2, the offshore wind is increasing every year, because turbines could have more potential capacity than onshore, taking into account that it could be bigger and generate more energy per turbine (Wind Europe 2017).

The importance of the Floating Offshore Wind Turbines is increasing, because it allows the installation of larger wind turbines, which makes them more economically attractive because of the production of energy and the longer lifetime. Floating turbines have also smaller impact in environmental surroundings, being noise and visual pollution smaller than in base fixed offshore turbines (Wind Europe 2017).

## 2.2. TYPES OF FLOATING PLATFORMS

The most used platforms for offshore wind turbines are the spar buoy, the semi-submersible platform and the tension-leg platform (TLP) (International Renewable Energy Agency (IRENA) 2016).



**Figure 3: Types of platform for off-shore wind turbine** (International Renewable Energy Agency (IRENA) 2016).

### 2.2.1. Spar-Buoys

The spar buoy (Figure 3) consists on a large deep cylinder, which could be divided in three parts, the floater, the transition piece and the tower. The spar is placed in vertical position, introducing ballast in its interior to place the centre of gravity below the centre of buoyancy in order to guaranty its equilibrium. Taking into account that the structure is suffering the wind and wave conditions, to avoid undesirable displacements, the spar will be fixed by three catenary mooring lines to the soil of the sea (International Renewable Energy Agency (IRENA) 2016). This type of platform will be the object of this thesis.

The main pros of this platform are (International Renewable Energy Agency (IRENA) 2016):

- Tendency for lower critical wave-induced motions.
- Simple design



- Lower installed mooring cost.

And cons are (International Renewable Energy Agency (IRENA) 2016):

- Offshore operations require heavy lift vessels.
- Needs deep water (more than 100 meters).

### 2.2.2. Semi-submersible

The semi-submersible platform (Figure 3) consist on cylinders connected each other by tubes. The columns provide the hydrostatic stability and the tubes provide the additional buoyancy and the connection between cylinders (International Renewable Energy Agency (IRENA) 2016). As in the previous case, the platform is kept in position by mooring lines, fixed on the soil.

The main pros of this platform are (International Renewable Energy Agency (IRENA) 2016):

- Constructed onshore or in a dry dock.
- Fully equipped platform, including turbine can float during the transportation.
- The transport is made using conventional tugs.
- Can be used in water less deep than the spar buoy (with 40 metres depth is enough).
- Lower installed mooring cost.

And the cons (International Renewable Energy Agency (IRENA) 2016):

- Tendency for higher critical wave-induced motions.
- Tends to use more material and larges structures.
- Complex fabrication.

### 2.2.3. Tension Leg Platform (TLP)

Highly buoyant, with central column and arms connected to tensioned tendons which ensure stability of the platform using suction piles (International Renewable Energy Agency (IRENA) 2016).

The main pros of this platform are (International Renewable Energy Agency (IRENA) 2016):

- Tendency for lower critical wave-induced motions.
- Low mass.
- Can be assembled onshore on a dry dock.

- Can be used in water depth to 50-60 metres, depending on metocean conditions.

And the cons (International Renewable Energy Agency (IRENA) 2016):

- Harder to keep stable during transport and installation.
- Depending on the design, a special purpose vessel may be required.
- Some uncertainty about impact of possible high-frequency dynamic effects on turbine.
- Larger installation mooring cost.

### 2.3. DEFINITION OF MOTIONS IN A FLOATING STRUCTURE

The definition of motions of a floating structure are defined as the motions of a ship. In a steadily translating system there are six motions which affect a ship, or any floating structure (Journée & Massie 2001).

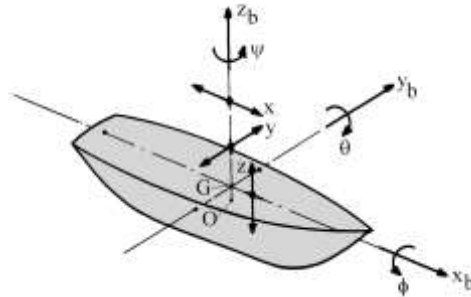


**Figure 4: Definition of ship motions in six degrees of freedom** (Journée y Massie 2001).

As shown in Figure 4 there are three translations of the ship centre of gravity, in the  $x$ ,  $y$ ,  $z$ -axis directions. Surge in  $x$ -direction, sway in  $y$ -direction and heave in  $z$ -direction. Figure 4 also defines the three rotations about these axes, roll about the  $x$ -axis, pitch, about the  $y$ -axis and yaw, about the  $z$ -axis (Journée & Massie 2001).

## 2.4. EXTERNAL LOADS IN FLOATING OFFSHORE WIND TURBINES

Wind turbines are subjected to very specific loads and stresses (Hau 2005). The main problem is to maintain the structure stability when there are storms and hurricanes which are considered the extreme conditions. Although there are the extreme conditions, it should be also studied the loads in normal conditions, because in long periods of time could create fatigue. Furthermore, there are other loads needed to be taking into account, the alternating loads, produced by the rotation of the rotor, which act on the structure during a long period of time, also creating fatigue.

Another problem to be faced is the dimension of the turbine elements, needed to convert energy from wind speed. If the dimension of the rotor increases, the dimensions of the tower will also need to increase, generating an increment of loads in the structure (Hau 2005). Large structures are elastic and the changing loads create a complex aero elastic coupling which induces vibrations and resonances and can produce high dynamic load components (Hau 2005).

At last there is the problem of hydrodynamic loads, caused by the waves and sea currents. These loads affect the platform more than the turbine, generating great tensions in the tower and the floater, and generating fatigue in the structure.

### 2.4.1. Hydrostatic pressure

Hydrostatic pressure results from the weight of the fluid column above the point at which that pressure is measured (Journée & Massie 2001). At a free water surface the pressure will be considered as 0 (atmospheric pressure). The hydrostatic pressure is calculated with the following equation (Journée & Massie 2001):

$$p = \rho * g * h$$

Where:

- $\rho$  is the mass density of the fluid. For sea water is 1025 kg/m<sup>3</sup>.
- $g$  is the acceleration of gravity.
- $h$  is the distance below the fluid surface.

#### 2.4.2. Archimedes law and buoyancy

Archimedes (285-212 BC) said that a body submerged in a fluid experiences an upward buoyant force (Journée & Massie 2001) equal to:

$$F_{\nabla} = \rho * g * \nabla$$

Where:

- $F_{\nabla}$  is the buoyant force.
- $\nabla$  is the volume of the submerged part of the solid.

#### 2.4.3. Gravity and inertial loads

This kind of loads are simple to calculate, despite the fact that at the beginning of the design phase, the masses are not known, because a mass can only be calculated as a consequence of the complete load spectrum (Hau 2005).

The gravity loads are the loads resulting from the death weight of the components of the turbine, the rotor, blades and support structure. These loads can be significant in the life of the blades, because when the turbine is working, with the rotation of the rotor, it generates different load cases in the blades. It occurs, approximately between  $10^7$  and  $10^8$  times in the service life of the turbine, so it generates fatigue stresses in blades which should be taken into account during the structural design.

The centrifugal loads are not very significant, because of the low rotational speed. On some rotors, the rotor blades are inclined downwind out of the plane of rotation, in a slight V-shaped form (Hau 2005). This angle of the rotor blades has the effect that the centrifugal forces, in addition to the tensile forces, create a bending moment distribution along the blade length which counters the bending moments created by the aerodynamic thrust (Hau 2005). However, complete compensation can only be achieved for one rotor speed and one wind speed (Hau 2005).

The gyroscopic loads are caused by gyroscopic effects, when the rotor is yawed into the wind. These loads generate gyroscopic moments, however they are not playing an important role in the dimensioning of the structure, because the yaw of the rotor is approximately 0.5 degrees/second, so it is negligible (Hau 2005). It will also be economically unviable to design the structure taking into account the gyroscopic moments.

#### 2.4.4. Aerodynamic loads

These loads are generated by the interaction between the wind and the structure, taking into account all the elements of it. There are static and dynamic loads (IEC 61400-1 2005). There are three different types of aerodynamic loads:

- Uniform and steady-state air flow (Figure 5): This kind of loads is an idealization, because a steady wind flow does not exist in the atmosphere. It is useful to calculate the mean load level occurring over a relatively long period of time (Chakrabarti 2005). The wind loads are determined by the effective wind speed varying from the blade root to the tip and the geometrical shape of the rotor blades influences the load distribution over the length of the blade (Hau 2005).



**Figure 5: Steady-state air flow** (Hau 2005).

- Vertical wind shear and cross wind (Figure 6): The wind flow produces unsteady, cyclically varying loads as soon as it strikes the rotor asymmetrically (Hau 2005). One of the asymmetries is caused by the increase in wind speed with height. During this process, the rotor is subjected to higher wind speeds and higher loads in the upper rotational sector. It occurs another asymmetry of flow at the rotor, caused by fast changes in wind direction, which is another reason for keeping the rotor axis inclination as small as possible to be affected by the directionality of the wind as less as possible (Chakrabarti 2005).

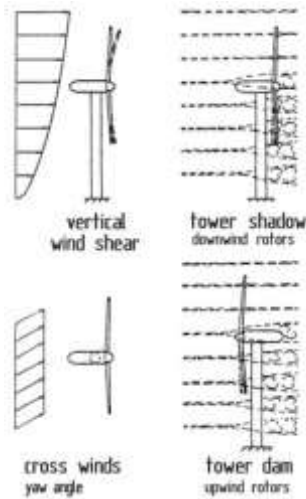


Figure 6: Vertical wind shear and cross wind (Hau 2005).

- Wind turbulence (Figure 7): When an structure is designed for a long-term period, there will occur variations of the mean wind speed during this time, creating non-cyclic fluctuating loads on the wind turbine (Hau 2005). The presence of turbulence specially generates fatigue in the structure, particularly in the rotor blades. In some cases, when extreme wind occurs, it can generate loads which could break the blades under fatigue, that's why in some cases the blades are allowed to rotate, to receive less loads and avoid stresses (Bredmose et al. 2020).

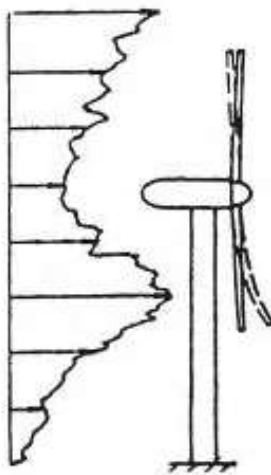


Figure 7: Wind turbulence (Hau 2005).

### 2.4.5. Tower interference

The rotor of a horizontal-axis wind turbine rotates very near to the tower. This separation should be as smaller as possible, to limit the length of the nacelle. The size of this separation makes the aerodynamic flow around the tower influences the rotor (Hau 2005). This influence is minimum when the rotor is placed upwind (Figure 8), because the wind flow goes through the rotor before arriving to the tower. These effects can be minimized when the distance between the rotor and the tower is at least one diameter (Hau 2005). When the rotor is placed downwind (Figure 8) the problem is different, because the tower generates a separation in the wind flow (Figure 9), named flow wake (Hau 2005). The flow wake depends on the Reynolds number (Hau 2005), generating different shapes of the wake (Figure 10). Inside this flow wake there are generated turbulences and a decreasing of the mean wind velocity.

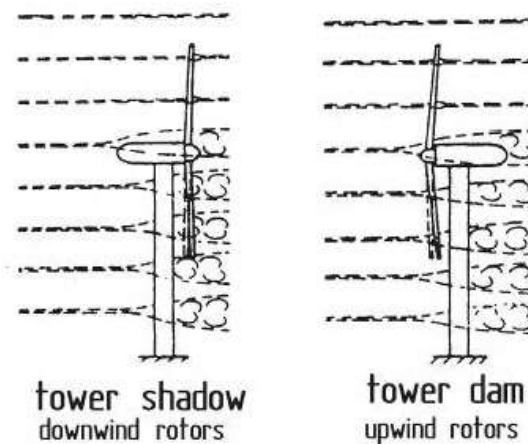


Figure 8: Position of the rotor related to wind direction (Hau 2005).

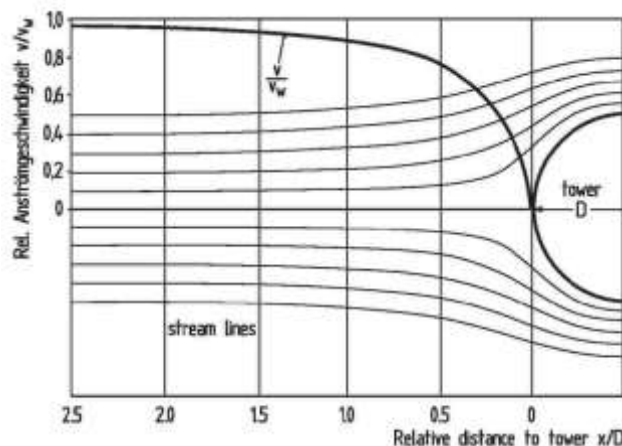


Figure 9: Flow field due to the tower dama head of a cylindrical tower with diameter D(Hau 2005).



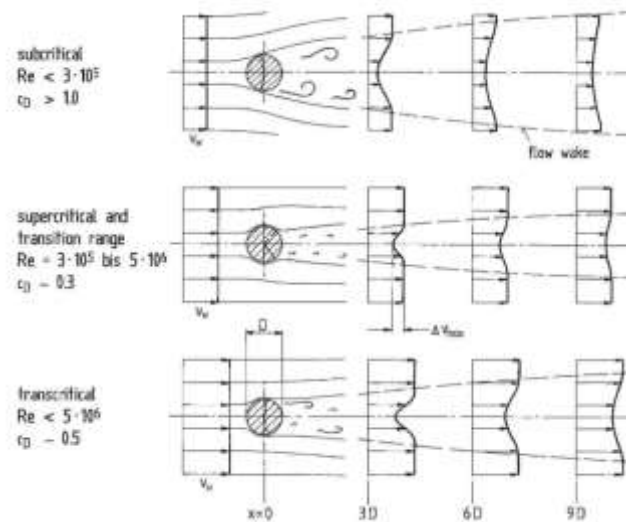


Figure 10: Flow around a circular cylinder in dependence on the Reynolds number (Hau 2005).

#### 2.4.6. Hydrodynamics

One of the biggest challenges in these calculations is to create a numerical formulation that adjusts itself to the reality of hydrodynamics characteristics because sea waves have a random appearance, and their description will only be possible in a statistical or spectral form (Chakrabarti 2005). The marine conditions for load and safety considerations are divided into the normal marine conditions which will occur more frequently than once per year during normal operation of an offshore wind turbine, and the extreme marine conditions which are defined as having a 1-year or 50-year recurrence period (IEC 61400-3 2009). There are some approaches to determine these loads, with different assumptions and limitations (Joao Cruz 2016). In hydrodynamics there are two types of methods, linear and non-linear. Linear methods are used to moderate situations, because the wave conditions are regular and the calculation time is less than in non-linear methods (Joao Cruz 2016). Non-linear methods are more suitable for non-moderate situations, and are more accurate than linear methods. Numerical models need to address some challenges (Joao Cruz 2016):

- “The necessity to account for radiation and diffraction forces, namely when these are of the same order of magnitude as the inertial forces” (Joao Cruz 2016).
- “The need to recognise and incorporate the frequency dependence of the above forces, in addition to memory effects” (Joao Cruz 2016).

- "Estimation of the mean and slow drift varying forces" (Joao Cruz 2016).
- "When relevant, consider shallow water effects, current and wave-current interactions in the calculations" (Joao Cruz 2016).
- "Estimation of the mooring dynamics and their effect on the overall system response" (Joao Cruz 2016).
- "When relevant, account for dissipative phenomena such as slamming loads and vortex induced vibrations (VIV)" (Joao Cruz 2016).

## 2.5. WINDCRETE FLOATER DESCRIPTION

WindCrete is a monolithic concrete spar platform including both the tower and the floater in a unique concrete member (Molins et al. 2016). The monolithic characteristic means that joints between the tower and the floater are avoided, thus the fatigue resistance is increased since weak points are driven out (Trubat et al. 2019). The whole structure is in compression state by the use of active reinforcement, and it is designed to avoid tension at any point during the life span of the platform.

Windcrete can be divided in four parts (Molins et al. 2016):

- Wind Turbine Generator: Formed by the rotor and blades, there will be connected to the tower by a special steel plate designed to take advantage of the post-tensioned tendons in the tower (Figure 11) (Molins et al. 2016).

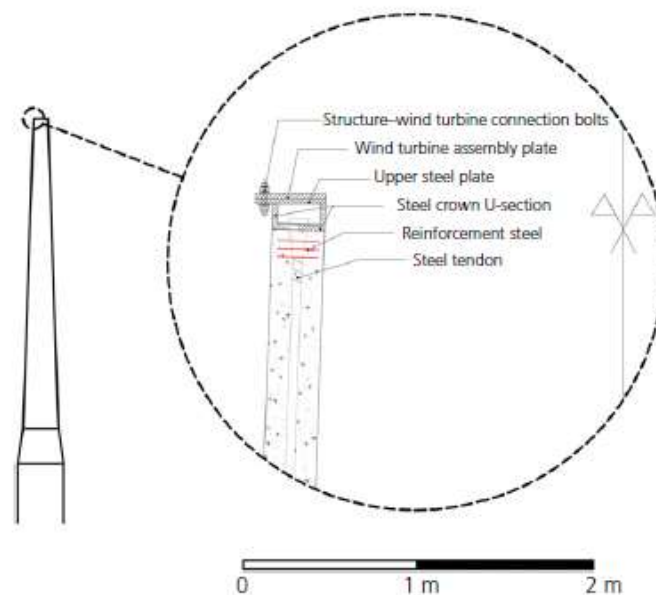


Figure 11: Steel crown detail (Molins et al. 2016).

- Concrete tower: is a truncated cone piece, designed to resist the bending moment during the service life of the structure with a minimum thickness that allows the colocations of post-tensioning tendons with the corresponding concrete cover.
- Substructure: According to the design basis (Trubat et al. 2019), the substructure can be divided in three parts:
  - Bottom semi-sphere: Placed in the base of the floater with the same diameter as the cylinder. This shape is favourable in structural terms, distributing the hydrostatic pressures in a

compression field around the base, while the post-tensioning steel tendons have continuity along the whole structure (Cobra et al. 2019).

- Cylinder buoy: Is the main part that ensures the buoyancy needed, as well as allows the placing of the ballast in its base to achieve the needed pitch and roll stiffness (Molins et al. 2016).
  - Tapered transition piece: Is the piece which guaranties the transition between the floater and the tower. Is designed to minimize the curvature changes in geometry, and it is the place where the losses of post-tensioning steel are bigger (Molins et al. 2016).
- Station keeping system: designed with three mooring lines distributed each  $120^\circ$ . They should be installed close to the centre of gravity of the structure to avoid pitch coupling motions that will increase the tension range of the mooring lines, and thus reducing its lifespan (Molins et al. 2016).

The Figure 12 shows an overview of windcrete, where will be easy to differentiate each part of the structure.



Figure 12: Windcrete overview (Cobra et al. 2019).

## 2.6. CONSTRUCTION, TRANSPORT AND INSTALLATION

Considering the dimensions of the structure, and its monolithic condition, construction is expected to be done in a dry dock or similar facility, with enough dimension to place all the structure, from where will be possible to launch the structure directly to the sea (Molins et al. 2016).

The structure is designed to be built in horizontal position by using a slipform. The use of slipforms avoids the presence of concrete joints, allowing the continuous construction of the structure (Molins et al. 2016).

The absence of joints improves the durability of the structure, avoiding the penetration of water into the concrete mixture (Molins et al. 2016).

Depending on the facility, the launching of the structure could be done by two different methods (Cobra et al. 2019). In case of a dry dock it will be done by the flotation of the structure (Molins et al. 2016). The other method, in case of having other facility is by the use of sliding guides or wheel skates to slip the structure into the sea (Molins et al. 2016). In both cases, the construction process needs to be done near the coast (few metres).

The towing process to the installation zone can be done by using a simple towing ship, as shown in Figure 13, available in most of commercial harbours (Molins et al. 2016).



**Figure 13: Towing of Windcrete.**

<https://www.windcrete.com/construction-installation/> (visited on 03/06/2020)

Once in the desired location, the erection process will be performed by flooding the structure in a controlled manner in order to not surpass the maximum bending moment allowed (Molins et al. 2016). The best way to reduce the maximum bending moment is to sink the whole structure guarantying that when it becomes vertical, only a small part of the tower will be above the mean sea level, as shown in Figure 14 (Molins et al. 2016).

Maintaining the majority of the structure submerged gives some advantages, a part from the reduction of bending moment, it makes easier to place in the top of the tower the wind turbine (Cobra et al. 2019).

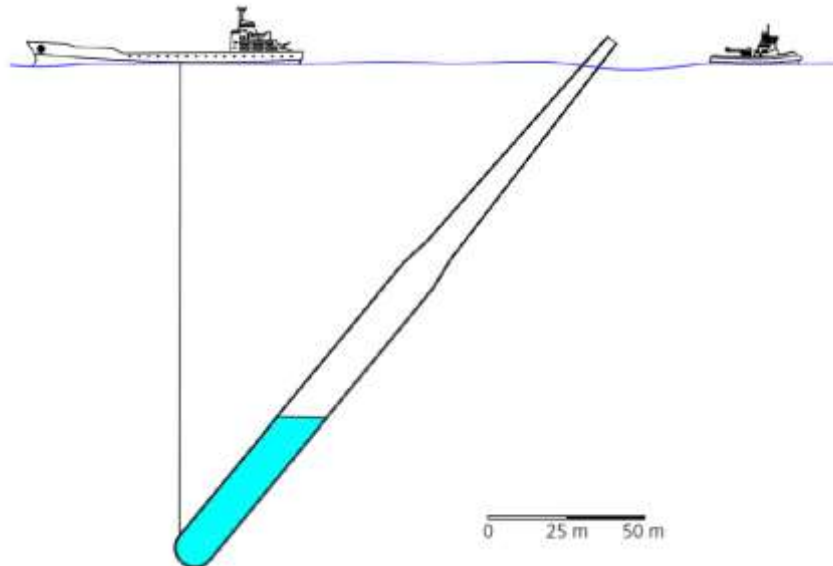


Figure 14: Erection process (Molins et al. 2016).

After having the tower in vertical position, as said before, it will be installed the wind turbine on the top. This installation will be done with a catamaran, or similar vehicle, equipped with a crane, as shown in Figure 15. The process is not complicated, because of the low height of the tower, due to the submerged position of the structure. It reduces the difficulty and also the cost of the operation (Molins et al. 2016).

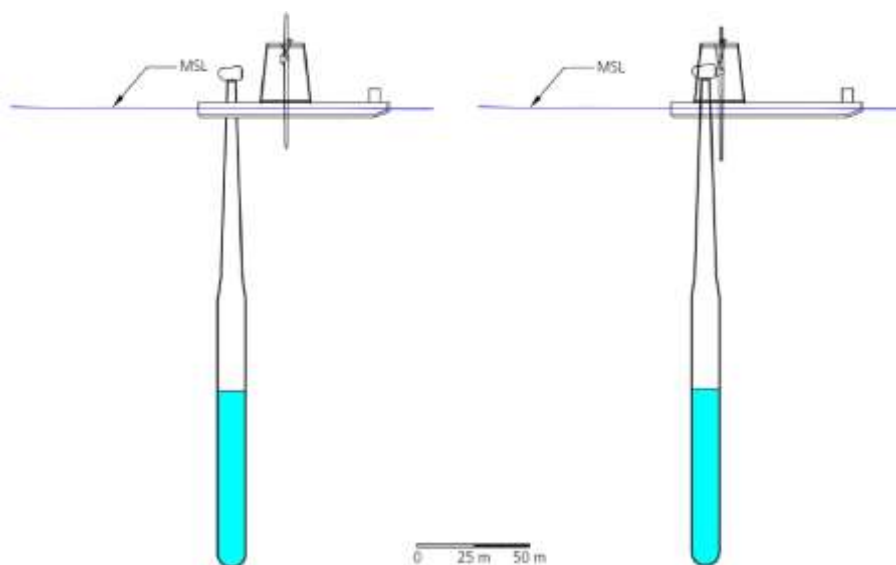
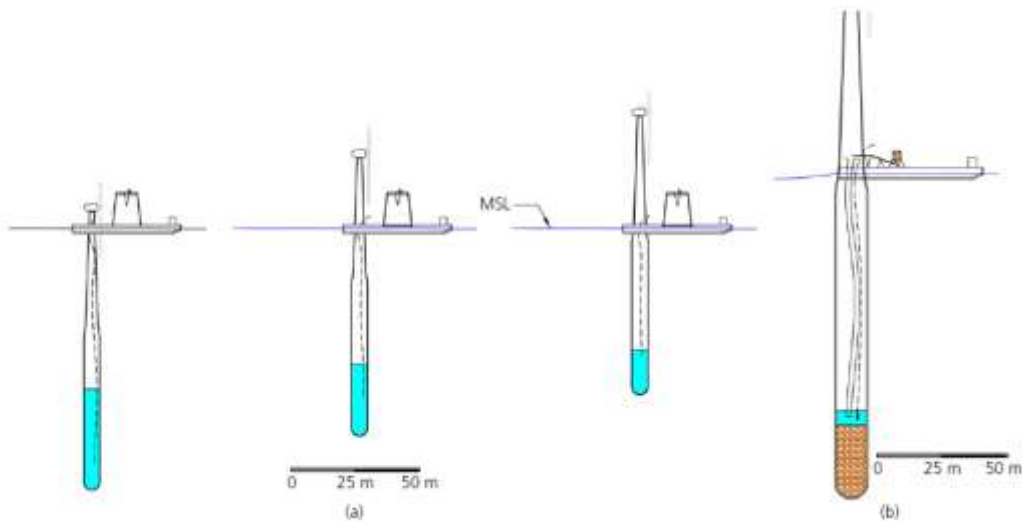


Figure 15: Wind Turbine installation (Molins et al. 2016).

Once having installed the wind turbine, it is time to ballast and emerge the structure. The structure is emerging by pumping out the water introduced to submerge the structure, maintaining stability with the water ballast, as shown in the Figure 16 (Molins et al. 2016). The most critical situation occurs once the structure reaches the required level above MSL, where the hydrostatic stiffness is enough to maintain the structure in a vertical position but the restoring moments are significantly reduced if compared with the final design (Molins et al. 2016). Then, the aggregates can be introduced inside the floater by way of a lateral opening, which can be the definitive maintenance door, using conveyor belts from an outside ship moored to the structure, as shown in the Figure 16b (Molins et al. 2016).



**Figure 16: Structure emerging (a) and ballasting (b) (Molins et al. 2016).**

## 2.7. FAST AND OPENFAST SOFTWARE

FAST (Fatigue, Aerodynamics, Structures, Turbulence) is a simulator used to analyse offshore wind turbines, created by NREL (National Renewable Energy Laboratory). FAST is an engineering tool used for simulating the coupled dynamic response of wind turbines (National Renewable Energy Laboratory 2017). It joins aerodynamics and hydrodynamics models for offshore structures, control and electrical system dynamics models, and structural dynamics models to enable coupled nonlinear aero-hydro-servo-elastic simulation (National Renewable Energy Laboratory 2017). Each module of FAST corresponds to different physical domain of the coupled aero-hydro-servo-elastic solution, most of it, separated by spatial boundaries (Jonkman y Buhl 2005). Figure 18 shows the control volumes associated with each module for a floating wind turbine. FAST could make the analysis of several wind turbine configurations, included two or three blade rotor, upwind or downwind... It could also be modelled the place of the turbine, differentiating onshore or offshore wind turbines, and bottom fixed or floating wind turbines (National Renewable Energy Laboratory 2017). FAST is based on a 24 degrees of freedom (Figure 17) problem for a floating offshore wind turbine with a three-bladed rotor (Jonkman 2013)

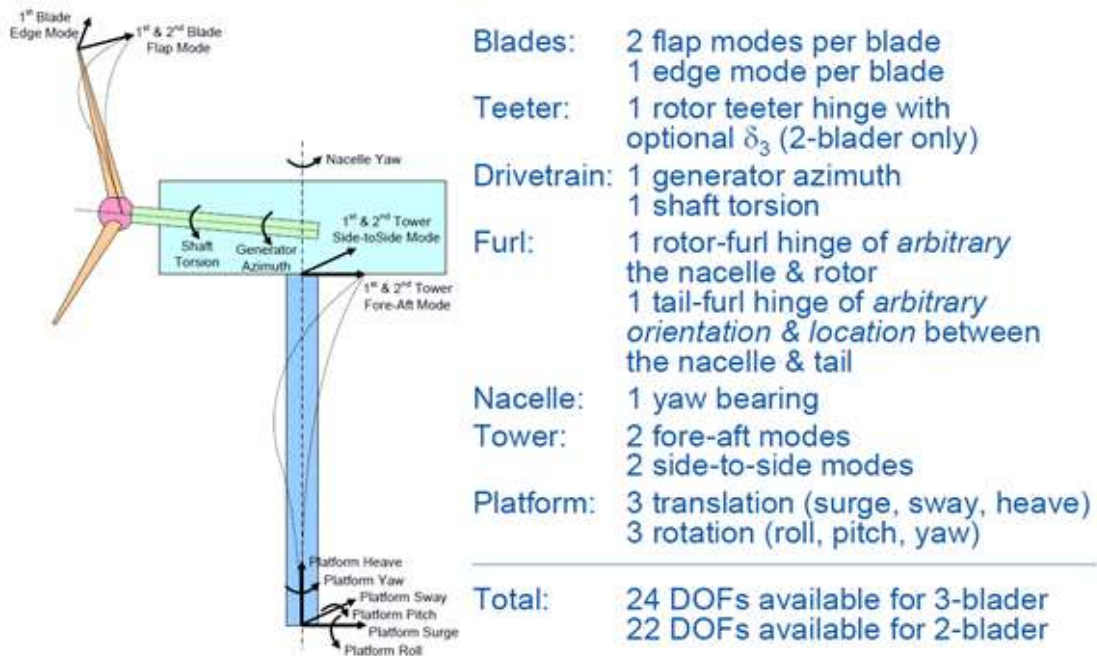


Figure 17: Degrees of freedom of a floating wind turbine (Jonkman 2013).



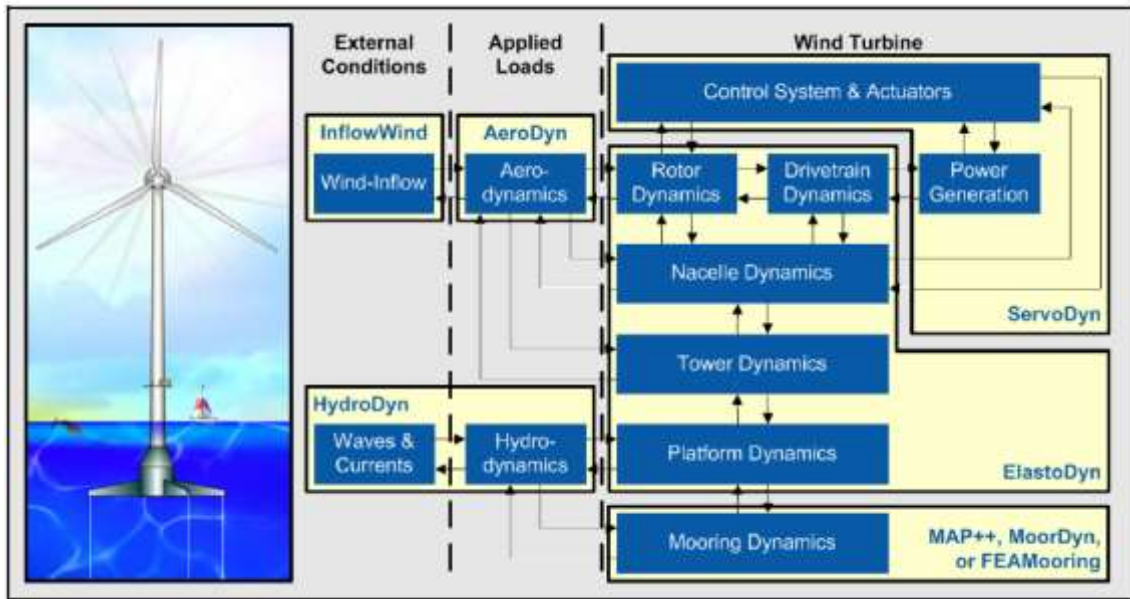


Figure 18: FAST control volumes for floating systems (Jonkman y Jonkman 2016).

OpenFAST “represents a transition to better support an open-source developer community across research laboratories, industry, and academia around FAST-based aero-hydro-servo-elastic engineering models of wind turbines and wind-plants” (National Renewable Energy Laboratory 2017).

FAST and OpenFAST are constantly in evolution being part of a research group with the objective of developing the software, to increase testing coverage (National Renewable Energy Laboratory 2017), and testing rigorously the results (Jonkman 2010).

### 2.7.1. Subroutines

#### 2.7.1.1. *Aerodyn*

Aerodyn is a model used to predict aerodynamics of horizontal-axis wind turbine (Moriarty & Hansen 2005), coupled to FAST and OpenFAST for aero-elastic simulation (Jonkman 2012). It was originally developed by Windward Engineering, and nowadays by NREL.

Aerodyn calculates the aerodynamic loads in the tower and the blades of the turbine. These calculations are based on the principles of actuator lines, where a 3-D flow around the body is approximated in a 2-D local flow distributed in a transversal section of the turbine (Moriarty & Hansen 2005). To make these calculations, it will take, as inputs, the turbine displacements and velocities.

When coupled to FAST, aerodyn receives as inputs the instantaneous structural position, orientation and velocities of the blades, hubs and tower for making its calculations (Jonkman 2012).

#### **2.7.1.2. *Hydrodyn***

Hydrodyn is a module added to FAST that allows the calculation of the time-domain hydrodynamic loads, for fixed-bottom or floating wind turbines (Jonkman 2014). This module is the generator of waves used in each load case, defining the significant height, the peak period and if they are regular or not. It is used to be an undocumented part of FAST, and it is a module with separated input files and source code (Jonkman 2014).

The inputs given to hydrodyn module are the substructure displacement, the substructure velocity and the substructure acceleration in each moment of time (Jonkman 2014). With these data, the module gives the hydrodynamic loads in the structure.

#### **2.7.1.3. *Servodyn***

Servodyn is the control and electrical-drive model for wind turbines (Jonkman 2014). Is a fundamental part of FAST and “includes control and electrical-drive models for blade pitch, generator torque, nacelle yaw, high-speed shaft (HSS) brake, & blade-tip brakes” (Jonkman 2014). Knowing the structural motions, the reaction loads and the wind measurements, this module provides the controller commands for the good function of the turbine, and to avoid problems.

#### **2.7.1.4. *Elastodyn***

Elastodyn is the structural-dynamic model for horizontal-axis wind turbines, including structural models of the rotor, nacelle, tower and platform (Jonkman 2013b). Taking as input the aerodynamic loads, the hydrodynamic loads, the controller commands and the substructure reactions, it will calculate displacement, velocities, accelerations and reaction loads (Jonkman 2013b).

This module is the one which takes into account the 24 degrees of freedom of the turbine explained in chapter 2.3 to compute forces and bending moments in each part of the structure.

## 2.8. CODES AND STANDARDS

To design the structure it has been followed different standards, because each one defines different parameters that should be taking into account to make the correct design of the structure. There are three main standards that have been used during the development of this project, DNVGL, IEC and EHE.

### 2.8.1. DNVGL

DNV (DET Norske Veritas) GL (Germanischer Lloyd) standards “contain requirements, principles and acceptance for objects, personnel, organisations and/or operations” (DNVGL-ST-0119 2018). They provide principles, technical requirements and guidance for load and site conditions of wind turbines (DNVGL-ST-0437 2016). The main use of these standards has been the definition of Load Cases of study, and the verifications needed to ensure the good behaviour of the structure. There have been used four different documents of this standard.

#### 2.8.1.1. *DNVGL-ST-0437*

This standard is applicable for the determination of design loads for onshore and bottom mounted offshore wind turbines. Site conditions are also within the scope of this standard.

The standard is applicable to all types of wind turbines, however, it is most comprehensive for two or three bladed and grid connected horizontal axis wind turbines with active pitch and yaw systems (DNVGL-ST-0437 2016).

This standard will be used to define the main load cases used in the designing process of the concrete spar, and also give some topic to evaluate the loads in the structure.

#### 2.8.1.2. *DNVGL-ST-0119*

This offshore standard provides principles, technical requirements and guidance for design, construction and in-service inspection of floating wind turbine structures (DNVGL-ST-0119 2018).

This standard defines the structural design for floating wind turbine structure. It also gives notions for the motion control of the floater and the control system of the wind turbine. The standard also gives provisions for transportation, installation and inspection to the extent necessary in the context of structural design.

#### **2.8.1.3. DNVGL-ST-0126**

This standard is the standard used for the design of wind turbine support structures. The standard takes construction, transportation, installation and inspection issues into account to the extent necessary in the context of structural design (DNVGL-ST-0126 2016).

This standard will be used to define the load cases to be studied, and also the duration of them, being the extreme loads, and the fatigue load level only exceeded 0.01% of the time equivalent to 17.5h in 20 years.

#### **2.8.1.4. DNVGL-ST-C502**

This standard is specific on the design of offshore concrete structure. It has been used, with DNVGL-ST-0126 to define the required environmental load combinations in order to verify the serviceability limit state. These combinations are maximum value of the extreme loads cases, and the fatigue load level exceeding 0.01% of the equivalent to 17.5 hours in 20 years.

#### **2.8.2. IEC**

The IEC (International Electrotechnical Commission) standard takes construction, transportation, installation and inspection issues into account to the extent necessary in the context of structural design (IEC 61400-1 2005).

##### **2.8.2.1. IEC 61400-1**

This part of IEC standard specifies essential design requirements to ensure the engineering integrity of wind turbines, providing and appropriate level of protection against damage.

It defines the structural design verification methodology defining the load cases and the duration of them, as well as its calculation and the analysis of the Ultimate Limit State and Serviceability Limit State.

##### **2.8.2.2. IEC 61400-3**

This part of the standards defines de requirements in design for offshore wind turbines to ensure its integrity (IEC 61400-3 2009). This standard is focused on the engineering integrity of the structural components for offshore wind turbines as well as their subsystems such as control and protection mechanisms, internal electrical systems and mechanical systems.

### 2.8.3. EHE-08

The EHE-08 is the Spanish standard used in the project of concrete structures. It defines all the requirements to be taken into account in concrete structures, either in building or in civil engineering, in order to achieve an acceptable level of safety (EHE-08 2008). This standard will be used to make all the structural verifications of the concrete spar. All the expressions used to calculate all the dimensions and the resistance forces and moments will be taken from this standard.

### **3. DEFINITION OF THE PROBLEM**

#### **3.1. WINDCRETE PROPERTIES**

The design of the WindCrete platform is based on a first static predesign to assess the main platform characteristics in order to verify the design basis (Mahfouz et al. 2020). The objective of the predesign basis is to present a static pitch less than  $4^\circ$ , and a natural motions period bigger than 30 seconds. Furthermore, the relation between the draft, diameter and thickness of the floater and the tower ensures the structural response and the disposition of active and passive reinforcement.

The hub height of the platform is 135 metres above sea level. The tower height is 129.495 metres height above sea level. This difference allows the location of an operating crane at the access platform.

The tower is a trunk cone made of concrete, with a base diameter of 13.2 metres and a top diameter of 6.5 metres to ensure the connection with the wind turbine. The thickness of the structure is variable, having a thickness of 0.5 metres in the tower base, and a thickness of 0.28 metres in the top of the tower.

The substructure consist on a tapered transition piece of 10 metres length with a base diameter of 18.6 metres and a top diameter of 13.2 metres to ensure the connection with the tower base and a thickness of 0.5 metres, a cylindrical spar of 135.7 metres length, 18.6 metres of diameter and a thickness of 0.5 metres and a hemisphere of 9.3 metres radius, with 0.5 metres of thickness at the bottom of the structure. So, the total draft of the platform is 155 metres.

The required hydrostatic stiffness in the pitch/roll degree of freedom is achieved by adding a solid aggregate ballast at the platform with a density of  $2500\text{kg/m}^3$  (Mahfouz et al. 2020). The internal height of the ballast is 44.14 metres from the keel (44.64 from the bottom of the structure).

The mass of the structure is  $3.9805\text{e}+07$  kg, and its centre of masses is placed 98.41 metres under the sea level. The centre of buoyancy is placed 77.29 metres under the sea level. And the inertia of the structure, measured form the centre of masses has the following values:

- $I_{xx} = 1.5536\text{e}+11 \text{ kg}\cdot\text{m}^2$
- $I_{yy} = 1.5536\text{e}+11 \text{ kg}\cdot\text{m}^2$
- $I_{zz} = 1.9025\text{e}+09 \text{ kg}\cdot\text{m}^2$

Figure 19 shows the dimensions of the windcrete.

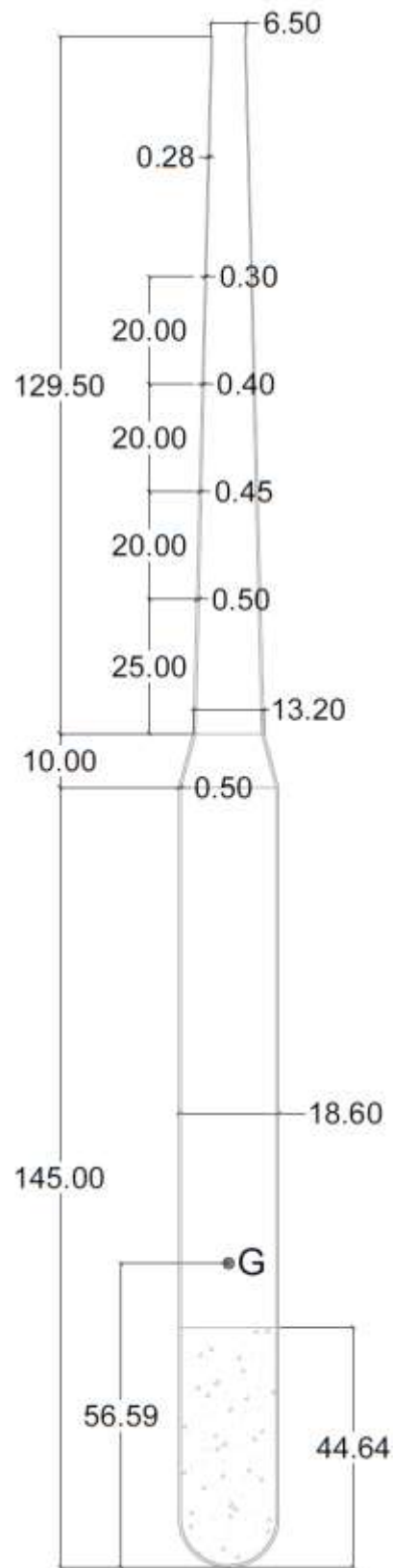


Figure 19: Windcrete dimensions.

### 3.2. MODAL ANALYSIS OF THE STRUCTURE

The floating platform will move and rotate due to waves and wind, furthermore it is subjected to the wind turbine loads, which are cyclic with a minimum rotor speed of 4.6 rpm and a maximum rotor speed of 7.6 rpm (Molins et al. 2016) which corresponds to a rotor frequency of 0.076 Hz and 0.126 Hz respectively and a blade passing frequency of 0.23 Hz and 0.38 Hz, respectively. It will be necessary to do a modal analysis to see if the structure, taking into account the self-weight of the floater, the tower and the turbine, does not vibrate in resonance with the turbine, which means that the value of frequency of the vibration modes of the structure is not between the values of rotor frequency and blade passing frequency (Figure 20).

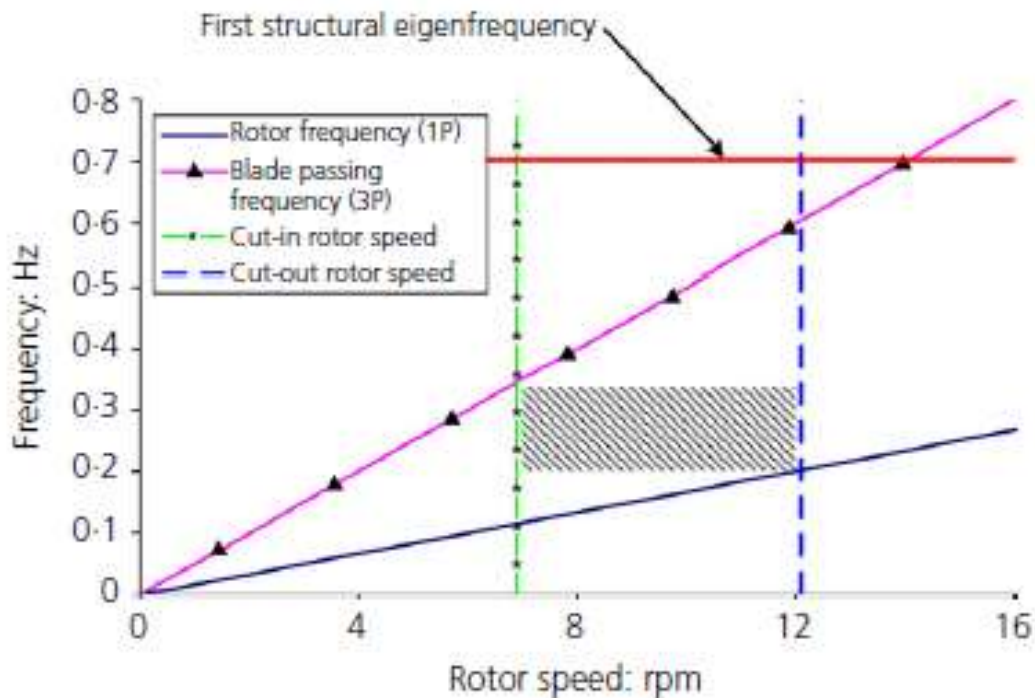


Figure 20: Campbell's diagram (Molins et al. 2016).

According to the Figure 20 the values of frequency should be out of the surface delimited by the cut-in rotor speed, the cut-out rotor speed, the blade passing frequency and the rotor frequency. However, they will be also accepted the values into the black rectangle.

This analysis will be done with Autodesk Robot Structural Analysis, creating a beam model, where the beams will have the sizes of the floater, the transition piece and the tower. The material will be an 80 MPa strength concrete, and it will be necessary to add an extra load representing the weight of the turbine



and the ballast. Trying to make it as realistic as possible, this extra load will be eccentric, because the real turbine is.

The hydrostatic behaviour of the platform is simulated by a 6 DOF spring system that simulates the rigid body behaviour of the spar. The horizontal motions and z rotation are based on the mooring response, the heave motion on the hydrostatic force, and the pitch and roll rotations due to the buoyancy and weight restoring moments (Journée y Massie 2001). The values of the stiffness are the followings:

- $K_x = 505 \text{ kN/m}$
- $K_y = 505 \text{ kN/m}$
- $K_z = 1376 \text{ kN/m}$
- $H_x = 117160 \text{ kN}\cdot\text{m/Deg}$
- $H_y = 117160 \text{ kN}\cdot\text{m/Deg}$
- $H_z = 89963 \text{ kN}\cdot\text{m/Deg}$

Where K is the linear stiffness and H is the rotation stiffness.

With all these values, the structure has been modelled by Robot. In the Figure 21 it will be shown the model with the size of the beams, the eccentric load and the elastic supports. The spar is not exactly the same as the real one because, for example, the bottom of the spar is a semi-sphere, and in the model is a cylinder, but the percentage of error is negligible (Table 1), so it will be an acceptable model:

	CoG (m from water surface)	Ixx (kg/m <sup>2</sup> )	Izz (kg/m <sup>2</sup> )
Real spar	-98.41	1.553e11	1.9025e9
Model	-100.03	1.586e11	2.023e9
Error (%)	1.649	2.35	6.34

**Table 1: Center of gravity and inertia of the real spar and the model of Robot Structural Analysis (values taken from AutoCad).**



**Figure 21: 3-D model of the structure made by Robot Structural Analysis.**

The modal analysis will give 12 vibration modes, first 6 shows the rigid body behaviour of the structure, and the others are the vibration modes of the structure. It should be taking into account that the first 6 modes of vibration represent the 6 degrees of freedom of rigid body motion which have been defined in the model to obtain correct values. In Table 2 it will be shown the real frequencies of these modes, and the ones obtained by Robot.

Mode	Real frequency (Hz)	Robot frequency (Hz)
1	0.01221	0.01
2	0.01221	0.01
3	0.03052	0.03
4	0.02441	0.04
5	0.02441	0.04
6	0.09155	0.12

**Table 2: Frequencies of the rigid body behaviour obtained with Robot (Mahfouz et al. 2020).**

It will be studied the modes 7, 8, 9 and 10, which are the vibration modes, and should be different from the vibration of the turbine. In Table 3 it will be shown the results of the 4 modes of vibration.

Mode	Frequency (Hz)	Period (s)
7	0.52	1.91
8	0.53	1.90
9	1.57	0.64
10	1.57	0.64

**Table 3: Modal analysis results obtained with Robot.**

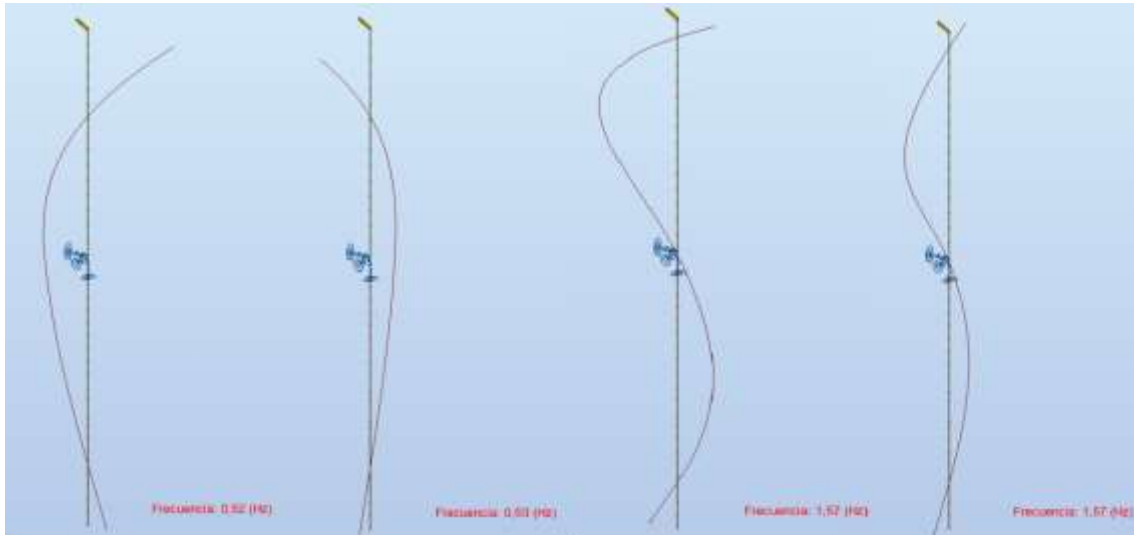


**Figure 22: Modes of vibration 7, 8, 9 and 10 respectively, taken from Robot.**

As shown in Table 2 and Table 3, every values of frequency are out of the limits defined by the Campbell's diagram (Figure 20) for rotor frequency and blade passed frequency.

### 3.3. ENVIRONMENTAL DATA

The structure will be placed near Gran Canaria Island, in Spain, so it will be necessary to know some data, specially wind velocities and wave's heights and peak periods. All this information will be taken from COREWIND data (Cobra et al. 2019).

The design water depth at Gran Canaria Island is 200 metres. This value have been taken from the tide gauge in Arinaga Port (Cobra et al. 2019).

#### 3.3.1. Wind

The wind data has been taken from SIMAR point 4038006 from the Spanish Ports Authority (Cobra et al. 2019), with coordinates 15°19'48.00" W and 27°45'0.00" N.

##### 3.3.1.1. Normal wind profile

The wind speed profile along the tower fits with the following logarithmic expression, used to know the wind velocity in the reference height (Cobra et al. 2019):

$$V(z) = V_{hub} * \frac{\ln\left(\frac{z}{z_0}\right)}{\ln\left(\frac{z_{hub}}{z_0}\right)}$$

So the 10-minute mean wind speed profile is shown in the Table 4 (Cobra et al. 2019):

Normal Wind Profile	
Height	Speed
[m]	[m/s]
10	9.83
20	10.48
50	11.33
100	11.98
119	12.14
150	12.36

Table 4: Normal wind speed profile (Cobra et al. 2019).

##### 3.3.1.2. Extreme wind profile

In this case, the expression which fits better with the wind velocity profiles is the following (Cobra et al. 2019):

$$V(z) = V_{hub} * (z/z_{hub})^{0.12}$$

So, the extreme wind speed profile for a return period of 50 year is shown in Table 5 (Cobra et al. 2019):

Extreme Wind Profile Tr=50 years	
Height	Speed
[m]	[m/s]
10	29.77
20	32.35
50	36.11
100	39.24
119	40.07
150	41.20

Table 5: Extreme condition wind speed profile (Tr =50 years) (Cobra et al. 2019).

### 3.3.2. Waves

The wave data have been also taken from the data provided by the SIMAR point 4038006, from the Spanish Ports Authority (Cobra et al. 2019).

#### 3.3.2.1. Extreme waves

Return period (years)	Hs (m)	Tp (s)
50	5.11	9.0-11.0
20	4.69	9.0-11.0
10	4.40	9.0-11.0
1	3.35	8.0-10.0

Table 6: Wave data for Gran Canaria (Cobra et al. 2019).

#### 3.3.2.2. Scatter diagrams

The wave data will be taken from scatter diagrams, shown in the following figures:

Significant Wave Height [m]	WIND SPEED (1-hour at 10 m)										
	0.00 - 2.00	2.00 - 4.00	4.00 - 6.00	6.00 - 8.00	8.00 - 10.00	10.00 - 12.00	12.00 - 14.00	14.00 - 16.00	16.00 - 18.00	18.00 - 20.00	>20.00
0.00 - 1.00	2.083	8.396	12.354	8.754	4.174	1.685	0.588	0.144	0.044	0.010	0.001
1.00 - 2.00	3.012	12.063	18.533	12.298	5.582	2.195	0.777	0.248	0.062	0.010	0.006
2.00 - 3.00	0.384	1.387	2.041	1.568	0.785	0.295	0.126	0.055	0.012	0.003	0.002
3.00 - 4.00	0.014	0.060	0.109	0.076	0.034	0.009	0.007	0.003			
4.00 - 5.00			0.005	0.003							
5.00 - 6.00											
6.00 - 7.00											
> 7.00											

Table 7: Wind-Wave scatter diagram (Cobra et al. 2019).

		Significant Wave Height (m)					
		0-1	1-2	2-3	3-4	4-5	Total
Peak Period (s)	1-2	0.037	0.001	0	0	0	0.038
	2-3	0.771	0.3	0	0	0	1.071
	3-4	2.603	1.845	0	0	0	4.448
	4-5	4.524	5.132	0.003	0	0	9.659
	5-6	5.392	10.973	0.049	0	0	16.414
	6-7	4.907	14.608	0.465	0	0	19.980
	7-8	4.211	9.569	2.593	0.012	0	16.385
	8-9	3.504	5.006	2.552	0.11	0	11.172
	9-10	2.836	3.119	1.087	0.147	0.001	7.190
	10-11	2.252	1.865	0.522	0.073	0.003	4.715
	11-12	1.766	1.250	0.275	0.028	0	3.319
	12-13	1.244	0.823	0.161	0.005	0	2.233
	13-14	0.827	0.542	0.12	0.001	0	1.490
	14-15	0.512	0.326	0.085	0.002	0	0.925
	15-16	0.27	0.21	0.052	0.003	0	0.535
	16-17	0.129	0.119	0.034	0.001	0	0.283
	17-18	0.04	0.058	0.005	0	0	0.103
	18-19	0.01	0.018	0	0	0	0.028
	19-20	0.001	0.006	0.001	0	0	0.008
	20-21	0	0.002	0	0	0	0.002
	21-22	0	0.001	0	0	0	0.001
<b>Total</b>	<b>35.84</b>	<b>55.77</b>	<b>8.004</b>	<b>0.382</b>	<b>0.004</b>	<b>100.000</b>	

Table 8: Significant wave height-Peak period frequency for Gran Canaria (Cobra et al. 2019).

With all these data is possible to define the conditions of the different load cases of study, defining the wind and wave conditions.

To define the peak period and the wave height it will be used the previous tables. Having the wind velocity, using the Table 7, where is shown the probability of each significant wave height. Making a weighted average of all the heights will be obtained the most probable value of  $H_s$ .

This value will be introduced in Table 8, and making the same procedure as before it will be obtained the value of the Peak Period.

### 3.4. LOAD CASES

To determine the behaviour of the structure and provide an acceptable level of safety, it will be calculated under different situations. These situations are defined in the standards (DNVGL-ST-0437 2016). According to these standards, the turbine is a class I turbine, which reference wind velocity is 50 m/s.

There will be studied 5 different load cases, corresponding with two different situations. Three of the load cases correspond to a normal situation of power production, when the turbine is working, and the others correspond to a situation where the turbine is parked, without producing energy. The Table 9 will show the data of each load case:

Design situations	D L C	Wind Condition	Wave Condition			Events	Type of analysis	Partial Safety Factor	Time of analysis
			Model	Height	Direction				
Power production	1.1	NTM $V_{in} < V_{hub} < V_{out}$	NSS	$H_s = E[H_s   V_{hub}]$	$B = 0^\circ$	$Yaw = 0^\circ, \pm 8^\circ$	U	1.25*1.2	3*20 min+600s
	1.2	NTM $V_{in} < V_{hub} < V_{out}$	NSS	Joint prob. distr. of $H_s, T_p, V_{hub}$	$B = 0^\circ$	$Yaw = 0^\circ, \pm 8^\circ$	F	1	3*20 min
	1.3	ETM $V_{in} < V_{hub} < V_{out}$	NSS	$H_s = E[H_s   V_{hub}]$	$B = 0^\circ$	$Yaw = 0^\circ, \pm 8^\circ$	U	1.35	3*20 min+600s
	1.6	NTM $V_{in} < V_{hub} < V_{out}$	SSS	$H_s = H_{s,SSS}$	$B = 0^\circ$	$Yaw = 0^\circ, \pm 8^\circ$	U	1.35	3*20 min+600s
Parked (standing still or idling)	6.1	EWM $V_{hub} = V_{ref}$	ESS	$H_s = H_{s,50}$	$B = 0^\circ, \pm 30^\circ$	$Yaw = 0^\circ, \pm 8^\circ$	U	1.35	9*1 hour
	6.2	EWM $V_{hub} = V_{ref}$	ESS	$H_s = H_{s,50}$	$B = 0^\circ, \pm 30^\circ$	$-180^\circ < Yaw < 180^\circ$	U	1.1	6*1 hour

Table 9: Design load cases (DNVGL-ST-0437 2016).

Where:

- $V_{in}$  is the cut-in wind speed, which is the speed that makes the turbine start moving.
- $V_{out}$  is the cut-out wind speed, which is the maximum speed allowed by the turbine, if it is more than this value, the blades will turn into horizontal position to stop working.
- NTM normal turbulence model.
- ETM extreme turbulence model.
- $H_s$  is the significant wave height.

- $V_{\text{hub}}$  is the 10-minute average wind speed at hub height.

According to the standards, and to the design basis of the turbine (Cobra et al. 2019) the hub height is 135.5 metres, the cut-in wind speed is 3 m/s and the cut-out wind speed is 25 m/s.

As shown in the Table 9 in every case there are different groups of time. In the Power production situations there are 3 calculations of 20 minutes for each case, that occurs because of the yaw misalignment, which should be analysed in every case (BS EN 61400 2009). The same happens with the parked cases, but in that ones, there is a yaw misalignment and a wind direction misalignment, that's why more cases are needed.

#### 3.4.1. DLC 1.1.

Analysis of DLC 1.1 is only required for calculations of the ultimate loads acting on the RNA (Rotor Nacelle Assembly) (DNVGL-ST-0437 2016). The calculations should be based on statistical extrapolation of the load response results of multiple simulations of stochastic sea states and turbulent inflow for a range of mean wind speeds (DNVGL-ST-0437 2016). The significant wave height for each individual sea state shall be taken as the expected value of the significant wave height conditioned on the relevant mean wind speed (BS EN 61400 2009).

The wind velocity, according to the Design Basis (Cobra et al. 2019) goes between the values of 3 m/s and 25 m/s. It will be taking into account all these velocities increasing the value in 2m/s in each case, calculating the significant wave height and the peak period for each velocity.

#### 3.4.2. DLC 1.2.

DLC 1.2 should consider the misalignment of wind, wave and current and the multi-directionality of metocean conditions (DNVGL-ST-0437 2016). Taking into account that this is a fatigue load calculation it should be considered 700 generator switching operations per year. Furthermore, 300 changes per year in the mean wind speeds from  $V_{\text{in}}$  to  $V_{\text{r}}$  and back should be taken into account also 50 changes per year in the mean wind speeds from  $V_{\text{r}}$  to  $V_{\text{out}}$  and back (DNVGL-ST-0437 2016).

As in the previous case the wind velocity, according to the Design Basis (Cobra et al. 2019) goes between the values of 3 m/s and 25 m/s. It will be taking into



account all these velocities increasing the value in 2m/s in each case, calculating the significant wave height and the peak period for each velocity.

#### 3.4.3. DLC 1.3.

DLC 1.3 studies the ultimate loading resulting from extreme turbulence conditions. Normal sea state conditions should be assumed for this design load case and the significant wave height for each individual sea state shall be taken as the expected value of the significant wave height conditioned on the relevant mean wind speed (BS EN 61400 2009).

For these case the significant wave height will be considered of 2 metres and the peak period will be calculated according to the design basis (Cobra et al. 2019), giving a value of 7.249 seconds.

#### 3.4.4. DLC 1.6.

In DLC 1.6 the offshore wind turbine shall be considered in the event of a combination with a severe sea state.

The values of the significant wave height and the peak period will be taken from the design basis (Cobra et al. 2019) for extreme waves with a return period of 50 years, having a significant wave height of 5.11 metres and a peak period of 10 seconds (Table 6).

#### 3.4.5. DLC 6.1.

In DLC 6.1 should be assumed the Extreme Wind Speed Model in combination with a stochastic wave model and the response shall be computed by using a full dynamic simulation (DNVGL-ST-0437 2016). It will be assumed a yaw misalignment of  $\pm 8^\circ$  and a wind misalignment of  $\pm 30^\circ$ .

As in the previous case, the values of the significant wave height and the peak period will be taken from the design basis (Cobra et al. 2019) for extreme waves with a return period of 50 years, having a significant wave height of 5.11 metres and a peak period of 10 seconds (Table 6).

### 3.4.6. DLC 6.2

In DLC 6.2 should be also assumed the Extreme Wind Speed Model. A grid failure in an early stage of the storm with the extreme wind situation shall be assumed. A yaw error of up to  $\pm 180^\circ$  shall be assumed if no independent power supply is available. It also will be assumed a wind misalignment of  $\pm 30^\circ$  (DNVGL-ST-0437 2016). To make a good study of this case there will be computed different situations with different yaw misalignments to see the real behaviour of the structure in this load case.

As in the previous cases, the values of the significant wave height and the peak period will be taken from the design basis (Cobra et al. 2019) for extreme waves with a return period of 50 years, having a significant wave height of 5.11 metres and a peak period of 10 seconds (Table 6).

### 3.5. Design conditions

The windcrete spar should be designed to fulfil the constraints defined in the design basis (Mahfouz et al. 2020). Apart from the verifications of the load cases defined in chapter 3.4, there are defined excursion and acceleration limits, which will be shown in Table 10:

Limit for	Windcrete
<b>OPERATION</b>	
Yaw (10 min. max).	< 15°
Yaw (10 min. std).	< 3°
Pitch (max.).	[-5.5°, +5.5]
Pitch (10 min. average).	[-4.0°, +4.0°]
Roll (max.).	[-3.5°, +3.5°]
Pitch (10 min. std).	< 1°
Roll (10 min. std).	< 1°
<b>IDLING CONDITION</b>	
Pitch (10 min. average).	[-5°, +5°]
Pitch (10 min. max.).	[-7°, +7°]
<b>EMERGENCY STOP</b>	
Max. pitch.	[-15°, +15°]
<b>EXCURSION RESTRICTION</b>	
Horizontal offset (alarm limit) (mean during operation).	15 m
Horizontal offset (WTG shutdown). Maximum during parked conditions.	30 m
<b>ACCELERATIONS LIMITS</b>	
Operation (acc. XY/acc. Z)	2.8 m/s <sup>2</sup>
Survival (acc. XY/acc. Z)	3.5 m/s <sup>2</sup>

Table 10: Excursion and acceleration limits (Mahfouz et al. 2020).

## 4. ANALYSIS OF THE RESULTS

In this chapter will be analysed the values given by OpenFAST for each load case and these values will be compared with the limits defined in chapter 3.5.

### 4.1. Motions and accelerations

#### 4.1.1. DLC 1.1.

LC	MaxPitch [deg]	Mean Pitch [deg]	Max Roll [deg]	Mean Roll [deg]	Max Yaw [deg]	Max Nacelle XY acceleration [m/s <sup>2</sup> ]	Max Nacelle Z acceleration [m/s <sup>2</sup> ]
36	5.16	3.11	0.91	-0.19	1.56	0.64	0.20
13	5.16	3.11	0.91	-0.19	1.56	0.64	0.20
36	3.40	1.37	2.85	0.47	4.94	1.12	0.27
13	5.07	3.02	1.30	0.63	1.35	0.56	0.13
36	3.40	1.37	2.85	0.47	4.94	1.12	0.27
29	3.71	1.34	2.83	0.41	3.79	1.59	0.34
36	3.71	1.34	2.83	0.41	3.79	1.59	0.34

Table 11: Motions and accelerations for DLC 1.1 given by OpenFAST, underlining the values out of the limits defined by the design bases.

As shown in Table 11 all the values are into the limits defined in Table 10, where the maximum value of Pitch angle should be smaller than 5.5°, the maximum pitch should be smaller than 4° and the maximum Roll should be smaller than 3.5°.

Taking into account this fact it is considered that the turbine performs as expected.

#### 4.1.2. DLC 1.2.

LC	MaxPitch [deg]	Mean Pitch [deg]	Max Roll [deg]	Mean Roll [deg]	Max Yaw [deg]	Max Nacelle XY acceleration [m/s <sup>2</sup> ]	Max Nacelle Z acceleration [m/s <sup>2</sup> ]
80	<u>6.83</u>	2.50	0.88	0.21	1.66	1.57	0.47
66	5.14	3.17	0.91	-0.21	2.77	1.17	0.26
129	3.81	1.29	3.64	0.45	4.26	1.46	0.34
61	5.20	2.90	1.62	0.61	2.59	1.43	0.32
135	4.95	1.23	3.35	0.40	5.14	1.82	0.39
131	2.95	1.25	1.45	0.45	3.55	<u>2.85</u>	0.59
131	2.95	1.25	1.45	0.45	3.55	<u>2.85</u>	0.59

Table 12: Motions and accelerations for DLC 1.2 given by OpenFAST, underlining the values out of the limits defined by the design bases.

As shown in Table 12 in load case 80 the maximum Pitch is out of the limits defined in Table 10, where the maximum value of Pitch angle should be smaller than 5.5°. It happens also than in case 131, the maximum nacelle acceleration is bigger than the limit defined in Table 10 in the value of operation, which is 2.8m/s<sup>2</sup>.

The load case 80 corresponds to a wind speed of 11.1 m/s, without yaw misalignment and a significant wave height of 3.5 metres with a peak period of 9.6 seconds. And the load case 131 corresponds to a wind speed of 23.4 m/s, without yaw misalignment and a significant wave height of 1.5 metres with a peak period of 7 seconds.

Taking into account the amount of cases, it will be considered that the turbine performs as expected, also because the maximum acceleration in case 131 is very similar to the limit, and is smaller than the survival limit.

#### 4.1.3. DLC 1.3.

LC	MaxPitch [deg]	Mean Pitch [deg]	Max Roll [deg]	Mean Roll [deg]	Max Yaw [deg]	Max Nacelle XY acceleration [m/s <sup>2</sup> ]	Max Nacelle Z acceleration [m/s <sup>2</sup> ]
30	<u>5.73</u>	2.86	0.93	0.22	2.25	1.38	0.33
15	<u>5.73</u>	2.86	0.93	0.22	2.25	1.38	0.33
30	4.84	1.31	3.45	0.44	5.28	1.39	0.31
13	5.18	2.80	1.32	0.59	2.86	1.20	0.27
30	4.84	1.31	3.45	0.44	5.28	1.39	0.31
20	3.85	1.72	2.39	0.47	2.90	2.26	0.51
33	3.85	1.72	2.39	0.47	2.90	2.26	0.51

Table 13: Motions and accelerations for DLC 1.3 given by OpenFAST, underlining the values out of the limits defined by the design bases.

As shown in Table 13 in load cases 30 and 15 the maximum Pitch is out of the limits defined in Table 10, where the maximum value of Pitch angle should be smaller than 5.5°.

The load case 30 corresponds to a wind speed of 21 m/s, with a yaw misalignment of 8° and a significant wave height of 2 metres with a peak period of 7.25 seconds. And the load case 15 corresponds to a wind speed of 11 m/s, with a yaw misalignment of 8° and a significant wave height of 2 metres with a peak period of 7.25 seconds.

Taking into account that there are only two cases of 36, and the value is near the limit, it will be considered that the turbine performs as expected.

#### 4.1.4. DLC 1.6.

LC	MaxPitch [deg]	Mean Pitch [deg]	Max Roll [deg]	Mean Roll [deg]	Max Yaw [deg]	Max Nacelle XY acceleration [m/s <sup>2</sup> ]	Max Nacelle Z acceleration [m/s <sup>2</sup> ]
14	<u>5.85</u>	3.10	0.68	0.21	1.55	1.93	0.28
15	5.22	3.19	0.93	-0.21	1.84	1.61	0.30
39	4.13	1.34	3.34	0.47	4.48	2.03	0.36
13	5.14	3.17	1.32	0.65	1.88	1.64	0.27
39	4.13	1.34	3.34	0.47	4.48	2.03	0.36
38	4.42	1.30	2.86	0.48	3.77	2.39	0.42
37	3.61	1.26	2.77	0.47	3.11	2.02	0.45

Table 14: Motions and accelerations for DLC 1.6 given by OpenFAST, underlining the values out of the limits defined by the design bases.

As shown in Table 14 there is only one value underlined, this value corresponds to load case 14, which corresponds to a wind speed of 11 m/s, without yaw misalignment and a significant wave height of 5.11 metres with a peak period of 10 seconds.

Taking into account that the limit of the Pitch angle is 5.5° and the value obtained is 5.85° just in one case, it could be concluded that the turbine performs as expected, like in the previous cases.

#### 4.1.5. DLC 6.1.

LC	MaxPitch [deg]	Mean Pitch [deg]	Max Roll [deg]	Mean Roll [deg]	Max Yaw [deg]	Max Nacelle XY acceleration [m/s <sup>2</sup> ]	Max Nacelle Z acceleration [m/s <sup>2</sup> ]
4	4.70	1.45	2.78	-1.06	3.01	1.96	0.22
5	4.39	1.46	1.30	0.07	1.96	1.54	0.26
6	4.10	1.42	3.06	1.25	2.54	1.68	0.24
6	4.10	1.42	3.06	1.25	2.54	1.68	0.24
4	4.70	1.45	2.78	-1.06	3.01	1.96	0.22
4	4.70	1.45	2.78	-1.06	3.01	1.96	0.22
3	3.94	1.44	2.96	1.25	2.21	1.73	0.32

Table 15: Motions and accelerations for DLC 6.1 given by OpenFAST, underlining the values out of the limits defined by the design bases.

As shown in Table 15, all the maximum values of load cases are into the limits defined in Table 10, so the turbine performs well in this DLC, without any exception.

#### 4.1.6. DLC 6.2.

LC	MaxPitch [deg]	Mean Pitch [deg]	Max Roll [deg]	Mean Roll [deg]	Max Yaw [deg]	Max Nacelle XY acceleration [m/s <sup>2</sup> ]	Max Nacelle Z acceleration [m/s <sup>2</sup> ]
3	<u>11.22</u>	3.23	<u>9.91</u>	-0.93	9.68	2.05	0.31
7	<u>9.03</u>	3.29	<u>7.73</u>	0.87	5.89	2.10	0.25
3	<u>11.22</u>	3.23	<u>9.91</u>	-0.93	9.68	2.05	0.31
16	<u>9.37</u>	3.26	<u>8.07</u>	0.88	5.81	2.43	0.25
3	<u>11.22</u>	3.23	<u>9.91</u>	-0.93	9.68	2.05	0.31
16	<u>9.37</u>	3.26	<u>8.07</u>	0.88	5.81	2.43	0.25
3	<u>11.22</u>	3.23	<u>9.91</u>	-0.93	9.68	2.05	0.31

**Table 16: Motions and accelerations for DLC 6.2 given by OpenFAST, underlining the values out of the limits defined by the design bases.**

As shown in Table 16, the values of maximum Pitch and Yaw are bigger than the limits defined in Table 10. This act happened because there is an extreme situation with a return period of 50 years, so it cannot be evaluated with the values of normal operation, because it is an exceptional situation.

Despite this fact, it should be underlined that, although the extreme situation, all the mean values are into the limits, so, in general the structure performs as expected, however there will be necessary to analyze the extreme values.

## 4.2. Forces

### 4.2.1. DLC 1.1.

LC	Max Line Tension [kN]	Max Fairlead Tension [kN]	Max Anchor Tension [kN]	Max Tower Base MomentXY [kN·m]
36	4947.97	4076.63	6963.05	560717.90
36	4294.21	4077.85	7217.94	522772.85
13	4294.21	4077.85	7217.94	522772.85
36	4947.97	4076.63	6963.05	560717.90

Table 17: Tension in DLC 1.1, given by OpenFAST.

### 4.2.2. DLC 1.2.

LC	Max Line Tension [kN]	Max Fairlead Tension [kN]	Max Anchor Tension [kN]	Max Tower Base MomentXY [kN·m]
75	4950.86	4295.76	7266.66	602989.10
66	4843.79	4739.67	7682.86	647653.87
80	4752.27	4670.64	8037.97	734177.69
69	4315.07	3862.98	6186.11	736632.95

Table 18: Tension in DLC 1.2, given by OpenFAST.

### 4.2.3. DLC 1.3.

LC	Max Line Tension [kN]	Max Fairlead Tension [kN]	Max Anchor Tension [kN]	Max Tower Base MomentXY [kN·m]
30	5021.69	4624.45	7841.07	556219.87
30	5021.69	4624.45	7841.07	556219.87
14	5021.69	4624.45	7841.07	556219.87
15	4424.91	4171.42	6982.56	638316.04

Table 19: Tension in DLC 1.3, given by OpenFAST.

### 4.2.4. DLC 1.6.

LC	Max Line Tension [kN]	Max Fairlead Tension [kN]	Max Anchor Tension [kN]	Max Tower Base MomentXY [kN·m]
35	4685.10	3453.37	4925.14	534541.65
14	4356.42	4243.72	7105.17	723835.87
17	4320.06	4081.38	7247.45	689426.78



13	4462.44	3956.07	6879.10	808723.45
----	---------	---------	---------	-----------

Table 20: Tension in DLC 1.6, given by OpenFAST.

#### 4.2.5. DLC 6.1.

LC	Max Line Tension [kN]	Max Fairlead Tension [kN]	Max Anchor Tension [kN]	Max Tower Base MomentXY [kN·m]
6	5111.10	3795.09	6210.26	466181.97
4	4423.76	3824.32	5999.26	577022.40
5	4614.58	3817.83	6370.50	502202.00
4	4423.76	3824.32	5999.26	577022.40

Table 21: Tension in DLC 6.1, given by OpenFAST.

#### 4.2.6. DLC 6.2.

LC	Max Line Tension [kN]	Max Fairlead Tension [kN]	Max Anchor Tension [kN]	Max Tower Base MomentXY [kN·m]
3	5376.31	4890.22	7476.53	1041968.79
3	5376.31	4890.22	7476.53	1041968.79
3	5376.31	4890.22	7476.53	1041968.79
3	5376.31	4890.22	7476.53	1041968.79

Table 22: Tension in DLC 6.2, given by OpenFAST.

#### 4.2.7. Analysis

Taking into account that the object of this project is to analyze the windcrete structure, the main value of the previous tables is the value of the tower base moment.

The maximum tower base values are in the DLC 6.2, however, it will be analyzed the moment in all the structure for cases 1.6, 6.1 and 6.2 to verify the tension in each point of structure and make the de serviceability limit state design with the extreme loads (DNVGL-ST-0437 2016).

DLC 1.2. will be used to analyze also the serviceability limit state for a fatigue load with a probability of 0.01% of occurrence. Taking into account the exceptionality of this load, it will be taken the maximum value of loads for this case, in order to be conservative.

## **5. STRUCTURAL DESIGN**

### **5.1. ANALYSIS OF THE SERVICEABILITY LIMIT STATE (SLS)**

The concrete structure is constantly subjected to stresses since the moment of its construction. The higher stresses come when the structure is in service at open sea, affected by the self-weight of the structure, the wind and the water conditions. It occurs because the post-tensioning steel is centred in the section and does not create bending moment, only axial forces.

All of these conditions produce stresses and fatigue that have to be resisted by the structure, avoiding the appearance of cracks, because in a marine environment it could generate great resistance problems on the concrete, for instance, corrosion of the reinforcement, a loose of the concrete section or water leaks to the floater.

The following analysis will be made to obtain the pre-stress forces needed to avoid the problems mentioned before; defining limits on tension and compression stresses.

#### **5.1.1. Data provided**

The bending moments and the axial forces acting on the structure have been obtained with the software OpenFAST developed by NREL (National Renewable Energy Laboratory). The input data of the software is the description of the structure and the turbine, and also the description the environmental and marine conditions.

According to the standards (DNVGL 2018), there will be checked the extreme situations, which correspond to DLC 1.6, 6.1 and 6.2, and also it will be checked DLC 1.2. The envelope of bending moment of all these DLCs along the structure and the axial force corresponding to that moment is represented in the following figures:

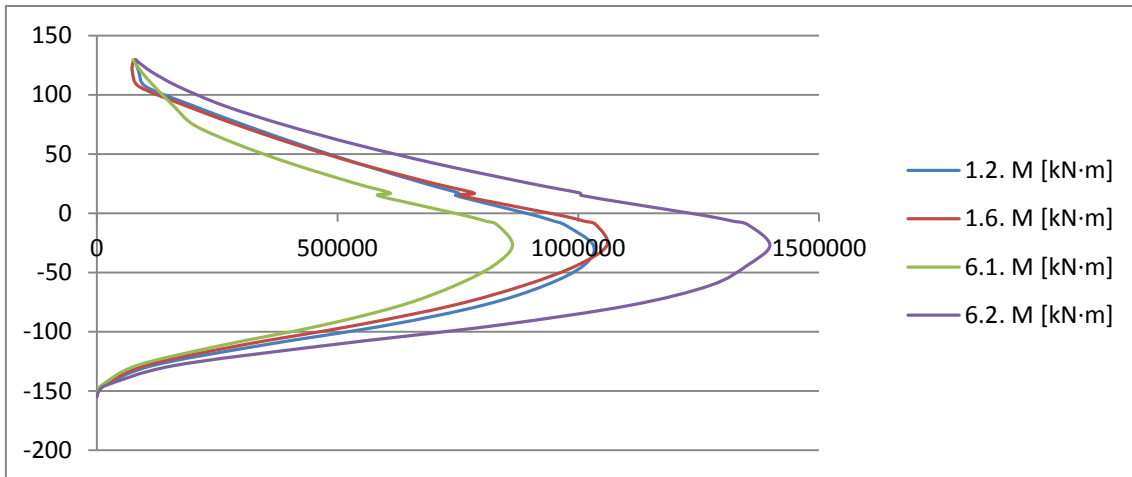


Figure 23: Diagram of bending moment due to action of wind and waves for each DLC [kN\*m].

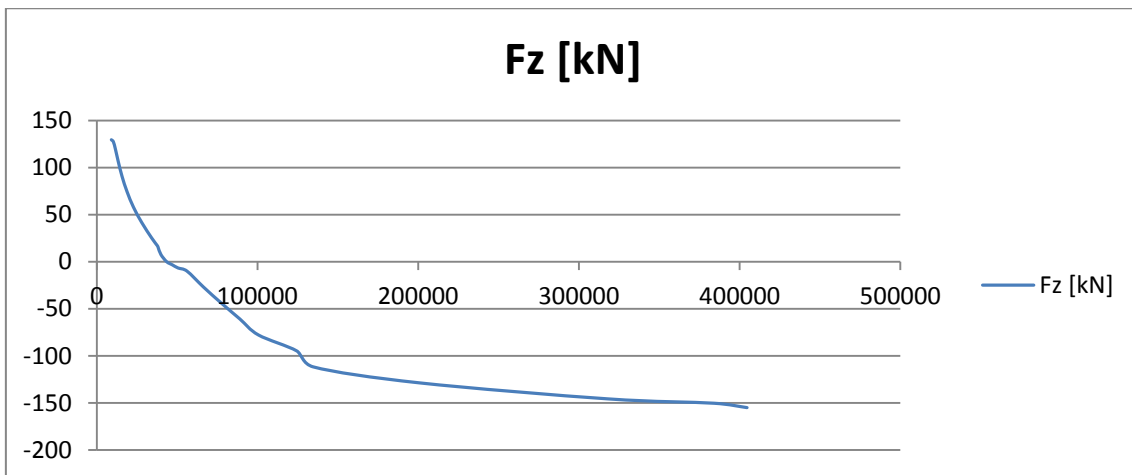


Figure 24: Diagram of axial forces due to action of wind, waves and self-weight corresponding to DLC 6.2 [kN].

The design of the structure will be done according to the Spanish code for concrete structures (EHE-08 2008). The concrete tower of the floating offshore wind turbine is 129.5 meters height. The length of the floater is 145 meters and the transition piece is 10 meters. The external radius of the floater is 9.3 meters, the external radius of the platform base is 6.6 meters, and the external radius in the top of the tower is 3.25 meters.

The tower thickness is variable, starting with a thickness of 0.5 meters at its base and finishing with a thickness of 0.28 meters in its top. And the thickness of the floater and the transition piece is 0.5 meters. These dimensions allow to locate whichever diameter of post-tensioning tendons in almost all the structure, with the exception of the top of the tower, which diameter is delimited to 10 cm in order to respect the concrete cover (chapter 5.1.4). This will be interesting, because, as shown in the previous figures, the values of the bending moment

are considerably large. In order to guaranty the buoyancy equilibrium of the structure once it is placed, there will be inside the floater a ballast column of 44.14 meters height. The whole dimensions of the structure are shown in the Figure 25:

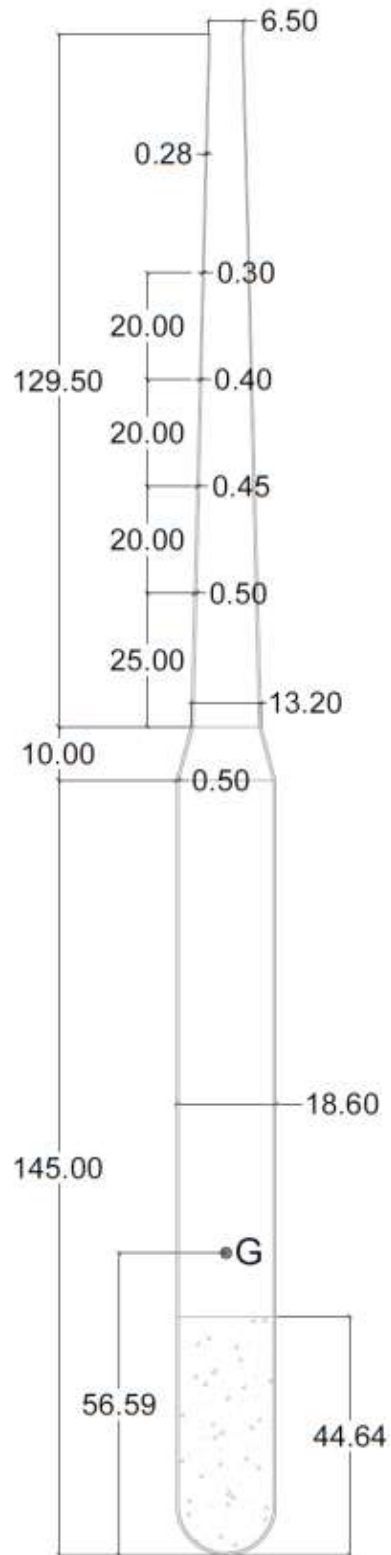


Figure 25: scheme of the structure.

### 5.1.2. Materials

The steel used for the active reinforcement is the Y-1860-S7, the steel for passive reinforcement is a B-500-S, and the concrete is a 80 MPa compression strength concrete with an exposition class IIIb-Qb.

### 5.1.3. Post-tensioning design

As said before, for making the calculations to determine the quantity of active steel needed it will be followed the EHE-08.

According to the EHE-08, the safety factors for a post-tensioning structure are the following:

	Serviceability Limit State (SLS)		Ultimate Limit State (ULS)	
	Favourable	Unfavourable	Favourable	Unfavourable
Permanent actions	$\gamma_{G,SLS} = 1.0$	$\gamma_{G,SLS} = 1.0$	$\gamma_{G,SLS} = 1.0$	$\gamma_{G,SLS} = 1.35$
Post-tensioning force	$\gamma_{G,SLS} = 0.9$	$\gamma_{G,SLS} = 1.1$	$\gamma_{G,SLS} = 1.0$	$\gamma_{G,SLS} = 1.0$

Table 23: Safety factors imposed by the EHE-08.

First of all it will be necessary to define the limits of the post-tensioning force. These limits are defined by two conditions. The first one is the non-presence of tensions larger than  $f_{ctm}$  in the whole structure, and the other is that the compressions should not be bigger than  $0.6 \cdot f_{ck}$ , because out of the boundaries defined by these limits there could appear transversal cracks, that can deteriorate the structure in less time than expected. The parameters that have influence on the value of the post-tensioning forces are the following:

- $\sigma$  [MPa]: Stress in the structure.
- $P_0$  [kN]: post-tensioning steel force.
- $N$  [kN]: axial force.
- $M$  [kN\*m]: bending moment.
- $A_c$  [mm<sup>2</sup>]: area of the concrete section.
- $W$  [m<sup>3</sup>]: section modulus.

To define the limits of the post-tensioning force, it is necessary to check the stresses in all the structure. The stresses acting in the moment of the application of post-tensioning force ( $t=0$ ), as well as also the stresses that appear in a long term states ( $t \rightarrow \infty$ ).

-  $t = 0s$

In this case, the most unfavourable situation is when the bending moment is acting on the structure, and the forces to neutralize it are the axial force and the post-tensioning force. In this case, it will be assumed an immediate loose of 10% of the post-tensioning force. The first conditions to satisfy, is the no presence of tensions in all the structure, so:

$$\sigma = -\frac{0.9 * \gamma_{P,f,SLS} * P_{0,1}}{A_c} - \frac{\gamma_{G,f,SLS} * N}{A_c} + \frac{\gamma_{G,unf,SLS} * M}{W} \leq f_{ctm}$$

The other condition is to not pass the compression value of  $0.6f_{ck}$ , so:

$$\sigma = -\frac{0.9 * \gamma_{P,unf,SLS} * P_{0,2}}{A_c} - \frac{\gamma_{G,unf,SLS} * N}{A_c} + \frac{\gamma_{G,unf,SLS} * M}{W} \geq -0.6f_{ck}$$

-  $t \rightarrow \infty$

For long term states, the conditions to follow are the same as in the previous case, however, the assumed losses are now the 20%, so:

$$\sigma = -\frac{0.8 * \gamma_{P,f,SLS} * P_{0,3}}{A_c} - \frac{\gamma_{G,f,SLS} * N}{A_c} + \frac{\gamma_{G,unf,SLS} * M}{W} \leq f_{ctm}$$

$$\sigma = -\frac{0.8 * \gamma_{P,unf,SLS} * P_{0,4}}{A_c} - \frac{\gamma_{G,unf,SLS} * N}{A_c} + \frac{\gamma_{G,unf,SLS} * M}{W} \geq -0.6f_{ck}$$

After some operations, the next equations are obtained:

-  $t=0s$

$$P_{0,1} \geq \frac{-f_{ctm} * A_c + \frac{\gamma_{G,unf,SLS} * M * A_c}{W} - \gamma_{G,f,SLS} * N}{0.9 * \gamma_{P,f,SLS}}$$

$$P_{0,2} \leq \frac{0.6 * f_{ck} * A_c - \frac{\gamma_{G,unf,SLS} * M * A_c}{W} - \gamma_{G,unf,SLS} * N}{0.9 * \gamma_{P,unf,SLS}}$$

-  $t \rightarrow \infty$

$$P_{0,3} \geq \frac{-f_{ctm} * A_c + \frac{\gamma_{G,unf,SLS} * M * A_c}{W} - \gamma_{G,f,SLS} * N}{0.8 * \gamma_{P,f,SLS}}$$

$$P_{0,4} \leq \frac{0.6 * f_{ck} * A_c - \frac{\gamma_{G,unf,SLS} * M * A_c}{W} - \gamma_{G,unf,SLS} * N}{0.8 * \gamma_{P,unf,SLS}}$$

The limit values of  $P_0$  depend on the elastic modulus and the acting external forces. As these values are different in each point of the structure, all the results will be given in the Appendix 1.

To determine the quantity of steel needed it is necessary to know the maximum stress that the steel could support. It is given by the following formula:

$$\sigma_{p0} \leq \min(0.70 * f_{pmax,k}, 0.85 * f_{pk}) = 1302 \text{ MPa}$$

Where:

- $f_{pmax,k} [kPa] = 1860 \text{ MPa}$ : maximum characteristic unitary load.
- $f_{pk} [kPa] = \frac{f_{pmax,k}}{\gamma_s} = 1691 \text{ MPa}$  where  $\gamma_s=1.15$ : characteristic elastic limit.

Then the area of post-tensioning steel will be:

$$A_p \geq \frac{P_0}{\sigma_{p0}}$$

The total area is formed by tendons, formed by strands, which are formed by 7 wires each one. The area of the strands is 150mm<sup>2</sup> and the diameter is 15.7mm.

For placing the steel area, it will be taken into account the values previously calculated, the construction process, to minimize, as much as possible the number of operations along the structure, and the dimensions of the structure, specially the thickness in each point. In the top of the tower it will be considered 15 strands per tendon, taking into account that the thickness in that point is 0.28 metres. The tendons will be able to carry 15 strands per tendon, with an external diameter of 9.5 cm (MK4 2010). When the thickness of the tower increases, there will be placed 34 strands per tendon. The tendons will be able to carry 37 strands each one, with an external diameter of 13.7 cm (MK4 2010). Giving a maximum number of tendons, in the most solicited section of 96, and in less solicited sections of 64, in the top of the tower, and 16, in the base of the floater, which values of post-tensioning forces are into the limits previously calculated. In Figure 26 it is shown a scheme of the amount of steel along the structure:

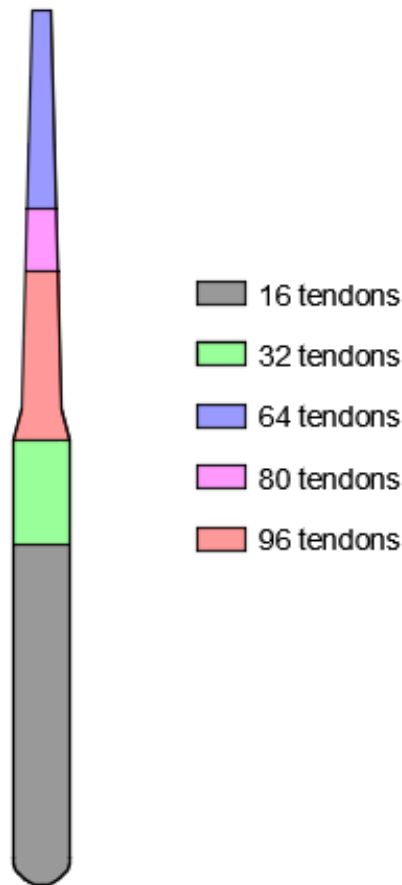


Figure 26: Quantity of Steel along the structure.

#### 5.1.4. Concrete cover

The concrete used for this system is adherent. According to the EHE-08, the concrete cover of the structure is:

$$r_{nom} = r_{min} + \Delta r$$

Where:

- $r_{nom}$  is the nominal concrete cover.
- $r_{min}$  is the minimum concrete cover.
- $\Delta r$  is the margin of the concrete cover, depending on the execution control, going from 0 to 10 mm. For being conservatives, it will be taken the value of 10mm.

To calculate the minimum concrete cover, there are some restrictions, shown in the Figure 27:



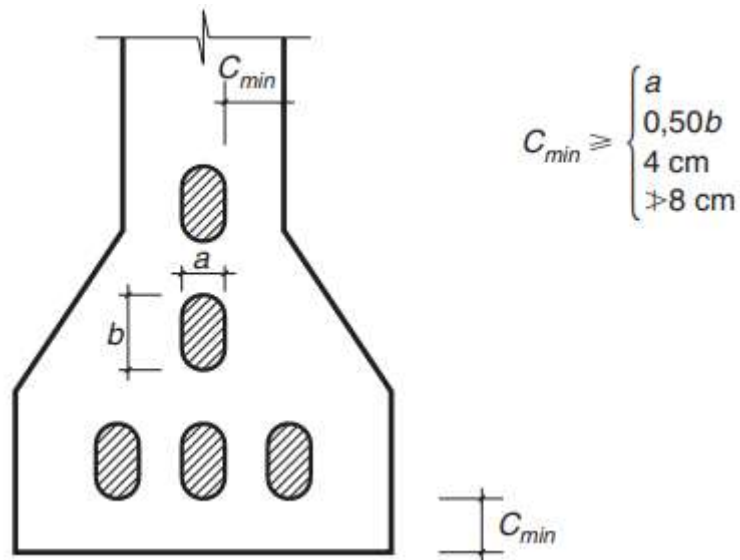


Figure 27: Limitations of the minimum concrete cover.

Taking into account that the diameter of the original tendon is approximately 14 cm, the minimum concrete cover will be 8 cm, adding the margin, nominal concrete cover will result on a 9 cm concrete cover.

So it is possible to place the designed tendon in the structure, because the margin is bigger than the nominal cover, with the exception of the top of the tower, where it has a thickness of 28 centimetres, being necessary to place a tendon of a maximum diameter of 10 cm.

### 5.1.5. Calculation of the losses

#### 5.1.5.1. *Direct losses*

##### 5.1.5.1.1. *Friction losses*

Losses produced by the contact between the tendon and the sheath. These losses depend on the position referenced by where the steel is being stressed. The angle, or the sum of the angles in the route of the tendon, the friction coefficient, and the curvature of the sheath.

$$\Delta P_1 = P_{max,o} * (1 - e^{-(\mu\Delta\theta+kx)})$$

Where:

- $\mu = 0.18$ . is the friction coefficient of the tendons composed by various elements and without superficial treatment, according to table 20.2.2.1.1.a of the EHE-08.

- $\Delta\theta$  is the sum of the angles of the route. The value oscillates between 0, 13 and 28 degrees.
- $k = 0.006 * \mu = 0.00108 m^{-1}$  is the curvature of the sheath, which diameter is bigger than 60mm.
- $x$  is the distance between the analysed section and the pace where the steel is stressed.

The Figure 28 shows the graph of the losses.

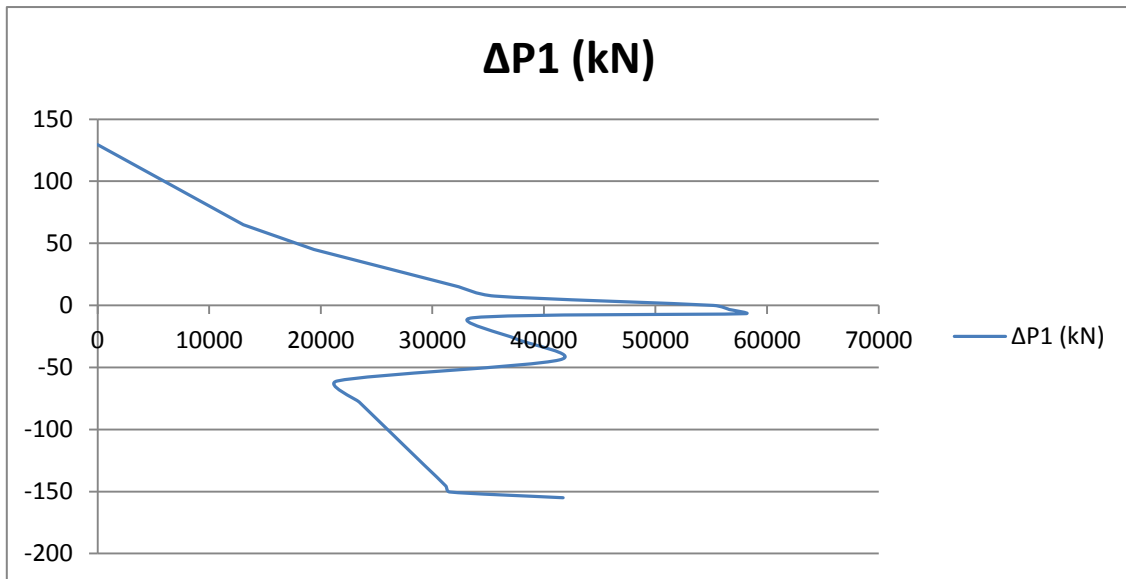


Figure 28: Friction losses of pre-stresses force along the structure.

The numerical values will be given on Appendix 1.

#### 5.1.5.1.2. Wedge Set Losses

These losses occur during anchoring operations with the penetrations of the slip of strands. They are calculated using the following formula:

$$\Delta P_2 = 2\Delta P_1(l_a)$$

Where:

$$l_a = \frac{a * E_p * A_p}{P_0 * (1 - e^{-(\mu\Delta\theta + kl_a)})}$$

Where:

- $E_p = 2.1 * 10^8 kPa$  is the Young Modulus of the steel.
- $l_a$  is the affected length of the structure.
- $a = 5mm$  is the slip of the stands.

The Figure 29 shows the graph of the losses.

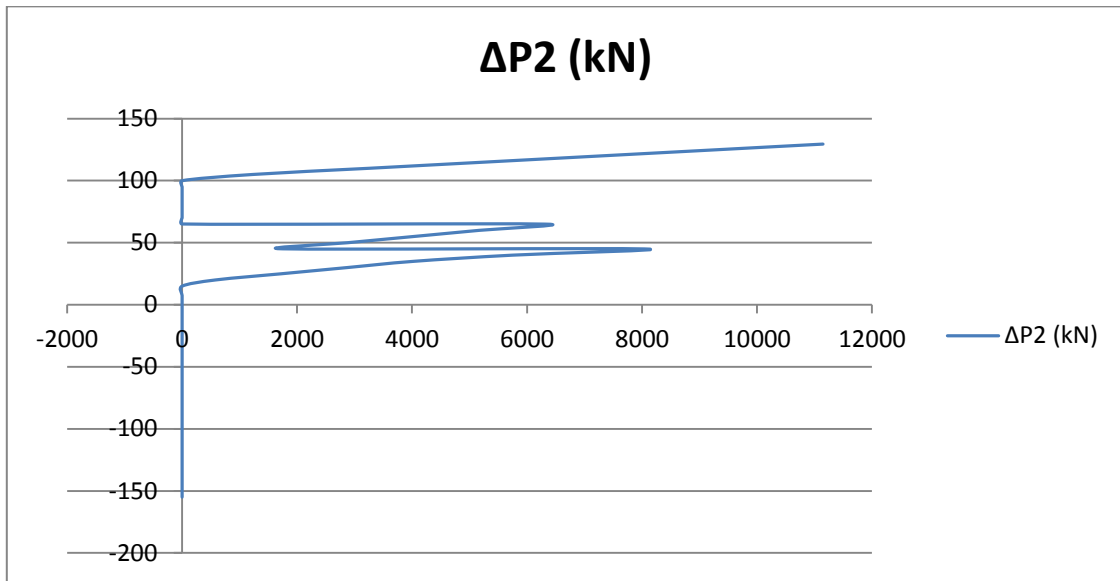


Figure 29: Wedge set losses along the structure.

The numerical values will be given on the Appendix 1.

#### 5.1.5.1.3. Elastic losses

These losses are due to the elastic shortening suffered by the concrete when it is compressed. This shortening reduces the compressive force of the steel. These losses are taken from this formula:

$$\Delta P_3 = \frac{n - 1}{2n} * \frac{E_p}{E_c} * Ap * \sigma_{cp}$$

Where:

- n is the number of operations of post-tensioning, in this case is the number of tendons, because there is only one operation of post-tensioning per tendon.
- $\sigma_{cp}$  is the stress in the steel after  $\Delta P_1$  and  $\Delta P_2$ .

The Figure 30 shows the graph of the losses.

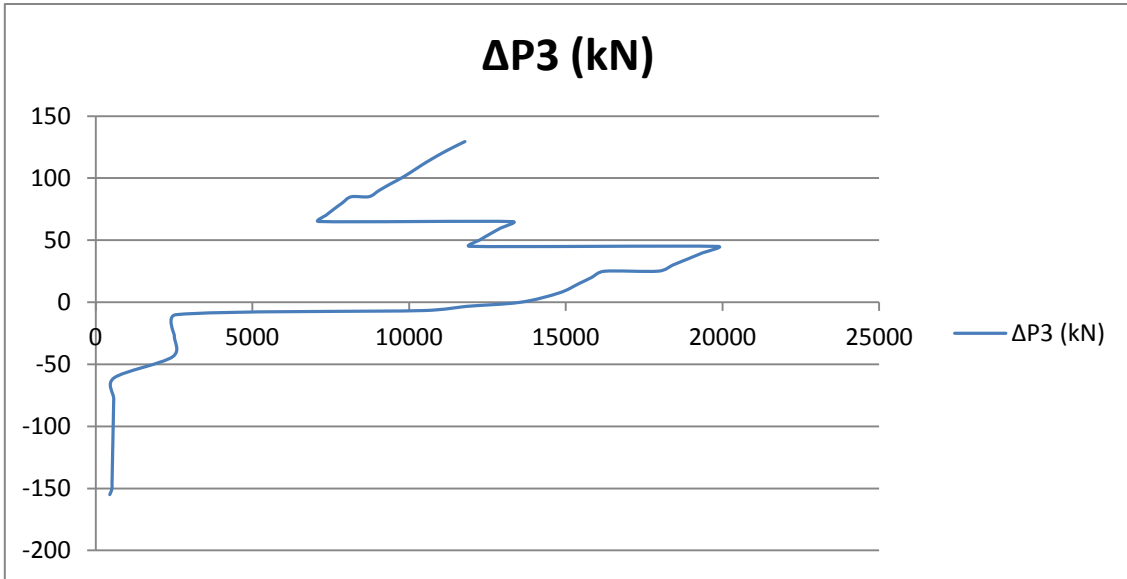


Figure 30: Elastic losses.

The numerical values will be given on the Appendix 1.

To achieve the desired values of post-tensioning force defined at the beginning the steel will be overstressed, without exceed the maximum values defined by the EHE-08 for exceptional situations of anchoring of:

$$\sigma_{p0} \leq \min(0.80 * f_{pmax,k}, 0.90 * f_{pk}) = 1456 \text{ MPa}$$

So the post-tensioning force to be introduced in the steel when anchoring to obtain the original values will be:

$$P_{0,SLS} = P_{max,0} + \Delta P_1 + \Delta P_2 + \Delta P_3$$

That new value of the post-tensioning force should also be inside the limits defined by the values of  $P_0$  maximum and minimum defined before.

#### 5.1.5.2. Time-dependent losses

There are three facts that affect these types of losses, the creep, the shrinkage and the relaxation of the concrete (EHE-08 2008).

The creep is the increase of deformation with time under a sustained constant load. The shrinkage occurs when the concrete has less water than it should, which reduces its volume without the influence of any load. Relaxation occurs when the deformation of the material remains constant, although the initial stresses have decreased.

The calculation of these losses is made by the following expression:

$$\Delta P_{dif} = \frac{n * \varphi(t, t_0) * \sigma_{cp} + E_p * \varepsilon_{cs}(t, t_0) + 0.8 * \Delta \sigma_{pr}}{1 + n * \frac{A_p}{A_c} * \left(1 + \frac{A_c * y_p^2}{I_c}\right) * (1 + \chi * \varphi(t, t_0))} * A_p$$

$$\Delta \sigma_{pr} = \rho_f * \frac{P_0 - \Delta P_1 - \Delta P_2 - \Delta P_3}{A_p}$$

Where:

- $n = \frac{E_p}{E_c}$
- $\varphi(t, t_0) = 0.775$  is the creep coefficient at infinite time (article 39.8 EHE-08).
- $\varepsilon_{cs}(t, t_0) = -1.26e^{-4}$  is the strain produced by the shrinkage of the concrete (article 39.7 EHE-08).
- $\chi = 0.8$  age coefficient.

The Figure 31 shows the graph of the losses.

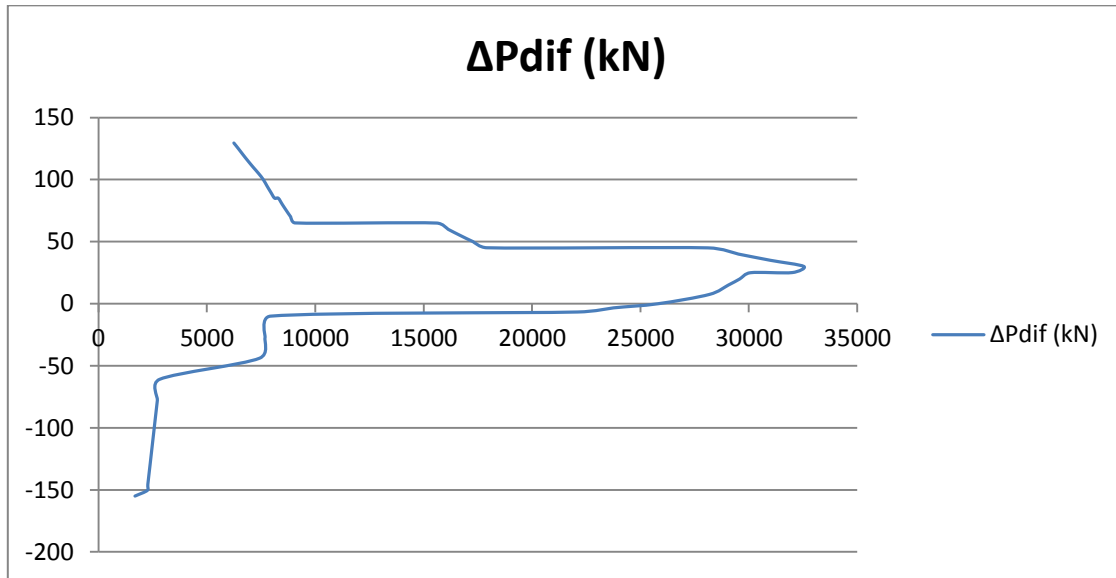


Figure 31: Time-dependent losses.

The numerical values will be given on the Appendix 1.

At the end, the post-tensioning force is represented in the Figure 32:

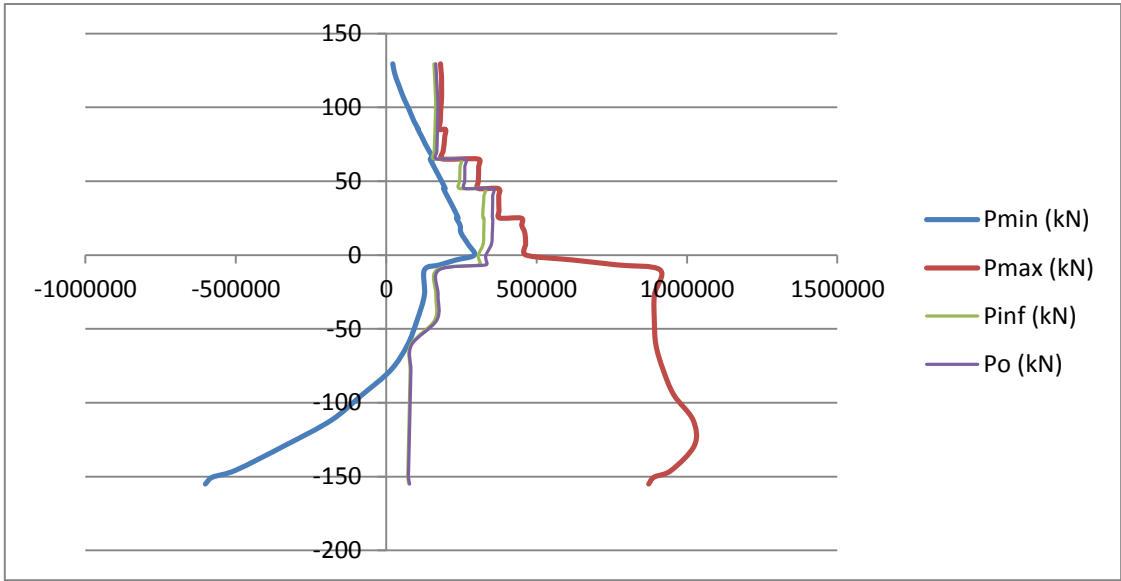


Figure 32: Initial and final post-tensioning forces, and limits along the structure.

### 5.1.6. SLS Cracking

After designing the post-tensioning steel it will be necessary to verify if the structure cracks in any place, because if it occurs, there will be necessary a solution to avoid the situation, because the presence of cracks allows the filtration of water into concrete, generating corrosion of the reinforcement, a loose of the concrete section or water ingress to the floater.

To ensure the non-presence of cracks it is enough to ensure the non-presence of tension bigger that the tensile strength of the concrete (4.8 MPa) in any point of the structure and also to ensure that the compressive stress in the concrete will not be bigger than  $0.6 \cdot f_{ck}$ , which has a value, for 80 MPa concrete, of 48 MPa. For knowing the values of the tension, it will be followed the next expression:

$$\sigma = -\frac{\gamma_{P,f,SLS} * P_0}{A_c} - \frac{\gamma_{G,f,SLS} * N}{A_c} + \frac{\gamma_{G,unf,SLS} * M}{W} \leq f_{ctm}$$

And the values of compression:

$$\sigma = -\frac{\gamma_{P,unf,SLS} * P_0}{A_c} - \frac{\gamma_{G,unf,SLS} * N}{A_c} + \frac{\gamma_{G,unf,SLS} * M}{W} \geq -0.6f_{ck}$$

Where  $P_0$  is the post-tensioning force after losses. It will be checked the immediate situation, where  $P_0$  will be the post-tensioning force after the immediate losses, and a long-term situation, where  $P_0$  will be the post-tensioning force after time dependent losses.

There are not any tensions bigger than  $f_{ctm}$  in the structure with the proposed post-tensioning steel.

The stresses in concrete are represented in the Figure 33 showing the immediate stresses, and the time-dependent stresses. The values will be shown in the Appendix 1.

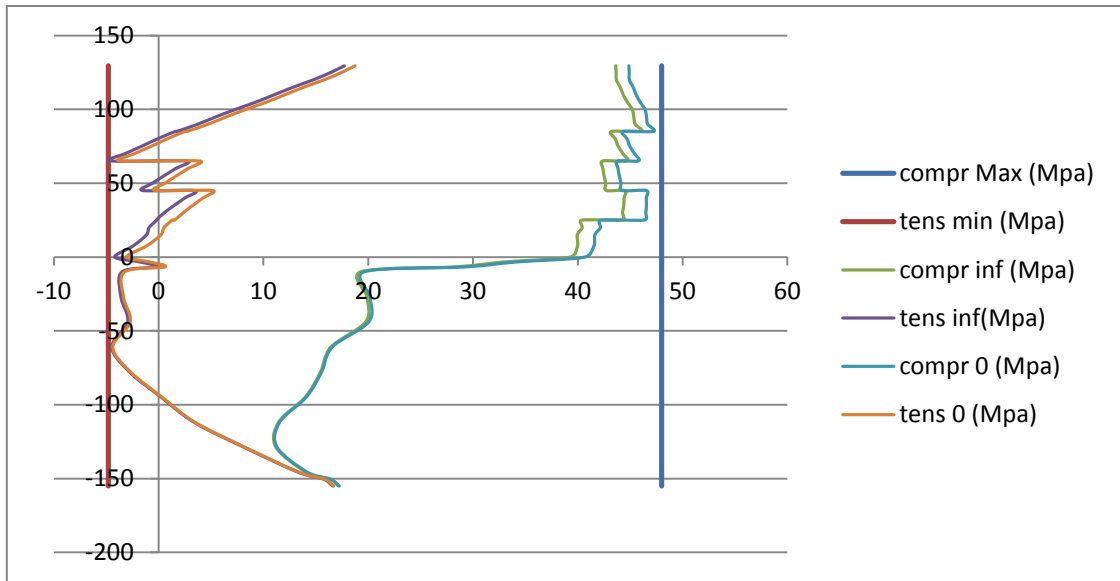


Figure 33: Tension and compression stresses



## 5.2. ANALYSIS OF COMPRESSIVE STRESSES UNDER PERMANENT LOADS

According to the standards, it should be verified that the concrete compressive stress under permanent loads should not be larger than  $0.45 \cdot f_{ck}$  (DNVGL-ST-0126 2016). The permanent loads will be the self-weight and the post-tensioning force acting on the structure, so there will not be taking into account the bending moments. To know the stresses it will be use the following formula:

$$\sigma = -\frac{\gamma_{P,unf,SLS} * P_0}{A_c} - \frac{\gamma_{G,unf,SLS} * N}{A_c} \geq -0.45 f_{ck}$$

Using the values of N and  $P_0$  defined in chapter 5.1.3 there will be verified that in any point of the structure will be compressions bigger than  $0.45 \cdot f_{ck}$ , which value, for an 80 MPa concrete, is 36 MPa.

In the Figure 34 will be represented the stresses along the structure, after immediate losses, and after time dependent losses. The results will be shown in the Appendix 1.

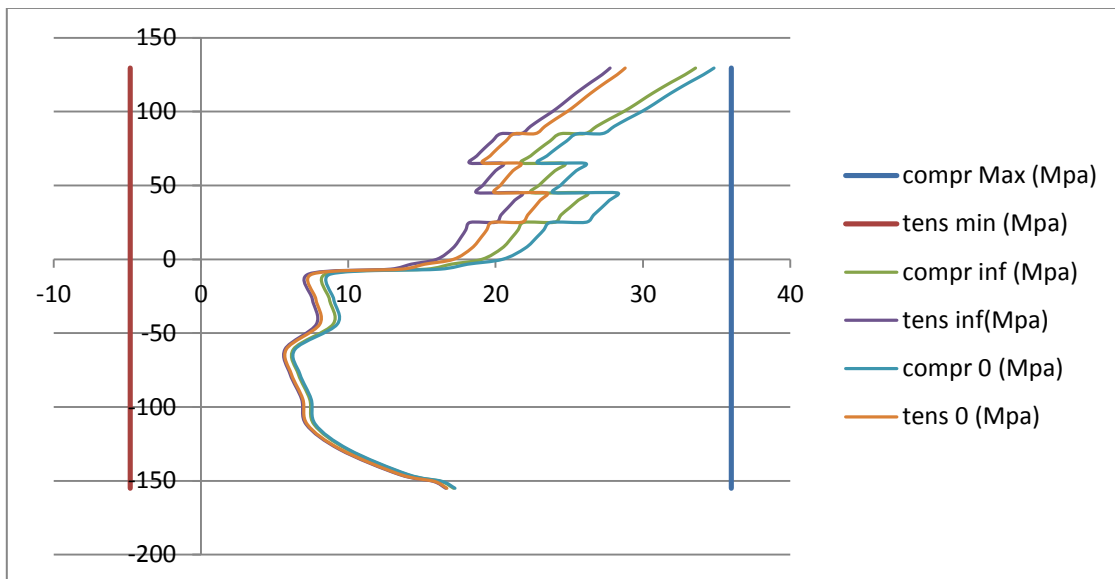


**Figure 34: Tension and compression stresses.**

### 5.3. ANALYSIS OF THE ULTIMATE LIMIT STATE (ULS)

#### 5.3.1. Bending moment

The Ultimate Limit State of the structure occurs when the structure collapses. It is assumed that it will happen due to bending moment, because is the most relevant force. So it should be checked that the design bending moment is smaller than the ultimate bending moment:

$$M_{Ed} \leq M_{Rd}$$

For knowing the value of the design bending moment it will be used the coefficients of Table 23 unfavourable actions, so:

$$M_{Ed} = M * \gamma_{G,unf,ULS}$$

Where:

- $M$  is the bending moment of provided data.
- $\gamma_{G,unf,ULS} = 1.35$ .

There are different conditions for each section of the structure, so it will be analysed each section to verify the previous condition.

Taking into account that the transversal section of the structure is a circular hollow section it is necessary to calculate the concrete compressive height, required to compute the resistance moment. The first step is the equilibrium of external and internal forces in the structure, as shown in the following figure:

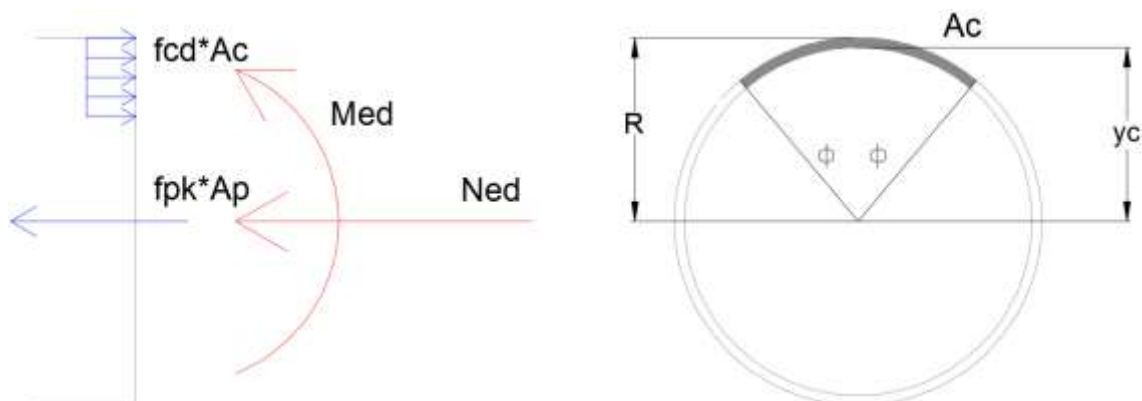


Figure 35: scheme of forces.

For making the analysis of the ULS, it should be done the equilibrium of forces, and according to the previous scheme, the equilibrium of forces is:

$$\sum F = 0$$

$$N_{Ed} + f_{pk} * A_p = f_{cd} * A_c$$

Where:

$$- N_{Ed} = N_i * \gamma_{G,unf,ULS}$$

After computing this equation it has reached the value of  $A_c$ , which is the value of the concrete compressive area. These values will be shown in the Appendix 1. After knowing the compressive area, it will be simple to know the angle  $\phi$ , just by a proportion between areas, and multiplying these values by  $\pi$  radians.

With this value, to know the distance between the centre of masses of the section, and the centre of masses of the compressive area it will be used the following formula:

$$y_c = \frac{R * \text{sen}(\phi)}{\phi}$$

And also it is possible to know the total compressive force made by the section:

$$N_c = A_c * f_{cd}$$

Finally, for equilibrium, the ultimate resistance moment is calculated using the following expression:

$$M_u = y_c * N_c$$

The values of the ultimate moment will be shown in the Appendix 1. After all this calculations, it has been verified the first condition in all the section, so it will not be necessary passive reinforcement to support the bending moment, although it will be paced minimum reinforcement to fulfil the condition of reinforcement concrete.

### 5.3.1.1. Passive reinforcement

The minimum geometric reinforcement is defined in the article 42.3.5 of the EHE-08.

Tipo de elemento estructural		Tipo de acero	
		Aceros con $f_y = 400 \text{ N/mm}^2$	Aceros con $f_y = 500 \text{ N/mm}^2$
Pilares		4,0	4,0
Losas <sup>(1)</sup>		2,0	1,8
Forjados unidireccionales	Nervios <sup>(2)</sup>	4,0	3,0
	Armadura de reparto perpendicular a los nervios <sup>(3)</sup>	1,4	1,1
	Armadura de reparto paralela a los nervios <sup>(3)</sup>	0,7	0,6
Vigas <sup>(4)</sup>		3,3	2,8
Muros <sup>(5)</sup>	Armadura horizontal	4,0	3,2
	Armadura vertical	1,2	0,9

Figure 36: minimum reinforcement in ‰.

The structure has been considered as a wall with passive steel whose elastic limit is 500MPa. So the minimum reinforcement will be the 3.2‰ of the concrete area in horizontal steel and 0.9‰ in vertical reinforcement. That results on a minimum horizontal reinforcement area of 16 cm<sup>2</sup>/m and a vertical reinforcement area of 4.5 cm<sup>2</sup>/m.

It is necessary also to determine the minimum mechanic reinforcement which follows the following formula according to 42.3.2 of the EHE-08:

$$A_s \geq 0.04 * A_c * \frac{f_{cd}}{f_{yd}}$$

This gives a minimum reinforcement of 24.53 cm<sup>2</sup>/m, in both directions, longitudinal and circumferential.

With these values, it will be placed, two lines of Ø20//0.250, one in the outer face, and the other in the inner face, resulting on an area of 25.14 cm<sup>2</sup>/m except in the top of the tower, where will be placed two lines of Ø16//0.150, obtaining an area of 26.80 cm<sup>2</sup>/m. This reinforcement should be checked in Ultimate Limit State for shear force.

According to 37.2.4 of the EHE-08, the concrete cover for the passive reinforcement should be, at least 10+40mm, taking into account the exposition class (IIIb) and the fact that is not an element built in situ.

### 5.3.2. Shear force

For checking the capacity of the structure to shear force it should be satisfied these both conditions:

$$V_{Rd} \leq V_{u1}$$

$$V_{Rd} \leq V_{u2}$$

Where  $V_{Rd}$  is the shear force acting on the structure,  $V_{u1}$  is the compressive force which makes the web fails, and  $V_{u2}$  is the tension force which makes the web fails.

$V_{u1}$  is obtained following the article 44.2.3.1 of the EHE-08, using the following formula:

$$V_{u1} = k * f_{1cd} * b_0 * d * \frac{\cot g \theta + \cot g \alpha}{1 + \cot g^2 \theta}$$

Where:

- $f_{1cd} = \left(0.9 - \frac{f_{ck}}{200}\right) * f_{cd} \geq 0.5 * f_{cd}$
- $b_0$  is the base of the element, without the tendons of post-tensioning steel.
- $K$  Is a coefficient deppendin of the axial force:
  - $K = 1.00$  for structures without post-tensioning steel of without compression forces.
  - $K = 1 + \frac{\sigma'_{cd}}{f_{cd}}$  for  $0 < \sigma'_{cd} \leq 0.25 * f_{cd}$
  - $K = 1.25$  for  $0.25 * f_{cd} < \sigma'_{cd} \leq 0.5 * f_{cd}$
  - $K = 2.5 * \left(1 - \frac{\sigma'_{cd}}{f_{cd}}\right)$  for  $0.5 * f_{cd} < \sigma'_{cd} \leq 1 * f_{cd}$
  - Where:
    - $\sigma'_{cd} = \frac{N_d - A_s' * f_{yd}}{A_c}$
- $\alpha$  angle between the reinforcement and the axis of the structure.
- $\theta$  angle of the compression struts.

$V_{u2}$  is obtained according to the article 44.2.3.2.2 of the EHE-08, using the following expression:

$$V_{u2} = V_{cu} + V_{su}$$

Where:

- $V_{su}$  is the contribution of the transversal reinforcement, and it follows the next expression:

$$V_{su} = z * sen\alpha * (cotg\alpha + cotg\theta) * \sum A_{\alpha} * f_{y\alpha,d}$$

Where:

- $A_{\alpha}$  is the area of transversal reinforcement.
- $z = \frac{M_d + N_d * z_0 - U'_s * (d - d')}{N_d + U_s - U'_s}$

Where:

- $U_s = A_s * f_{yd}$
- $d$  is the distance between the most compressive fiber and the center of gravity of the longitudinal reinforcement.
- $V_{cu}$  is the contribution of the concrete to resist the shear force, and it will be calculated with the following expression:

$$V_{cu} = \max \left( \left( \frac{0.15}{\gamma_c} * \xi * (100 * \rho_l * f_{cv})^{\frac{1}{3}} + 0.15 * \sigma'_{cd} \right) * \beta * b_0 * d; \left( \frac{0.075}{\gamma_c} * \xi^{\frac{3}{2}} * f_{cv}^{\frac{1}{2}} + 0.15 * \sigma'_{cd} \right) * b_0 * d \right)$$

Where:

- $f_{cv}=15$  MPa is the effective shear strength of the concrete.
- $\xi = \left( 1 + \sqrt{\frac{200}{d}} \right) < 2.0$

The values of the shear strength for the minimum reinforcement will be given in the Appendix 1.

In the following figure there is a scheme of the reinforcement:

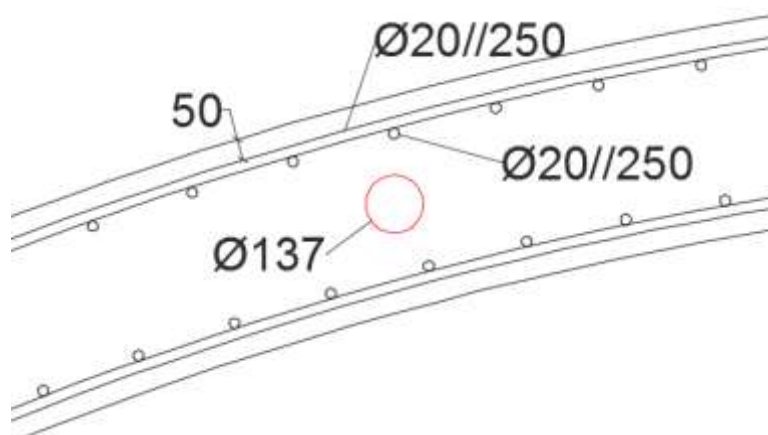


Figure 37: Scheme of the longitudinal active (red) and passive (black) reinforcement.

### 5.3.3. Torsion

For checking the torsional capacity of the structure it should be satisfied these conditions (EHE-08 2008):

$$T_d \leq T_{u1}$$

$$T_d \leq T_{u2}$$

$$T_d \leq T_{u3}$$

Where  $T_d$  is the torsional moment of design,  $T_{u1}$  is the maximum torsional moment resisted by the compressive struts of the concrete,  $T_{u2}$  is the maximum torsional moment resisted by the transversal reinforcement, and  $T_{u3}$  is the maximum torsional moment resisted by the longitudinal reinforcement.

$T_{u1}$  is obtained following the article 45.2.2.1 of the EHE-08, using the following expression it will be shown the calculations for the most critical section, which is the top of the tower:

$$T_{u1} = 2 * K * \alpha * f_{1cd} * A_e * h_e * \frac{\cot g \theta}{1 + \cot g^2 \theta}$$

Where:

- $f_{1cd} = (0.9 - f_{ck}/200) * f_{cd} \geq 0.5 * f_{cd} = 26.67 \text{ MPa}$  is the compressive strength of concrete.
- $K$  is a coefficient depending of axial force.
  - $K = 1.00$  for structures without post-tensioning steel of without compression forces.
  - $K = 1 + \frac{\sigma'_{cd}}{f_{cd}}$  for  $0 < \sigma'_{cd} \leq 0.25 * f_{cd}$
  - $K = 1.25$  for  $0.25 * f_{cd} < \sigma'_{cd} \leq 0.5 * f_{cd}$
  - $K = 2.5 * \left(1 - \frac{\sigma'_{cd}}{f_{cd}}\right)$  for  $0.5 * f_{cd} < \sigma'_{cd} \leq 1 * f_{cd}$
  - Where:
    - $\sigma'_{cd} = \frac{N_d - A_s' * f_{yd}}{A_c} = 25.72 \text{ MPa} > 0.25 * f_{cd} = 13.33 \text{ MPa} \rightarrow$   
 $K = 1.25$
- $\alpha = 0.75$  because there is reinforcement in both faces of the structure.
- $\theta$  is the angle of the compression struts
- $A_e = 30.39 \text{ m}^2$  is the area defined by the mean line of the section, taking into account the section and the empty part (Figure 38).

- $h_e = \frac{A_c}{u} = 0.268$  is the relation between the area of the concrete and the perimeter.

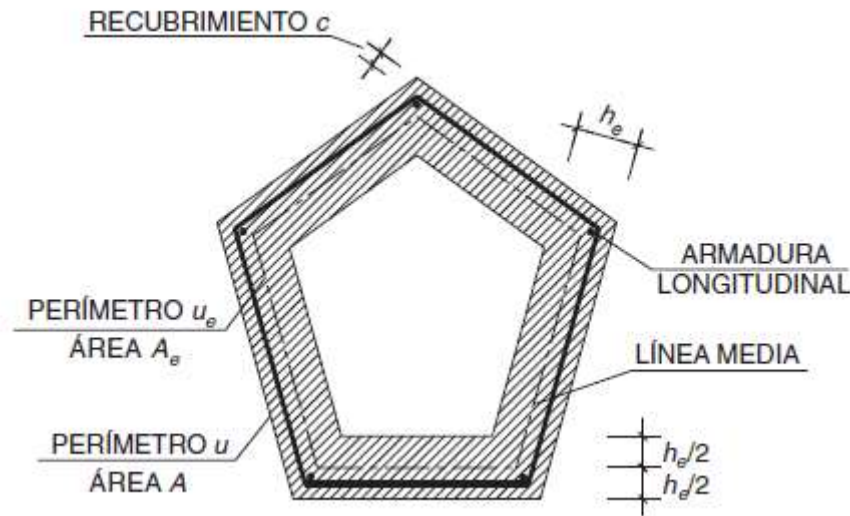


Figure 38: scheme of dimensions of a piece with torsional moment (EHE-08 2008).

$T_{u2}$  is obtained following the article 45.2.2.2 of the EHE-08, using the following expression:

$$T_{u2} = \frac{2 * A_e * A_t}{s_t} * f_{yt,d} * \cot \theta$$

Where:

- $A_t = 26.8 \text{ cm}^2/\text{m}$  is the area of the transversal reinforcement (active and passive).
- $s_t = 0.15\text{m}$  is the separation between transversal bars.
- $f_{yt,d} = \frac{500}{1.15} \text{ MPa}$  is the strength of the steel, being  $f_{yd}$  for passive reinforcement and  $f_{pd}$  for active reinforcement and its value should not be larger than 400 MPa.

$T_{u3}$  is obtained following the article 45.2.2.3 of the EHE-08, using the following expression:

$$T_{u3} = \frac{2 * A_e}{u_e} * A_l * f_{y1,d} * \tan \theta$$

Where:

- $A_l = 26.8 \text{ cm}^2/\text{m}$  (passive);  $A_l = 144000 \text{ mm}^2$  (active) is the area of the longitudinal reinforcement (active and passive).
- $u_e = 19.54 \text{ m}$  is the mean perimeter of the section (Figure 38).



- $f_{yl,d}$  is the strength of the steel, being  $f_{yd} = 500/1.15 \neq 400$  for passive reinforcement and  $f_{pd} = 1860/1.15 \neq 400$  for active reinforcement.

Obtaining the following values:

$$T_{u1} = 217107 \text{ kN} \cdot \text{m}$$

$$T_{u2} = 868629 \text{ kN} \cdot \text{m}$$

$$T_{u3} = 122141 \text{ kN} \cdot \text{m}$$

Being the design torsional moment 41705 kN\*m, the initial condition is fulfilled. It is also fulfilled in all the structure; so, with the reinforcement designed in the previous calculations will be enough.

The values of the torsional strength of the structure will be given in the Appendix 1.

#### 5.3.4. Interaction of forces

It will be necessary to verify the structure under the interaction of different concomitant stresses. Following the standards (EHE-08 2008), it will be verified the interaction of torsion with bending moment and axial force, and the interaction of torsion with shear force.

##### 5.3.4.1. *Torsion with Bending Moment and Axial force*

According to the article 45.3.2.1 of the EHE-08, in the zones of the structure where the bending moment generates tension, it will be determined the needed reinforcement separately. First it will be defined the reinforcement needed to support the bending moment, and then, it will be defined the reinforcement needed to support the torsional stress, and if it is bigger, it will be added to the structure. As shown in chapters 5.3.1 and 5.3.3 it will not be needed this addition of reinforcement.

In the compressive zone, it will be checked if there is necessary more reinforcement to support the compressive strength generated by the bending moment, axial force and the torsional moment. This quantity of reinforcement will be calculated following this expression (EHE-08 2008):

$$\rho_l * f_{yd} = \sigma_{md} - \alpha * f_{cd} * \left( 0.5 + \sqrt{0.25 - \left( \frac{\tau}{\alpha * f_{cd}} \right)^2} \right) \geq 0$$

Where:

- $\rho_l$  is the quantity of extra reinforcement needed.
- $\sigma_{md}$  is the compressive stress in concrete generated by the bending moment and axial force concomitant with torsion. In the most critical section it has de value of 17.53 MPa.
- $\tau = \frac{T}{2 * A_e * h_e}$  is the tangential stress generated by torsion. In the most critical section it has the value of 3.9 MPa.
- $\alpha = 0.75$
- $f_{cd} = \frac{f_{ck}}{1.5} = 53.33 \text{ MPa}$ .
- $f_{yd} = 400 \text{ MPa}$

So, with the previous values:

$$\rho_l * f_{yd} = -22.08$$

Being negative, it means that it will not be necessary extra reinforcement. Taking into account that it is the most critical section, it will not be necessary extra reinforcement in any section.

The values will be given in the Appendix 1.

#### 5.3.4.2. *Torsion with shear force*

According to EHE-08, the interaction of torsion and shear force should not generate excessive compressions in the concrete. According to the article 45.3.2.2 to verify this condition it should be satisfied the following expression:

$$\left(\frac{T_d}{T_{u1}}\right)^\beta + \left(\frac{V_d}{V_{u1}}\right)^\beta \leq 1$$

Where:

- $\beta = 2 * \left(1 - \frac{h_e}{b}\right)$
- $b$  is the thickness of the web, in this case will be two times the thickness of the structure.

In the most critical section, the value of  $b$  is 0.56 metres, the value of  $\beta$  is 1.043, so the value of the expression will be 0.57, which is less than one, so the condition is fulfilled to the most critical section, so, in consequence it is also fulfilled in all the structure.

The values will be given in the Appendix 1.

#### 5.4. ANALYSIS OF THE CONSTRUCTION PROCESS

Taking into account the dimensions of the structure, it will be necessary to analyse it during the construction process, especially when it is placed in horizontal position, simply supported in the bottom of the structure in four symmetrical points. It will be shown the calculation of the section of the floater, which is the ones that presents bigger tensions; however, at the end it will be presented the results and the reinforcement in each section of the windcrete.

The analysis of the structure will be made by the software Robot Structural Analysis, taking into account the self-weight and considering the structure simply supported in four radial points and a simply support in its vertical symmetrical axis to avoid the rotation (Figure 39).

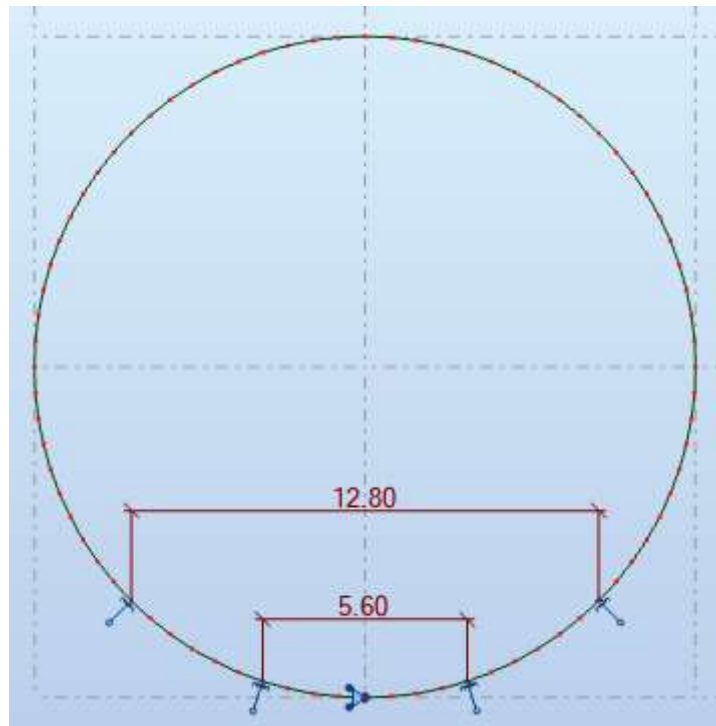


Figure 39: Model of the structure made by Robot.

With these boundary conditions, the structure will be analysed in ULS and SLS under the action of the self-weight.

#### 5.4.1. Ultimate Limit State (ULS)

According to the EHE-08, for the ULS it should be considered a safety factor of 1.35 for the self-weight acting of the structure. According to these conditions, the internal forces given by Robot are shown in the following figures:

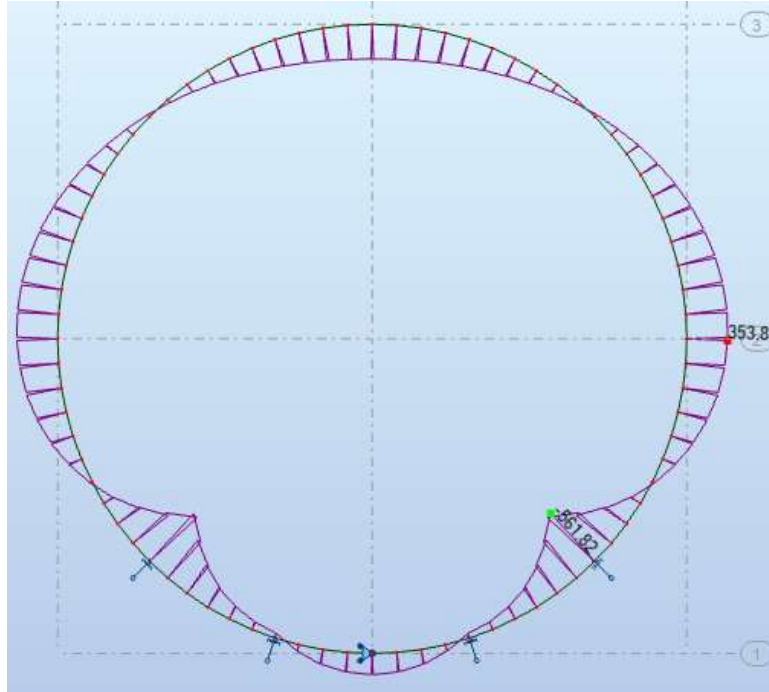


Figure 40: Bending moment diagram.

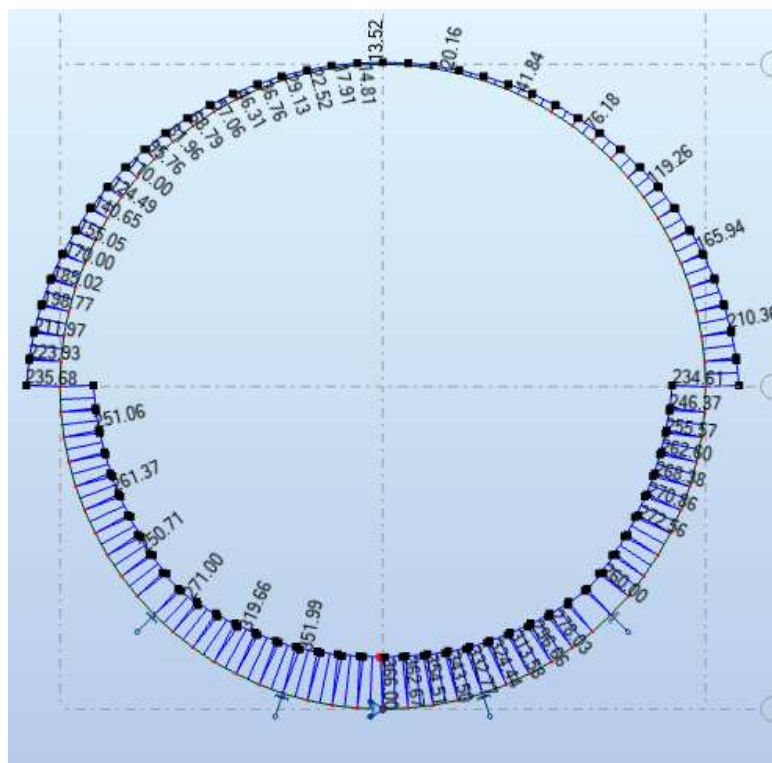


Figure 41: Axial forces.

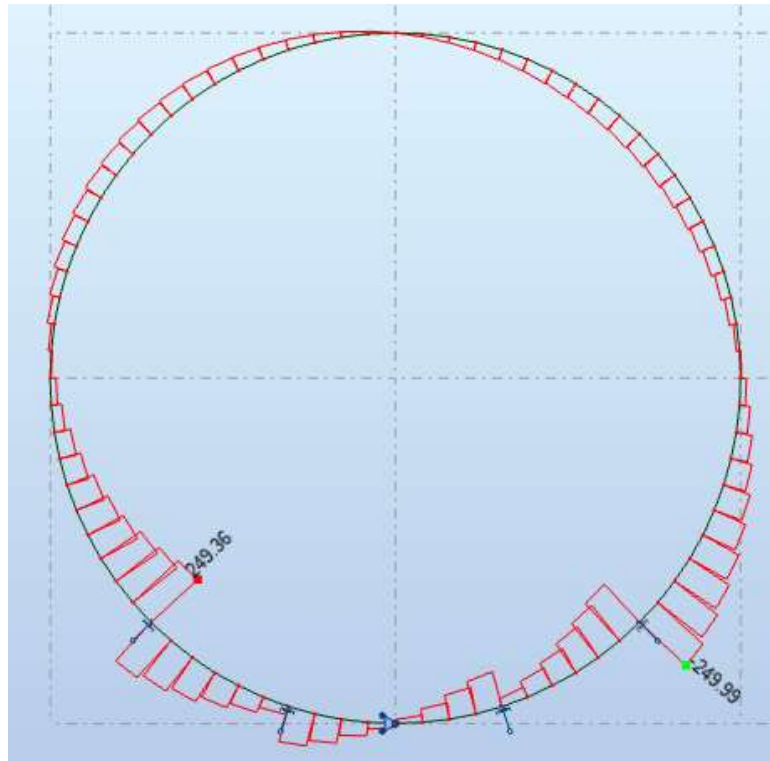


Figure 42: Shear forces.

#### 5.4.1.1. Bending Moment

As shown in the previous figures, the worst section, according to the bending moment is the section between supports, having a bending moment of 561.82 kN·m. In this zone it is also acting an axial force of 249.58 kN. This axial force is favourable to resist the bending moment acting on the structure, because it is a compression. To analyse and determine the reinforcement needed it will be followed the Eurocode 2 (EC-2 2010) method, using the following scheme:

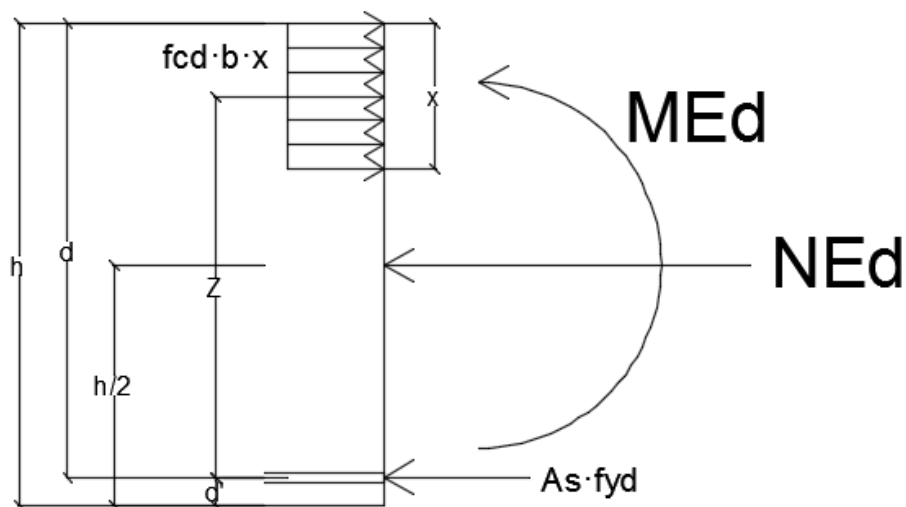


Figure 43: Scheme of equilibrium of forces.

Making the equilibrium of forces it will be obtained the following expression:

$$f_{cd} * b * x = N_{Ed} + A_s * f_{yd} + A_p * f_{pd}$$

Where:

- b is the base of the structure, it will be considered as 1000 mm.
- x is the size of the compressive zone of the concrete.
- $f_{cd}=f_{ck}/1.5$ .
- $f_{yd}=f_{yk}/1.15$ .
- $f_{pd}=f_{pk}/1.15$ .

In this equations, the unknown values are x and the area of reinforcement, so it will be necessary another equation to determine. This equation will be the equation of the resistant bending moment:

$$M_{Rd} = A_s * f_{yd} * z_y + A_p * f_{pd} * z_p + N_{Ed} * \left(\frac{h}{2} - \frac{x}{2}\right)$$

Where:

- $z_y = d_y - \frac{x}{2}$
- $d_y = h - c = 450mm$
- $z_p = d_p - \frac{x}{2}$
- $d_p = h - c - \phi = 430mm$
- $M_{Rd} \geq 561.82 \text{ kN} \cdot \text{m}$
- $N_{Ed} = 249.58 \text{ kN}$

After an iterative process, it will be computed a value of x of 127.95mm and a needed reinforcement area of 0 cm<sup>2</sup>/m, so it will be placed the minimum reinforcement of Ø20//0.250, obtaining an area of 12.57 cm<sup>2</sup>/m, and a resistant bending moment of 1378.7721 kN·m. In the top of the tower, taking into account the thickness, it will be placed Ø16//0.150, obtaining an area of 13.40 cm<sup>2</sup>/m

#### 5.4.1.2. Shear force

For checking the capacity of the structure to shear force it should be satisfied these both conditions:

$$V_{Rd} \leq V_{u1}$$

$$V_{Rd} \leq V_{u2}$$

Where  $V_{Rd}$  is the shear force acting on the structure (249.99 kN),  $V_{u1}$  is the compressive force which makes the web fails, and  $V_{u2}$  is the tension force which makes the web fails.

$V_{u1}$  is obtained following the article 44.2.3.1 of the EHE-08, using the following formula:

$$V_{u1} = k * f_{1cd} * b_0 * d * \frac{\cot g \theta + \cot g \alpha}{1 + \cot g^2 \theta}$$

Where:

- $f_{1cd} = \left(0.9 - \frac{f_{ck}}{200}\right) * f_{cd} \geq 0.5 * f_{cd} = 26.67 \text{ MPa}$
- $b_0$  is the base of the element, without the tendons of post-tensioning steel.
- $K$  Is a coefficient dependin of the axial force:
  - $K = 1.00$  for structures without post-tensioning steel of without compression forces (in this case, it is the value used).
  - $K = 1 + \frac{\sigma'_{cd}}{f_{cd}}$  for  $0 < \sigma'_{cd} \leq 0.25 * f_{cd}$
  - $K = 1.25$  for  $0.25 * f_{cd} < \sigma'_{cd} \leq 0.5 * f_{cd}$
  - $K = 2.5 * \left(1 - \frac{\sigma'_{cd}}{f_{cd}}\right)$  for  $0.5 * f_{cd} < \sigma'_{cd} \leq 1 * f_{cd}$
  - Where:
    - $\sigma'_{cd} = \frac{N_d - A_s' * f_{yd}}{A_c}$
- $\alpha = 90$  angle between the reinforcement and the axis of the structure.
- $\theta$  angle of the compression struts ( $\cot g \theta = 2$ ).

The final value of  $V_{u1}$  is 4800 kN.

$V_{u2}$  is obtained according to the article 44.2.3.2.1.2 of the EHE-08, taking into account that there is not shear reinforcement in this section, using the following expression:

$$V_{u2} = \frac{0.18}{\gamma_c} * \xi * (100 * \rho_l * f_{cv})^{\frac{1}{3}} + 0.15 * \sigma'_{cd} * b_0 * d$$

With a minimum value of:

$$V_{u2} = \frac{0.075}{\gamma_c} * \xi^{\frac{2}{3}} * f_{cv}^{\frac{1}{2}} + 0.15 * \sigma'_{cd} * b_0 * d$$

Where:

- $f_{cv} = f_{ck}$  is the effective strength of the concrete in front of shear forces.
- $\xi = \left(1 + \sqrt{\frac{200}{d}}\right) = 1.66 < 2.0$

- $\sigma'_{cd} = \frac{N_d}{A_c} = 7.86 \text{ MPa} < 0.3 * f_{cd} \approx 12 \text{ MPa}$  Taking into account the external axial force and the post-tensioning axial force (chapter 5.4.2.2).
- $\rho_l = \frac{A_s + A_c}{b_0 * d} = 0.0126 \leq 0.02$  is the geometric quantity of active and passive reinforcement.

The final value of  $V_{u2}$  is 525.72 kN, with a minimum value of 473.15 kN, both bigger than  $V_{Rd}$ .

#### 5.4.2. Serviceability limit state (SLS)

Taking into account that the structure will be used in a marine environment, it will be necessary to don't have any crack, so with the reinforcement defined in the previous chapter it will be checked the crack size, and if it is bigger than 0, it will be necessary to place some post-tensioning steel.

To know if the structure will have cracks it is necessary to know the moment of cracking, which depends on the tension capacity of the concrete. For a concrete with strength of 80 MPa, the tension capacity will be 5 MPa, according to the EC-2. So, the cracking moment will be obtained with the following expression:

$$M_{fis} = f_{ctm} * \frac{I_z}{x_{cdg}}$$

Where:

- $I_z = \frac{1}{12} * b * h^3 = 1.0417e10$
- $x_{cdg} = \frac{h}{2} = 250 \text{ mm}$

Obtaining a moment of 216.15 kN·m, which is smaller than  $M_{Ed}$ , which has de value, in SLS of 310.1 kN, so the section will crack. To determine the amount of post-tensioning steel needed it is necessary to know the maximum tension on the section, taking into account that there is not only a bending moment acting; there is also an axial force, which can be favourable in some cases. This tension will be calculated with the following formula:

$$\sigma = - \frac{\gamma_{G,f,SLS} * N_{Ed}}{A_c} + \frac{\gamma_{G,unf,SLS} * M_{Ed}}{W}$$

After testing all the sections with all the values given by Robot, the maximum tension acting on the concrete has the value of 9.62 MPa. This will be the tension that should be absorbed by the post-tensioning steel.



Taking into account that the post-tensioning steel goes parallel to the shape of the section, it will only introduce axial forces. To determine the needed steel it will be used the following expression:

$$\sigma = -\frac{\gamma_{P,f,SLS} * P_0}{A_c} - \frac{\gamma_{G,f,SLS} * N}{A_c} + \frac{\gamma_{G,unf,SLS} * M}{W} \leq 4.0 \text{ MPa}$$

It could be possible to determine the minimum  $P_0$  needed to avoid tension. It will be obtained a minimum  $P_0$  of 3121.9 kN. It is necessary to take into account that this force obtained will be the force after losses.

To start with the design of the post-tensioning steel it will be placed 22 strands per metre, taking into account that each strand will make a 198 kN force. So, the initial post-tensioning force will be  $P_0 = 4356 \text{ kN}$

#### 5.4.2.1. Immediate losses

##### 5.4.2.1.1. Friction losses

Losses produced by the contact between the tendon and the sheath. These losses depend on the position referenced by where the steel is being stressed. The angle, or the sum of the angles in the route of the tendon, the friction coefficient, and the curvature of the sheath.

$$\Delta P_1 = P_{max,o} * (1 - e^{-(\mu\Delta\theta+kx)})$$

Where:

- $\mu = 0.07$ . is the friction coefficient of the tendons composed by non-adherent elements and with lubrication, according to table 20.2.2.1.1.c of the EHE-08.
- $\Delta\theta$  is the sum of the angles of the route. The value oscillates between 0 and 180 degrees.
- $k = 0.006 * \mu = 0.00042 \text{ m}^{-1}$  is the curvature of the sheath, which diameter is bigger than 60mm.
- $x$  is the distance between the analysed section and the pace where the steel is stressed.

The value of friction losses oscillates between 0 and 901.42 kN. All the values will be shown in the Appendix 2.

#### 5.4.2.1.2. Wedge Set Losses

These losses occur during anchoring operations with the penetrations of the slip of strands. They are calculated using the following formula:

$$\Delta P_2 = 2\Delta P_1(l_a)$$

Where:

$$l_a = \frac{a * E_p * A_p}{P_0 * (1 - e^{-(\mu\Delta\theta + kl_a)})}$$

Where:

- $E_p = 2.1 * 10^8 \text{ kPa}$  is the Young Modulus of the steel.
- $l_a$  is the affected length of the structure.
- $a = 5\text{mm}$  is the slip of the stands.

With the previous values it will be obtained a  $l_a$  of 4169.45 mm, and the values of the losses will be shown in the Appendix 2.

#### 5.4.2.1.3. Elastic losses

These losses are due to the elastic shortening suffered by the concrete when it is compressed. This shortening reduces the compressive force of the steel. These losses are taken from this formula:

$$\Delta P_3 = \frac{n - 1}{2n} * \frac{E_p}{E_c} * A_p * \sigma_{cp}$$

Where:

- $n$  is the number of operations of post-tensioning, in this case is the number of tendons, because there is only one operation of post-tensioning per tendon.
- $\sigma_{cp}$  is the stress in the steel after  $\Delta P_1$  and  $\Delta P_2$ .

The value of these losses will be shown in the Appendix 2.

#### 5.4.2.2. Time dependent losses

There are three facts that affect these types of losses, the creep, the shrinkage and the relaxation of the concrete.

The creep is the increase of deformation with time under a sustained constant load. The shrinkage occurs when the concrete has less water than it should, which reduces its volume without the influence of any load. Relaxation occurs

when the deformation of the material remains constant, although the initial stresses have decreased.

The calculation of these losses is made by the following expression:

$$\Delta P_{dif} = \frac{n * \varphi(t, t_0) * \sigma_{cp} + E_p * \varepsilon_{cs}(t, t_0) + 0.8 * \Delta \sigma_{pr}}{1 + n * \frac{A_p}{A_c} * \left(1 + \frac{A_c * y_p^2}{I_c}\right) * (1 + \chi * \varphi(t, t_0))} * A_p$$

$$\Delta \sigma_{pr} = \rho_f * \frac{P_0 - \Delta P_1 - \Delta P_2 - \Delta P_3}{A_p}$$

Where:

- $n = \frac{E_p}{E_c}$
- $\varphi(t, t_0) = 0.775$  is the creep coefficient at infinite time (article 39.8 (EHE-08 2008)).
- $\varepsilon_{cs}(t, t_0) = -1.26e^{-4}$  is the strain produced by the shrinkage of the concrete (article 39.7 (EHE-08 2008)).
- $\chi = 0.8$  age coefficient.
- $y_p = 0.1425m$  is the distance between the centre of gravity of the section and the centre of gravity of the reinforcement.

The value of these losses will be shown in the APPENDIX 2. NUMERICAL RESULTS FOR CIRCUMFERENTIAL STRUCTURE.

It will be possible to see that the minimum value of post-tensioning force will be 3255.26 kN, which is bigger than the minimum value required. With this value of post-tensioning force the tension in the section will be 3.76 MPa, which is smaller than 4 MPa.

The final value of the post-tensioning steel force will be shown in the Appendix 2.

The post-tensioning steel will be placed with separated groups of two strands, taking into account that there will be non-adherent, so they will be placed in the internal face of the structure, near the passive reinforcement, because in the centre of the section will be placed the vertical reinforcement. The separation between strands will be 90 mm (Figure 44):

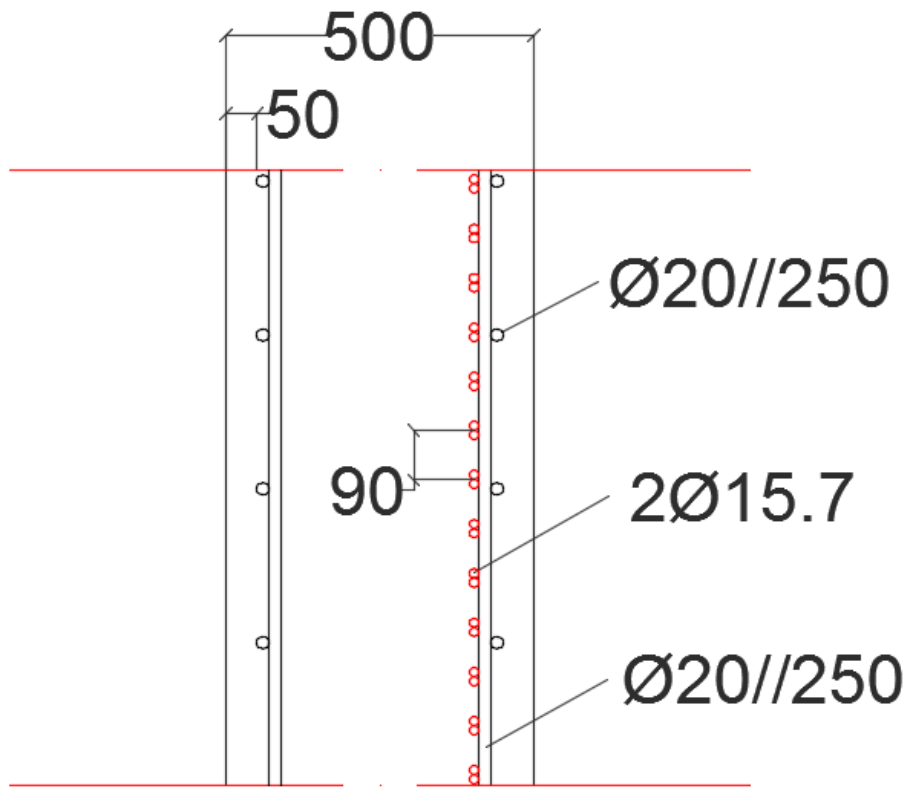


Figure 44: Scheme of the active (red) and passive (black) reinforcement.

### 5.4.3. Verification of tensions in other sections

The previous calculations for SLS will be done for every section, in order to define the needed active reinforcement to avoid the presence of cracks, and avoid using more steel than needed.

#### 5.4.3.1. Top of the tower

The concrete section in the top of the tower has a diameter of 6.5 metres and a thickness of 0.28 metres. It will be computed by Robot with radial simply supports.

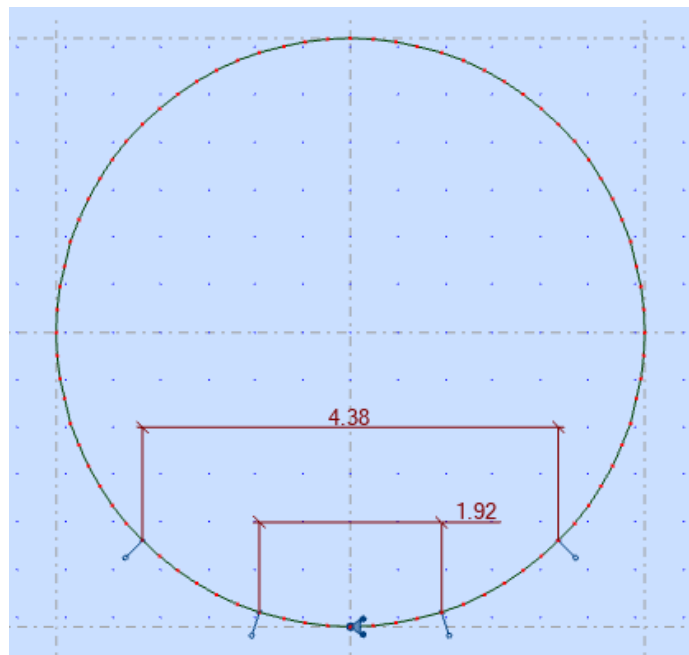


Figure 45: Model of the structure made by Robot

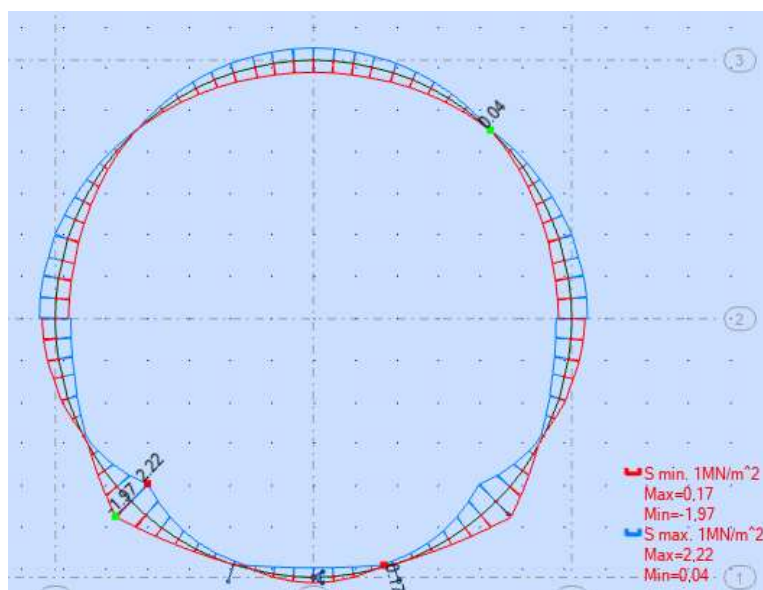


Figure 46: Tensions in the top of the tower.

As shown in Figure 46, the maximum tension in the structure is 1.97 MPa, which is smaller than 4 MPa, so there will not be needed passive reinforcement.

#### 5.4.3.2. Section of 0.28 metres thickness

The concrete section has a diameter of 8.8 metres. It will be computed by Robot with radial simply supports.

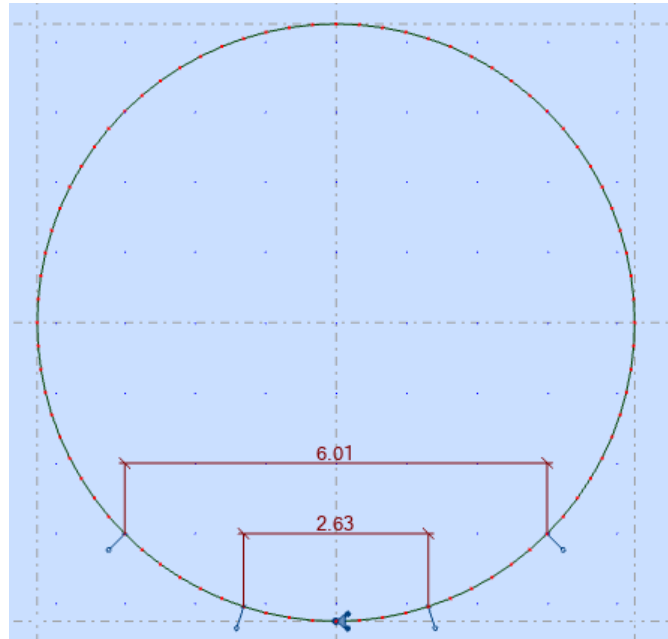


Figure 47: Model of the structure made by Robot.

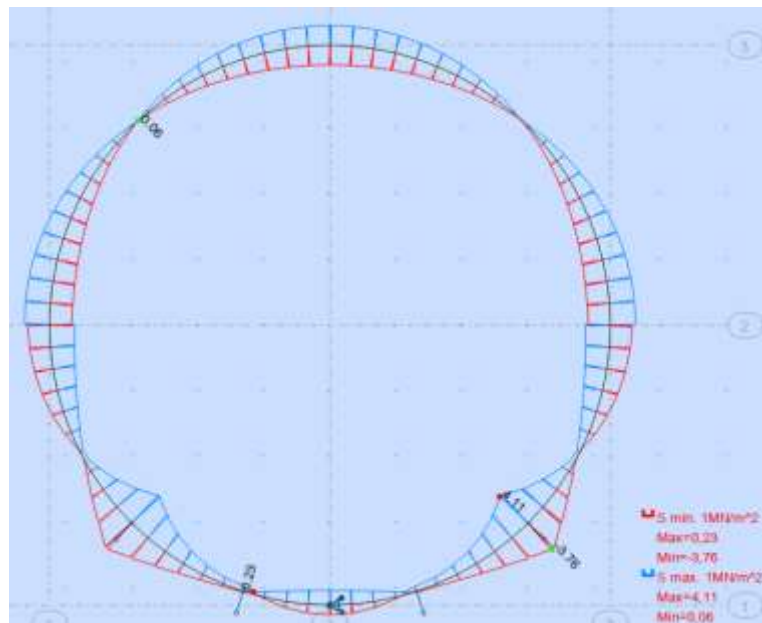


Figure 48: Tensions in the section

As shown in Figure 48, the maximum tension in the section is 3.76 MPa which is smaller than 4 MPa, so in all the 0.28 metres thickness section will not be necessary active reinforcement.

#### 5.4.3.3. Section of 0.3 metres thickness

In order to define the active reinforcement in each section, it will be chosen the biggest one for each thickness, being conservative. In this case will be analysed the section which diameter is 9.84 metres.

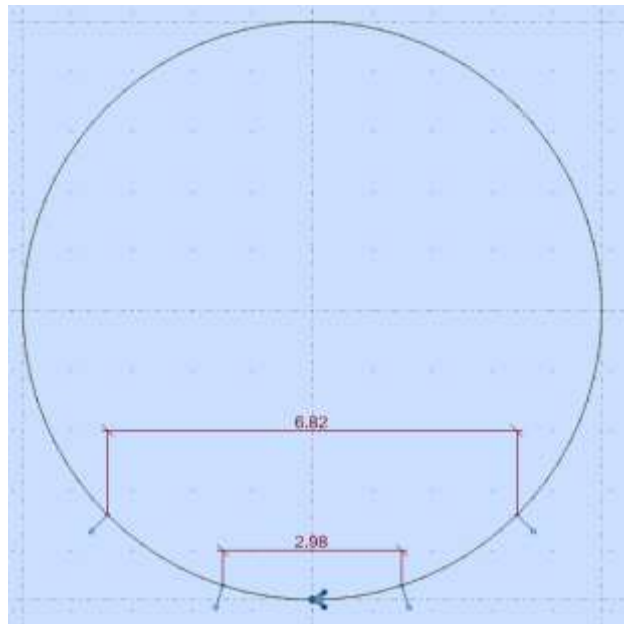


Figure 49: Model of the structure made by Robot.

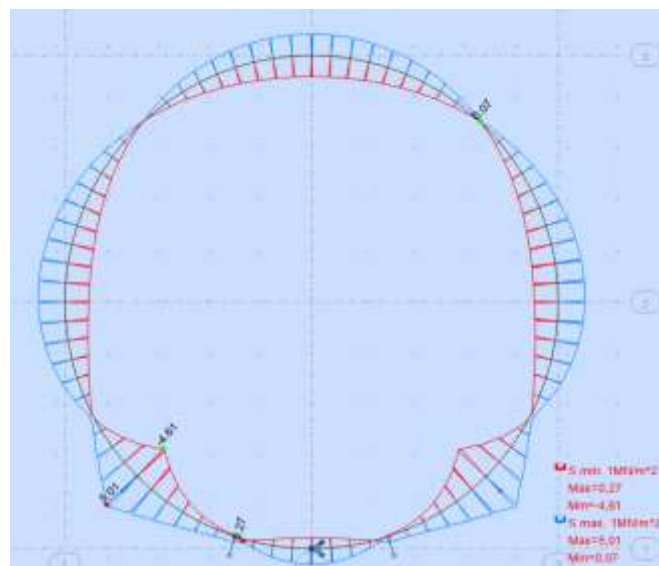


Figure 50: Tensions in the section.

As shown in Figure 50, the maximum tension in the section is 4.61 MPa, being this value bigger than 4 MPa, it will be necessary circumferential post

tensioning steel. After making the calculations shown in chapter 5.4.2 it will be placed two strands of 15.7 mm of diameter per metre of section. Giving an initial post-tensioning force of 396 kN/m and a force after losses of 307.62 kN/m, giving a final tension in the structure of 3.59 MPa. The scheme of the reinforcement in this section will be shown in the following figure:

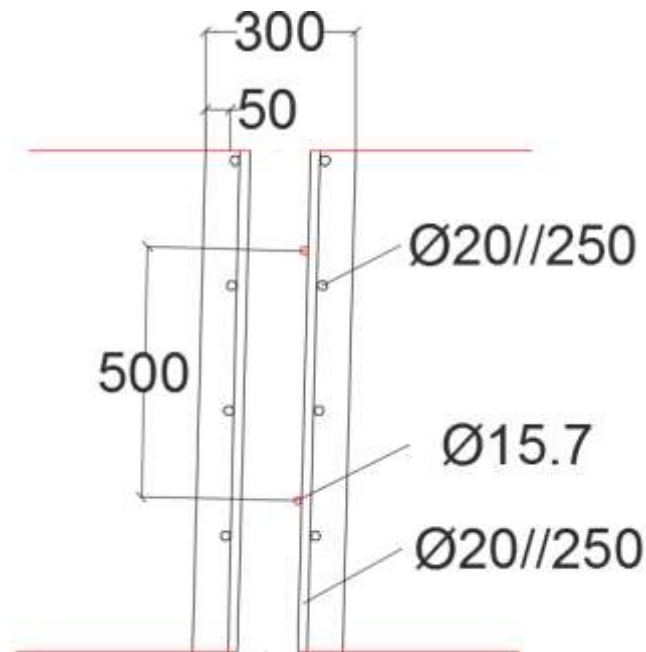


Figure 51: Scheme of the active (red) and passive (black) reinforcement.

#### 5.4.3.4. Section of 0.4 metres thickness

As in the previous case, it will be analysed the biggest section with this thickness. It corresponds to the section which diameter is 10.87 metres.



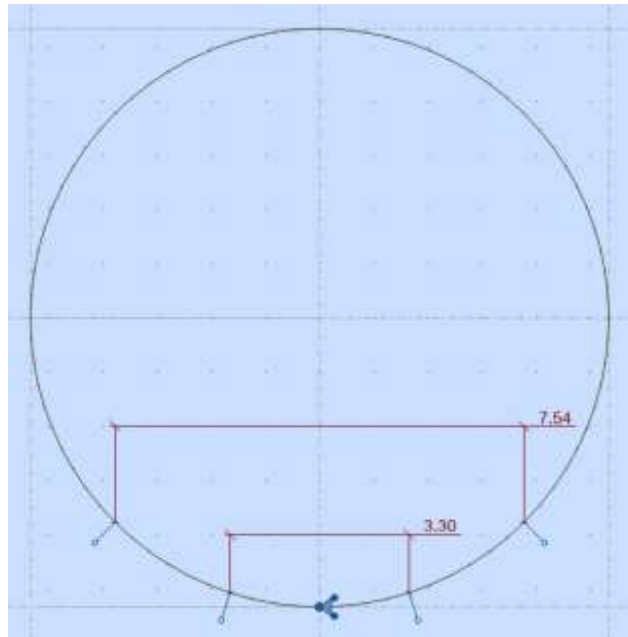


Figure 52: Model of the structure made by Robot.

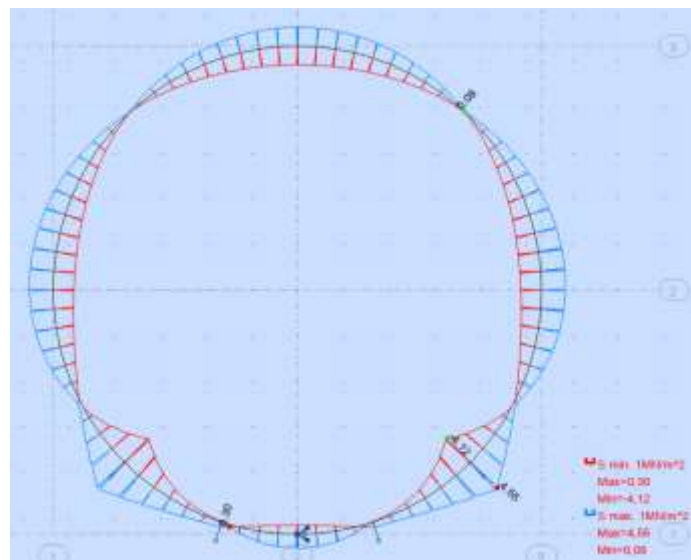


Figure 53: Tensions in the section.

As shown in Figure 53, the maximum tension in the section is 4.12 MPa, being this value bigger than 4 MPa, it will be necessary circumferential post tensioning steel. After making the calculations shown in chapter 5.4.2 it will be placed two strands of 15,7 mm of diameter per metre of section. Giving an initial post-tensioning force of 396 kN/m and a force after losses of 307.70 kN/m, giving a final tension in the structure of 3.42 MPa. The scheme of the reinforcement in this section will be shown in the following figure.

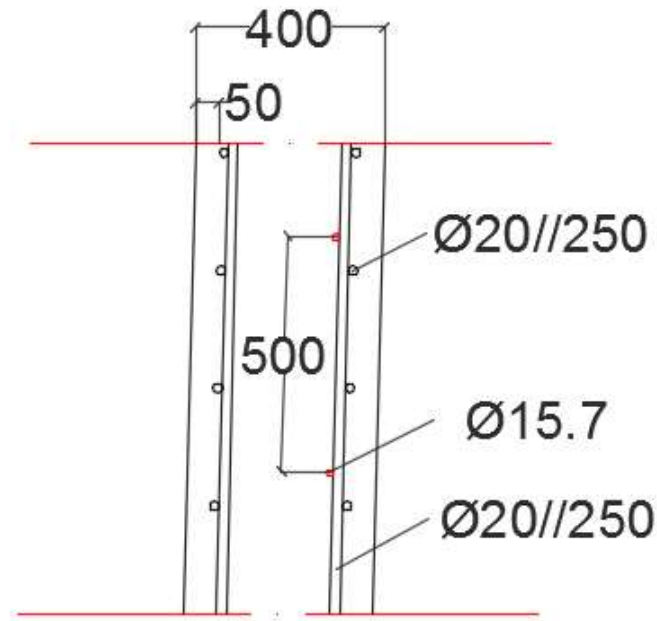


Figure 54: Scheme of the active (red) and passive (black) reinforcement.

#### 5.4.3.5. Section of 0.45 metres thickness

As in the previous cases, it will be analysed the biggest section with this thickness. It corresponds to the section which diameter is 11.91 metres.

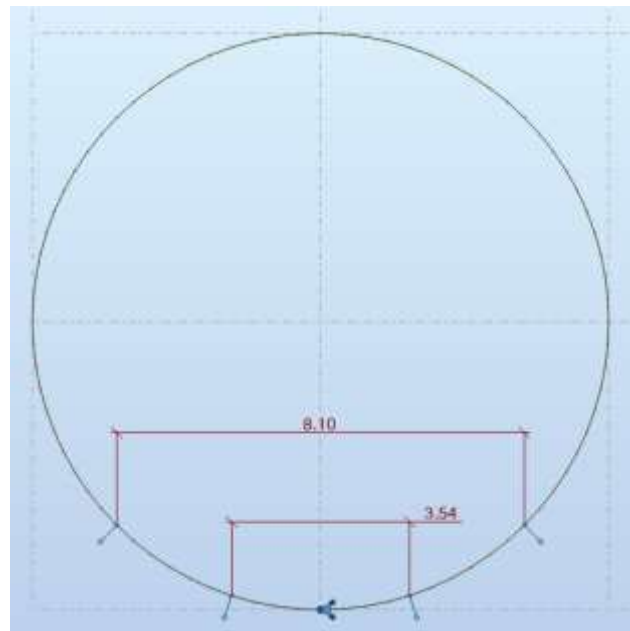


Figure 55: Model of the structure made by Robot.

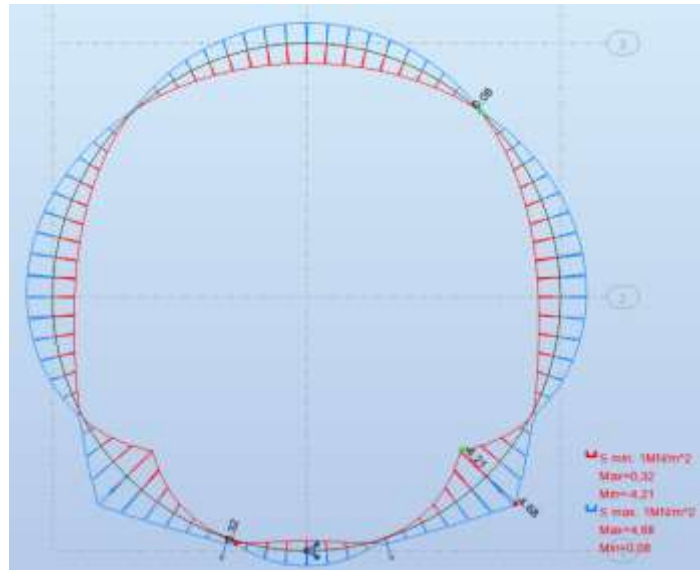


Figure 56: Tensions in the section.

As shown in Figure 56, the maximum tension in the section is 4.21 MPa, being this value bigger than 4 MPa, it will be necessary circumferential post tensioning steel. After making the calculations shown in chapter 5.4.2 it will be placed two strands of 15,7 mm of diameter per metre of section. Giving an initial post-tensioning force of 396 kN/m and a force after losses of 307.61 kN/m, giving a final tension in the structure of 3.59 MPa. The scheme of the reinforcement in this section will be shown in the following figure.

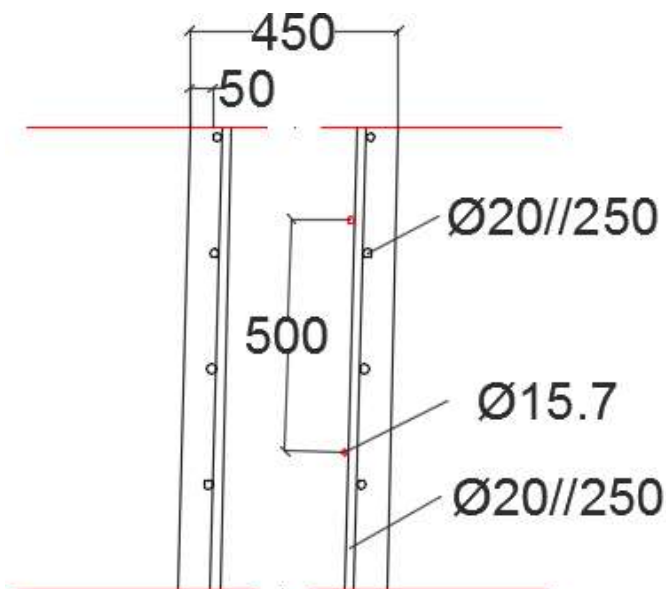


Figure 57: Scheme of the active (red) and passive (black) reinforcement.

#### 5.4.3.6. Section of 0.5 metres thickness

As in the previous cases, it will be analysed the biggest section with this thickness. It corresponds to the tower base section which diameter is 13.20 metres.

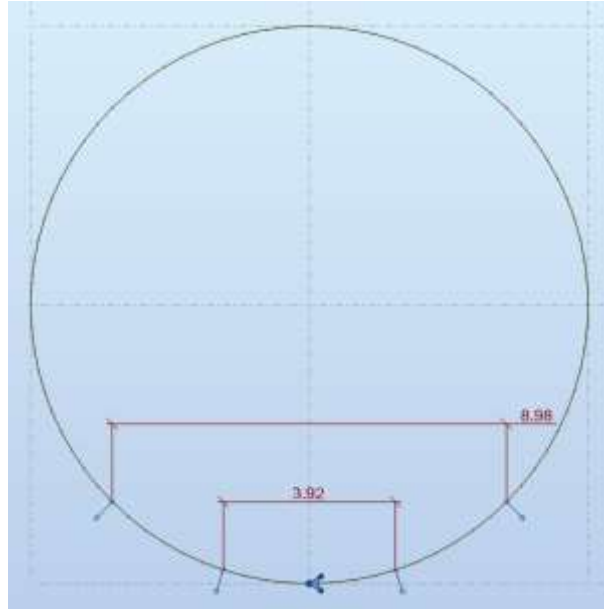


Figure 58: Model of the structure made by Robot.

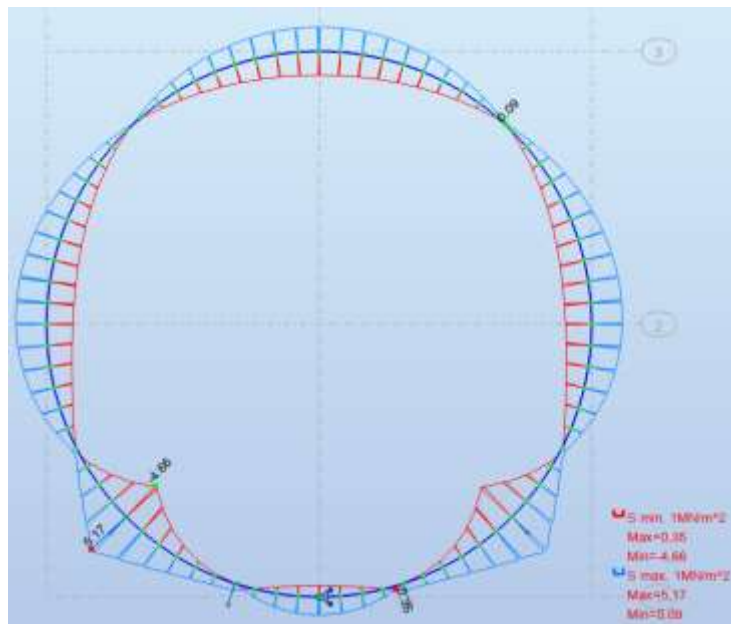


Figure 59: Tensions in the section.

As shown in Figure 59, the maximum tension in the section is 4.66 MPa, being this value bigger than 4 MPa, it will be necessary circumferential post tensioning steel. After making the calculations shown in chapter 5.4.2 it will be placed four strands of 15,7 mm of diameter per metre of section. Giving an

initial post-tensioning force of 792 kN/m and a force after losses of 612.58 kN/m, giving a final tension in the structure of 3.56 MPa. The scheme of the reinforcement in this section will be shown in the following figure.

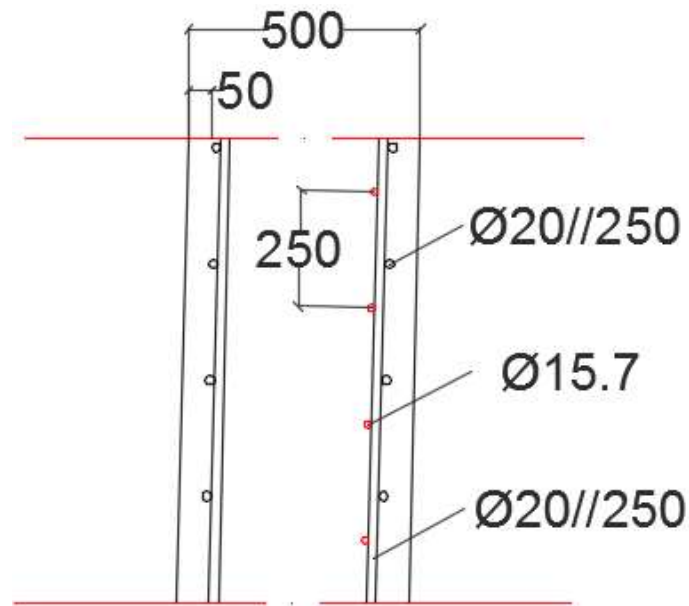


Figure 60: Scheme of the active (red) and passive (black) reinforcement.

#### 5.4.3.7. *Transition piece*

The transition piece is a special case, where there occurs an important variation of the section in few metres. That is why will be divided in three sections, in order to optimize the active reinforcement. The sections will be divided in three, four and three metres, respectively. The tensions in the base of the transition piece are the ones shown in chapter 5.4.2, and the tensions in the top of the piece are shown in chapter 5.4.3.6. For making a more accurate calculation it will be computed also the tension on an intermediate point of the section, which diameter will be 15.9 metres.

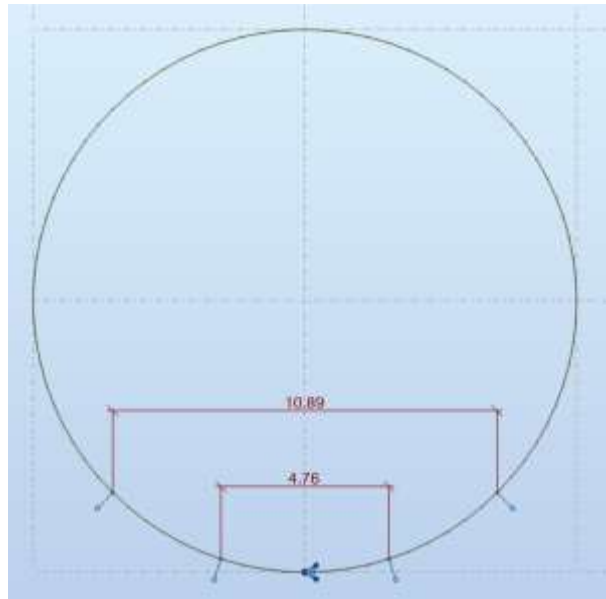


Figure 61: Model of the structure made by Robot.

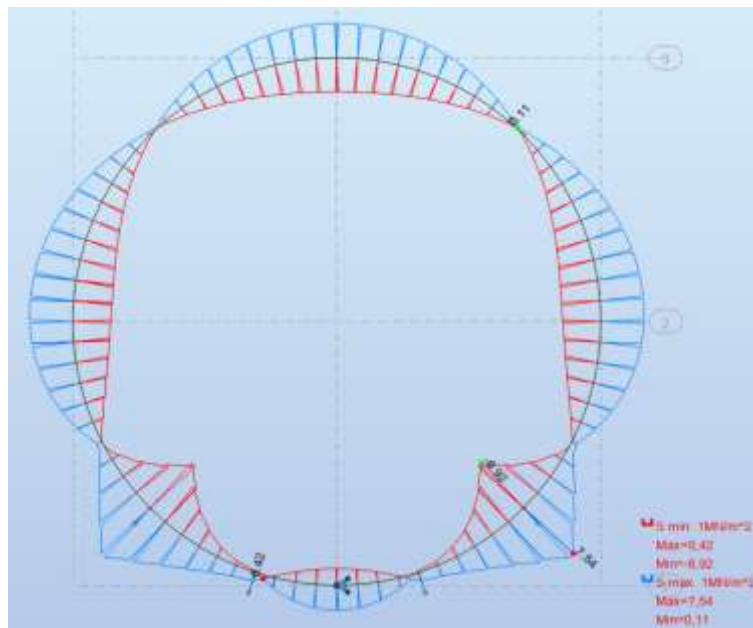


Figure 62: Tensions in the section.

As shown in Figure 62 the tension in this point is 6.92 MPa, so, with the tension in the top of the transition piece, the tension in the middle of the piece and the tension in the base, it will be defined the reinforcement along the section by a lineal regression (Table 24).

Z (m)	Tension (Mpa)	Strands/metre	Final tension (Mpa)
Sea level (0)	4.66	8	2.47
-1	5.11	8	2.92
-2	5.56	8	3.37
-3	6.02	16	1.69
-4	6.47	16	2.14
-5	6.92	16	2.60
-6	7.46	16	3.14
-7	8	22	2.12
-8	8.54	22	2.66
-9	9.08	22	3.20
-10	9.62	22	3.74

Table 24: Tension on the transition piece.

The following figures show the scheme of the reinforcement in each section of the transition piece.

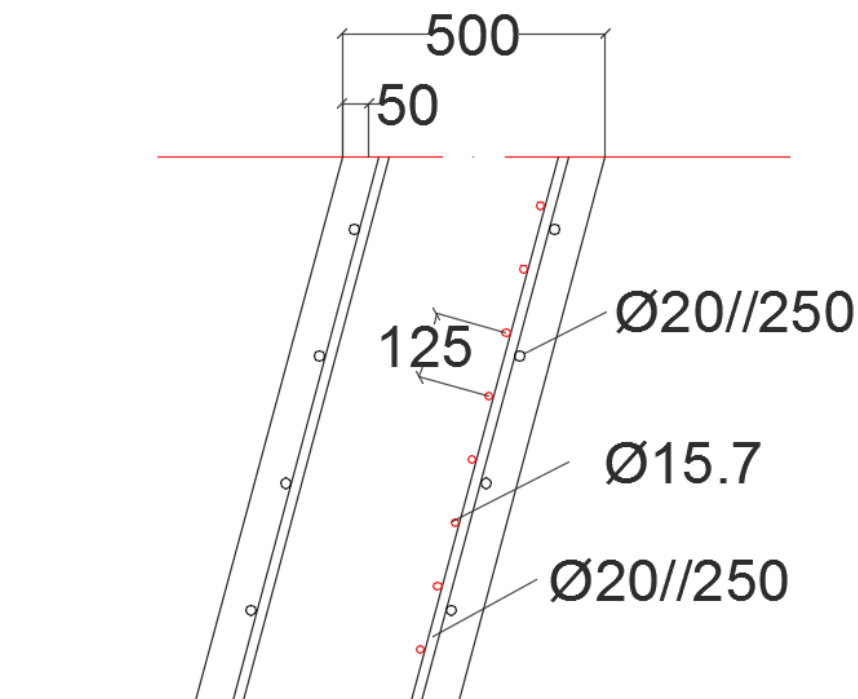


Figure 63: Scheme of the active (red) and passive (black) reinforcement from the sea level until 3 metres depth.

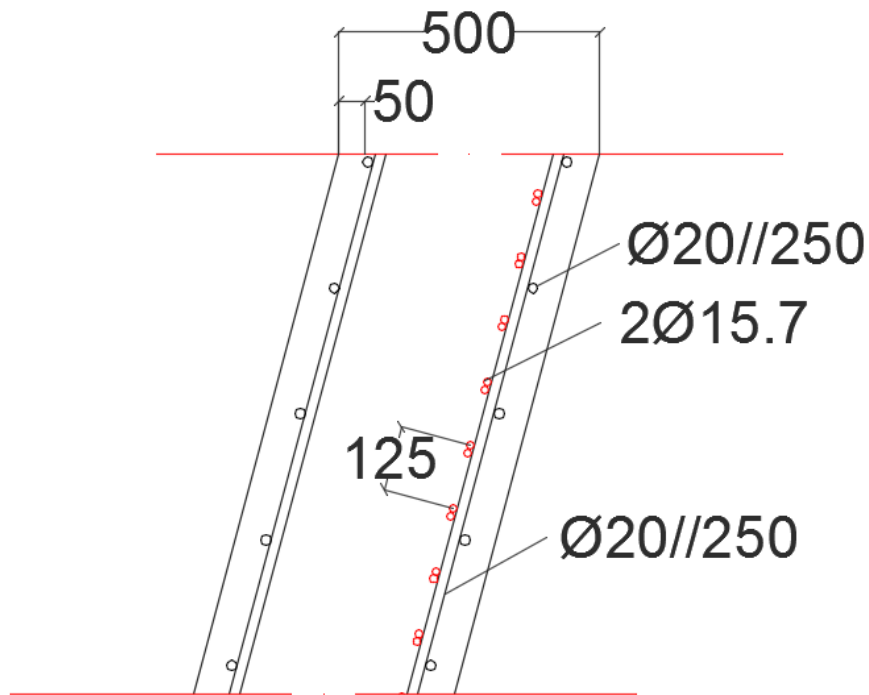


Figure 64: Scheme of the active (red) and passive (black) reinforcement from 3 until 7 metres depth.

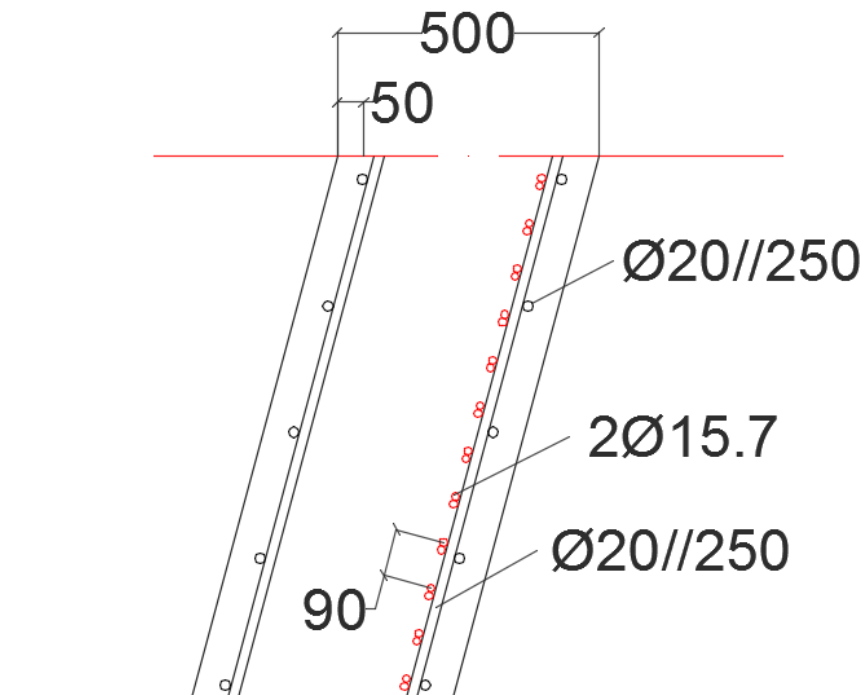


Figure 65: Scheme of the active (red) and passive (black) reinforcement from 7 until 10 metres depth.

All the results of these calculations for each section will be shown in the Appendix 2.



## 5.5. SUMMARY OF RESULTS AND BILL OF QUATITIES

### 5.5.1. Summary of the reinforcement

After all the calculations and structural verifications the summary of the reinforcement designed is:

- Longitudinal active reinforcement:
  - 64 tendons of 15 strands, from the top of the tower (129.5 metres above sea level) to the end of the transition piece (10 metres under sea level)
  - 16 tendons of 34 strands form 65 metres above sea level to 43.3 metres under sea level
  - 16 tendons of 34 strands from 45 metres above sea level until the bottom of the floater.
- Circumferential active reinforcement:
  - 22 strands per metre in the substructure.
  - 22, 16 and 8 strands per metre in the transition piece.
  - 4 strand per metre in the 0.5 metres thickness section of the tower.
  - 2 strands per metre in the rest of the tower until 85 metres height.
- Longitudinal passive reinforcement:
  - $\phi 20//250$  along all the structure.
- Circumferential passive reinforcement:
  - $\phi 20//250$  along all the structure.

### 5.5.2. Bill of quantities

- Volume of concrete:
  - Bottom of the floater (hemisphere): 257.37 m<sup>3</sup>.
  - Floater (cylinder): 3858.15 m<sup>3</sup>.
  - Transition piece (trunk cone): 241.90 m<sup>3</sup>.
  - Tower (trunk cone): 2060.12 m<sup>3</sup>.
  - TOTAL VOLUME: 6417.53 m<sup>3</sup>.
- Longitudinal active reinforcement:
  - Total weight: 454042.5 kg.
  - Ratio: 70.75 kg/m<sup>3</sup>.
- Circumferential active reinforcement:
  - Floater (cylinder): 250855.67 kg.
  - Transition piece (trunk cone): 9794.93 kg.
  - Tower (trunk cone): 10956.46 kg.

- Total weight: 271607.05 kg.
- Ratio: 42.32 kg/m<sup>3</sup>.
- Longitudinal passive reinforcement:
  - Total weight: 164176.13 kg.
  - Ratio: 25.58 kg/m<sup>3</sup>.
- Circumferential passive reinforcement:
  - Total weight: 319714.87 kg.
  - Ratio: 49.82 kg/m<sup>3</sup>.

## 6. CONCLUSIONS

After the complete analysis of the structure made by OpenFAST, it has been concluded that the worst situation comes with the DLC 6.2, which is the extreme case without power supply. It is an extreme case, with extreme wind, extreme waves and a grid failure, which main objective is to ensure the survival of the structure in this situation. In this load case, the worst situations comes when the wind speed is 41.2 m/s, and with a yaw misalignment of 90°.

After making the modal analysis of the structure, and due to the frequencies of vibration, it can be concluded that the structure will not have problems of resonance, taking into account that the frequency of vibration in all modes is out of the limits defined in Campbell's diagram (Figure 20). These limits are defined by cut-in wind speed, blade passed frequency, cut-out wind speed and rotor frequency.

As said before, the worst situation is produced by DLC 6.2, so the structure will be analysed for this load case, which represents an extreme situation.

Taking into account these extreme conditions, it has been defined the post-tensioning steel in Serviceability Limit State. Avoiding tensions bigger than the value of  $f_{ctm}$  of the concrete, which is 4.8 MPa for an 80 MPa compressive strength concrete, and avoiding compressions bigger than  $0.6 \cdot f_{ck}$  which will be 48 MPa for an 80 MPa concrete. These two conditions should be fulfilled since the installation of the structure ( $t=0s$ ) till the end of its service life ( $t=\infty$ ).

For making the design of the post-tensioning steel it has been considered a fictitious tendon that goes through the centre of gravity of the section, simplifying considerably the calculations, taking into account that it only introduces axial forces into the structure.

After this analysis it has been observed that the critical points of the structure are the tower, and the transition piece. The tower is critical because of the constant variation of the thickness, which creates larger tensions in the transition zones, where the thickness increase. The problem with the transition piece is that the frictional losses are larger than in the rest of the structure, due to the angle in the wall, which creates a considerable increment in this kind of losses, making necessary a larger amount of active reinforcement in order to fulfil the previous conditions, specially the non-presence of tension bigger than 4.8 MPa.

The Ultimate Limit State checking has been also performed, including the bending moment capacity, the resistance to shear force, the resistance to torsional moment, and the interaction of all of them. The critical section of the structure, especially considering the torsional moment is the top of the tower, due to its thickness, which is approximately half of the thickness in the floater, and due to the value of the torsional moment in this section, which is the larger value in all the structure. That is why the results of its calculation have been presented with more detail than in other sections of the structure. After making this analysis, it has been observed that the design is safe, taking into account that resisting forces are larger than the design moments and forces in every section.

Taking into account the dimension of the structure, it has been necessary the analysis of it in horizontal position, simulating the construction process. This analysis has been done for SLS, to see if it would be necessary some post-tensioning steel, and for ULS, to define the passive reinforcement.

After the SLS analysis it has been concluded that it is necessary the installation of active steel. Taking into account the dimensions of the structure, and that this active reinforcement should be compatible with the vertical tendons, it has been concluded that the best option is to use unbounded mono-strand tendons, because they present smaller friction losses. With this solution the strands could be independent and only have 15.7 mm of diameter, so they can be placed in the structure with any problem. In order to not disturb the vertical tendons they will be placed near the passive reinforcement in the interior face of the circular section, which will be the most stressed section in horizontal position. As they are always placed in the same position in the section relatively to the centre of gravity, they only generate axial force, which simplifies considerably the calculation. Although the calculation has been conservative, in less solicited section it has been placed less post-tensioning steel than in the floater, which is the most solicited section, in order to reduce the cost of the structure as much as possible.

After making the ULS analysis, taking into account the passive reinforcement designed in the vertical verification, it has been checked that the capacity of the structure is bigger than the tensions acting on it.

As a final conclusion it should be said that there are a lot of situations that should be taken into account in the design of this kind of structures, especially

when they have considerably big dimensions. Commonly, at the beginning of a design people only think on the built final structure, but as shown in this thesis, the construction process is also determinant, because the failure of the structure could occur during those construction and installation stages.

## 7. BIBLIOGRAFY

- BREDMOSE, H., RINKER, J., SKRZYPINSKI, W., ZAHLE, F., MENG, F., DYKES, K., GAERTNER, E., BARTER, G., BORTOLOTTI, P., SETHURAMAN, L. y SHIELDS, M., 2020. COREWIND D1.1: Definition of the 15 MW Reference Wind Turbine. , no. 815083, pp. 1-40.
- BS EN 61400, 2009. BSI British Standards Wind turbines. ,
- CHAKRABARTI, S.K., 2005. *Handbook of Offshore Engineering* [en línea]. S.l.: s.n. ISBN 9780080443812. Disponible en: <http://dx.doi.org/10.1016/B978-0-08-044381-2.50022-9>.
- COBRA, INNOSEA, JDR, DTU, FIHAC, UPC, UL INT GMBH y USTUTT, 2019. COREWIND D1.2 design basis. . S.l.:
- DNVGL-ST-0119, 2018. Floating wind turbine structures. , no. July.
- DNVGL-ST-0126, 2016. DNVGL-ST-0126 : Support structures for wind turbines. . S.l.:
- DNVGL-ST-0437, 2016. Loads and site conditions for wind turbines. , no. November.
- DNVGL, 2018. DNVGL-ST-C502 Offshore concrete structures. *Standard*, no. February. ISSN 00298018. DOI 10.1016/j.oceaneng.2012.11.007.
- EC-2, 2010. Eurocode 2 - Project of concrete structures. , pp. 259.
- EHE-08, 2008. Instrucción de Hormigón Estructural EHE-2008. *Boe N° 203*, pp. 704.
- HAU, E., 2005. *Wind turbines. Fundamentals, Technologies, Application, Economics*. S.l.: s.n. ISBN 0824715098.
- History of Europe's Wind Industry. *WindEurope* [en línea], 2020. Disponible en: <https://windeurope.org/about-wind/history/>.
- IEC 61400-1, 2005. INTERNATIONAL STANDARD. ,
- IEC 61400-3, 2009. INTERNATIONAL STANDARD. ,
- INTERNATIONAL RENEWABLE ENERGY AGENCY (IRENA), 2016. Floating Foundations: A Game Changer for Offshore Wind Power. [en línea], pp. 1-8. Disponible en: [http://www.irena.org/-/media/Files/IRENA/Agency/Publication/2016/IRENA\\_Offshore\\_Wind\\_Floating\\_Foundations\\_2016.pdf](http://www.irena.org/-/media/Files/IRENA/Agency/Publication/2016/IRENA_Offshore_Wind_Floating_Foundations_2016.pdf).
- JOAO CRUZ, M.A., 2016. *Floating Offshore Wind Energy: The Next Generation of*

- Wind Energy*. S.l.: s.n. ISBN 978-3-319-29398-1.
- JONKMAN, B.J. y JONKMAN, J.M., 2016. FAST v8.16.00a-bjj User's Guide. *Nrel*, pp. 58.
- JONKMAN, J., 2012. Aerodynamics Module NREL Wind Turbine. ,
- JONKMAN, J., 2013a. NREL Wind Turbine Modeling Workshop. , pp. 10 pp.
- JONKMAN, J., 2013b. Structural-Dynamics Module. ,
- JONKMAN, J., 2014a. Overview of Offshore Features. ,
- JONKMAN, J., 2014b. Overview of the ServoDyn Control & Electrical-Drive Module. ,
- JONKMAN, J.M., 2010. Overview of FAST. ,
- JONKMAN, J.M. y BUHL, M.L., 2005. FAST User's Guide. S.l. Disponible en: [www.nrel.gov](http://www.nrel.gov).
- JOURNÉE, J.M.J. y MASSIE, W.W., 2001. Offshore Hydromechanics, First Edition. . S.l.
- MAHFOUZ, M.Y., SALARI, M., HERNÁNDEZ, S., VIGARA, F., MOLINS, C. y TRUBAT, P., 2020. D1.3 Public design and FAST models of the two 15MW floater-turbine concepts. , no. April.
- MK4, 2010. Pretensado. ,
- MOLINS, C., CAMPOS, A., GIRONELLA, X. y TRUBAT, P., 2016. Spar concrete monolithic design for offshore wind turbines. *Proceedings of the Institution of Civil Engineers: Maritime Engineering*, vol. 169, no. 2, pp. 49-63. ISSN 17517737. DOI 10.1680/jmaen.2014.24.
- MORIARTY, P.J. y HANSEN, A.C., 2005. AeroDyn Theory Manual. . S.l.:
- NATIONAL RENEWABLE ENERGY LABORATORY, 2017. FAST v8 and the transition to OpenFAST. ,
- SESTO, E. y LIPMAN, N.H., 1992. Wind energy in Europe. ,
- TRUBAT, P., BAIRAN, J., YAGÜE, A. y MOLINS, C., 2019. Iowtc2019- 7564. , pp. 1-8.
- WALSH, C., 2019. Offshore wind in Europe. *Refocus* [en línea], vol. 3, no. 2, pp. 14-17. ISSN 14710846. DOI 10.1016/s1471-0846(02)80021-x. Disponible en: <https://windeurope.org/wp-content/uploads/files/about-wind/statistics/WindEurope-Annual-Offshore-Statistics-2019.pdf>.

WIND EUROPE, 2017. Floating Offshore Wind Vision Statement. [en línea], no. June, pp. 16. Disponible en: <https://windeurope.org/about-wind/reports/floating-vision-statement/>.



# APPENDIX 1. NUMERICAL RESULTS FOR THE LONGITUDINAL STRUCTURE

## 1. Post-tensioning steel area

Z (m)	Po1 (kN)	Po2 (kN)	Po3 (kN)	Po4 (kN)	Asmin (mm <sup>2</sup> )	Asmax (mm <sup>2</sup> )	As (mm <sup>2</sup> )
-155	-6.68E+05	9.70E+05	-7.51E+05	1.09E+06	-5.13E+05	7.45E+05	8.16E+04
-150.35	-6.42E+05	9.90E+05	-7.22E+05	1.11E+06	-4.93E+05	7.60E+05	8.16E+04
-145.7	-5.56E+05	1.05E+06	-6.26E+05	1.19E+06	-4.27E+05	8.09E+05	8.16E+04
-128.74	-3.72E+05	1.14E+06	-4.19E+05	1.28E+06	-2.86E+05	8.75E+05	8.16E+04
-111.78	-2.02E+05	1.13E+06	-2.28E+05	1.28E+06	-1.55E+05	8.71E+05	8.16E+04
-94.81	-9.03E+04	1.06E+06	-1.02E+05	1.20E+06	-6.94E+04	8.16E+05	8.16E+04
-77.85	1.71E+04	1.02E+06	1.93E+04	1.15E+06	1.48E+04	7.86E+05	8.16E+04
-60.89	7.86E+04	9.96E+05	8.85E+04	1.12E+06	6.79E+04	7.65E+05	8.16E+04
-43.93	1.14E+05	9.90E+05	1.29E+05	1.11E+06	9.89E+04	7.61E+05	1.63E+05
-26.96	1.41E+05	9.91E+05	1.59E+05	1.11E+06	1.22E+05	7.61E+05	1.63E+05
-10	1.41E+05	1.01E+06	1.59E+05	1.14E+06	1.22E+05	7.77E+05	1.63E+05
-6.67	1.98E+05	8.53E+05	2.22E+05	9.60E+05	1.71E+05	6.55E+05	3.07E+05
-3.33	2.58E+05	6.88E+05	2.90E+05	7.74E+05	2.23E+05	5.29E+05	3.07E+05
0	3.25E+05	5.16E+05	3.66E+05	5.81E+05	2.81E+05	3.97E+05	3.07E+05
7.5	3.02E+05	5.15E+05	3.40E+05	5.80E+05	2.61E+05	3.96E+05	3.07E+05
15	2.76E+05	5.12E+05	3.11E+05	5.76E+05	2.39E+05	3.93E+05	3.07E+05
20	2.73E+05	5.01E+05	3.07E+05	5.64E+05	2.36E+05	3.85E+05	3.07E+05
25	2.59E+05	4.99E+05	2.92E+05	5.61E+05	2.24E+05	3.83E+05	3.07E+05
25.1	2.66E+05	4.18E+05	2.99E+05	4.71E+05	2.30E+05	3.21E+05	3.07E+05
30	2.53E+05	4.17E+05	2.85E+05	4.69E+05	2.19E+05	3.20E+05	3.07E+05
35	2.40E+05	4.16E+05	2.70E+05	4.68E+05	2.07E+05	3.19E+05	3.07E+05
40	2.25E+05	4.16E+05	2.53E+05	4.68E+05	1.95E+05	3.19E+05	3.07E+05
45	2.12E+05	4.14E+05	2.38E+05	4.66E+05	1.83E+05	3.18E+05	3.07E+05
45.1	2.18E+05	3.40E+05	2.45E+05	3.83E+05	1.88E+05	2.61E+05	2.26E+05
50	2.05E+05	3.41E+05	2.30E+05	3.83E+05	1.77E+05	2.62E+05	2.26E+05
55	1.90E+05	3.41E+05	2.14E+05	3.84E+05	1.64E+05	2.62E+05	2.26E+05
60	1.76E+05	3.42E+05	1.98E+05	3.84E+05	1.52E+05	2.62E+05	2.26E+05
65	1.63E+05	3.41E+05	1.83E+05	3.83E+05	1.41E+05	2.62E+05	2.26E+05
65.1	1.74E+05	2.06E+05	1.96E+05	2.32E+05	1.51E+05	1.58E+05	1.44E+05
70	1.60E+05	2.10E+05	1.80E+05	2.36E+05	1.38E+05	1.61E+05	1.44E+05
75	1.45E+05	2.14E+05	1.63E+05	2.41E+05	1.25E+05	1.64E+05	1.44E+05
80	1.32E+05	2.16E+05	1.48E+05	2.43E+05	1.14E+05	1.66E+05	1.44E+05
85	1.17E+05	2.19E+05	1.32E+05	2.47E+05	1.01E+05	1.68E+05	1.44E+05
85.1	1.19E+05	1.95E+05	1.34E+05	2.19E+05	1.03E+05	1.50E+05	1.44E+05
90	1.04E+05	2.00E+05	1.17E+05	2.25E+05	9.01E+04	1.53E+05	1.44E+05
95	9.26E+04	2.01E+05	1.04E+05	2.26E+05	8.00E+04	1.54E+05	1.44E+05
100	8.07E+04	2.02E+05	9.08E+04	2.27E+05	6.97E+04	1.55E+05	1.44E+05
105	6.78E+04	2.04E+05	7.63E+04	2.30E+05	5.86E+04	1.57E+05	1.44E+05
110	5.67E+04	2.05E+05	6.38E+04	2.31E+05	4.90E+04	1.57E+05	1.44E+05
115	4.67E+04	2.05E+05	5.25E+04	2.30E+05	4.03E+04	1.57E+05	1.44E+05
120	3.63E+04	2.05E+05	4.08E+04	2.30E+05	3.13E+04	1.57E+05	1.44E+05
125	2.88E+04	2.02E+05	3.24E+04	2.28E+05	2.49E+04	1.55E+05	1.44E+05
129.50	2.42E+04	2.01E+05	2.73E+04	2.26E+05	2.09E+04	1.54E+05	1.44E+05

## 2. Post-tensioning losses

Z (m)	Pmax,0 (kN)	$\Delta P1$ (kN)	$\Delta P2$ (kN)	$\Delta P3$ (kN)	Po (kN)	$\Delta P$ (kN)	Pinf (kN)
-155	1.06E+05	4.17E+04	0	4.48E+02	6.41E+04	1.68E+03	6.24E+04
-150.35	1.06E+05	3.16E+04	0	5.18E+02	7.42E+04	2.26E+03	7.19E+04
-145.7	1.06E+05	3.12E+04	0	5.21E+02	7.45E+04	2.28E+03	7.22E+04
-128.74	1.06E+05	2.93E+04	0	5.34E+02	7.64E+04	2.39E+03	7.40E+04
-111.78	1.06E+05	2.73E+04	0	5.48E+02	7.84E+04	2.50E+03	7.59E+04
-94.81	1.06E+05	2.54E+04	0	5.61E+02	8.03E+04	2.61E+03	7.77E+04
-77.85	1.06E+05	2.34E+04	0	5.75E+02	8.22E+04	2.72E+03	7.95E+04
-60.89	1.06E+05	2.15E+04	0	5.88E+02	8.42E+04	2.83E+03	8.13E+04
-43.93	2.12E+05	4.14E+04	0	2.45E+03	1.69E+05	7.43E+03	1.61E+05
-26.96	2.12E+05	3.75E+04	0	2.51E+03	1.72E+05	7.68E+03	1.65E+05
-10	2.12E+05	3.36E+04	0	2.57E+03	1.76E+05	7.94E+03	1.68E+05
-6.67	4.00E+05	5.81E+04	0	1.05E+04	3.31E+05	2.21E+04	3.09E+05
-3.33	4.00E+05	5.66E+04	0	1.18E+04	3.32E+05	2.38E+04	3.08E+05
0	4.00E+05	5.52E+04	0	1.35E+04	3.31E+05	2.58E+04	3.05E+05
7.5	4.00E+05	3.56E+04	0	1.48E+04	3.50E+05	2.82E+04	3.21E+05
15	4.00E+05	3.24E+04	0	1.54E+04	3.52E+05	2.91E+04	3.23E+05
20	4.00E+05	3.02E+04	5.80E+02	1.58E+04	3.53E+05	2.96E+04	3.24E+05
25	4.00E+05	2.80E+04	1.73E+03	1.62E+04	3.54E+05	3.01E+04	3.24E+05
25.1	4.00E+05	2.80E+04	1.75E+03	1.80E+04	3.52E+05	3.20E+04	3.20E+05
30	4.00E+05	2.59E+04	2.88E+03	1.84E+04	3.53E+05	3.25E+04	3.20E+05
35	4.00E+05	2.37E+04	4.02E+03	1.89E+04	3.53E+05	3.10E+04	3.22E+05
40	4.00E+05	2.16E+04	5.75E+03	1.94E+04	3.53E+05	2.95E+04	3.24E+05
45	4.00E+05	1.94E+04	8.05E+03	1.99E+04	3.53E+05	2.81E+04	3.25E+05
45.1	2.94E+05	1.94E+04	1.75E+03	1.19E+04	2.61E+05	1.79E+04	2.43E+05
50	2.94E+05	1.78E+04	2.88E+03	1.22E+04	2.61E+05	1.73E+04	2.44E+05
55	2.94E+05	1.62E+04	4.02E+03	1.26E+04	2.61E+05	1.67E+04	2.44E+05
60	2.94E+05	1.46E+04	5.17E+03	1.29E+04	2.61E+05	1.61E+04	2.45E+05
65	2.94E+05	1.31E+04	6.32E+03	1.33E+04	2.61E+05	1.56E+04	2.45E+05
65.1	1.87E+05	1.30E+04	0	7.11E+03	1.67E+05	9.07E+03	1.58E+05
70	1.87E+05	1.20E+04	0	7.34E+03	1.68E+05	8.87E+03	1.59E+05
75	1.87E+05	1.10E+04	0	7.60E+03	1.69E+05	8.67E+03	1.60E+05
80	1.87E+05	1.00E+04	0	7.87E+03	1.70E+05	8.48E+03	1.61E+05
85	1.87E+05	9.01E+03	0	8.15E+03	1.70E+05	8.30E+03	1.62E+05
85.1	1.87E+05	8.99E+03	0	8.72E+03	1.70E+05	8.12E+03	1.62E+05
90	1.87E+05	8.00E+03	0	9.04E+03	1.70E+05	7.94E+03	1.63E+05
95	1.87E+05	6.98E+03	0	9.38E+03	1.71E+05	7.77E+03	1.63E+05
100	1.87E+05	5.97E+03	0	9.75E+03	1.72E+05	7.60E+03	1.64E+05
105	1.87E+05	4.96E+03	1.23E+03	1.01E+04	1.71E+05	7.38E+03	1.64E+05
110	1.87E+05	3.95E+03	3.25E+03	1.04E+04	1.70E+05	7.14E+03	1.63E+05
115	1.87E+05	2.94E+03	5.28E+03	1.07E+04	1.69E+05	6.90E+03	1.62E+05
120	1.87E+05	1.92E+03	7.30E+03	1.10E+04	1.67E+05	6.67E+03	1.61E+05
125	1.87E+05	9.10E+02	9.33E+03	1.14E+04	1.66E+05	6.45E+03	1.59E+05
129.50	1.87E+05	0.00E+00	1.11E+04	1.18E+04	1.65E+05	6.25E+03	1.58E+05

### 3. Verification of cracking

Z (m)	Ac (m <sup>2</sup> )	M (kNm)	N (kN)	$\sigma_{co}$ (MPa)	$\sigma_{cinf}$ (MPa)	$\sigma_{to}$ (MPa)	$\sigma_{tinf}$ (MPa)
-155	28.43	0	4.05E+05	-16.71	-16.64	-16.26	-16.21
-150.35	28.43	4.20E+03	3.84E+05	-16.41	-16.33	-15.82	-15.75
-145.7	28.43	1.68E+04	3.18E+05	-14.19	-14.10	-13.40	-13.33
-128.74	28.43	1.59E+05	2.01E+05	-11.29	-11.20	-8.22	-8.14
-111.78	28.43	4.73E+05	1.35E+05	-11.55	-11.45	-3.44	-3.37
-94.81	28.43	8.28E+05	1.24E+05	-14.09	-13.99	-0.31	-0.23
-77.85	28.43	1.11E+06	1.01E+05	-15.55	-15.44	2.68	2.77
-60.89	28.43	1.27E+06	8.90E+04	-16.56	-16.45	4.38	4.47
-43.93	28.43	1.35E+06	7.75E+04	-20.04	-19.75	2.72	2.96
-26.96	28.43	1.40E+06	6.64E+04	-20.17	-19.87	3.36	3.61
-10	28.43	1.35E+06	5.61E+04	-19.60	-19.29	3.25	3.50
-6.67	25.61	1.32E+06	5.06E+04	-29.24	-28.29	-0.60	0.18
-3.33	22.78	1.28E+06	4.70E+04	-34.10	-32.95	0.86	1.80
0	19.95	1.23E+06	4.35E+04	-40.63	-39.21	3.07	4.23
7.5	19.32	1.12E+06	3.99E+04	-41.50	-39.90	1.18	2.49
15	18.69	1.01E+06	3.82E+04	-41.59	-39.89	-0.18	1.22
20	18.29	9.66E+05	3.64E+04	-42.14	-40.36	-0.49	0.97
25	17.88	9.02E+05	3.42E+04	-42.15	-40.30	-1.27	0.25
25.1	16.16	9.01E+05	3.42E+04	-46.34	-44.16	-1.49	0.29
30	15.80	8.43E+05	3.24E+04	-46.44	-44.17	-2.31	-0.46
35	15.44	7.85E+05	3.05E+04	-46.50	-44.29	-3.22	-1.41
40	15.07	7.26E+05	2.86E+04	-46.48	-44.32	-4.19	-2.43
45	14.71	6.72E+05	2.69E+04	-46.50	-44.40	-5.11	-3.39
45.1	13.13	6.71E+05	2.69E+04	-44.17	-42.67	0.37	1.60
50	12.81	6.21E+05	2.53E+04	-44.08	-42.60	-0.58	0.63
55	12.49	5.69E+05	2.38E+04	-43.92	-42.45	-1.66	-0.46
60	12.17	5.20E+05	2.23E+04	-43.79	-42.33	-2.78	-1.59
65	11.84	4.75E+05	2.11E+04	-43.75	-42.30	-3.90	-2.72
65.1	8.97	4.74E+05	2.11E+04	-45.76	-44.65	3.75	4.66
70	8.73	4.30E+05	1.99E+04	-45.38	-44.26	2.32	3.24
75	8.49	3.86E+05	1.87E+04	-44.93	-43.80	0.74	1.65
80	8.25	3.47E+05	1.78E+04	-44.67	-43.54	-0.77	0.15
85	8.00	3.09E+05	1.68E+04	-44.29	-43.15	-2.47	-1.54
85.1	7.48	3.08E+05	1.68E+04	-47.16	-45.97	-2.70	-1.72
90	7.26	2.70E+05	1.59E+04	-46.61	-45.41	-4.70	-3.72
95	7.04	2.39E+05	1.51E+04	-46.50	-45.28	-6.44	-5.44
100	6.81	2.10E+05	1.43E+04	-46.36	-45.13	-8.31	-7.30
105	6.58	1.81E+05	1.36E+04	-45.89	-44.65	-10.27	-9.26
110	6.36	1.56E+05	1.29E+04	-45.49	-44.26	-12.03	-11.02
115	6.13	1.33E+05	1.22E+04	-45.21	-43.97	-13.79	-12.78
120	5.90	1.12E+05	1.15E+04	-44.85	-43.61	-15.72	-14.71
125	5.68	9.49E+04	1.07E+04	-44.83	-43.58	-17.39	-16.37
129.50	5.47	8.19E+04	9.08E+03	-44.79	-43.53	-18.68	-17.65

#### 4. Verification under permanent loads

Z (m)	$\sigma_{max}$ (MPa)	Po (KNm)	N (kN)	$\sigma_{co}$ (MPa)	$\sigma_{cinf}$ (MPa)	$\sigma_{to}$ (MPa)	$\sigma_{tinf}$ (MPa)
-155	36	1.06E+05	4.05E+05	17.24	17.15	16.70	16.62
-150.35	36	1.06E+05	3.84E+05	16.37	16.29	15.85	15.78
-145.70	36	1.06E+05	3.18E+05	14.06	13.97	13.54	13.46
-128.74	36	1.06E+05	2.01E+05	10.02	9.93	9.49	9.41
-111.78	36	1.06E+05	1.35E+05	7.77	7.68	7.22	7.14
-94.81	36	1.06E+05	1.24E+05	7.49	7.39	6.92	6.84
-77.85	36	1.06E+05	1.01E+05	6.72	6.62	6.14	6.06
-60.89	36	1.06E+05	8.90E+04	6.39	6.28	5.80	5.71
-43.93	36	2.12E+05	7.75E+04	9.25	8.97	8.07	7.83
-26.96	36	2.12E+05	6.64E+04	9.01	8.72	7.80	7.56
-10	36	2.12E+05	5.61E+04	8.80	8.50	7.56	7.31
-6.67	36	4.00E+05	5.06E+04	16.23	15.30	13.64	12.88
-3.33	36	4.00E+05	4.70E+04	18.10	16.97	15.18	14.26
0	36	4.00E+05	4.35E+04	20.47	19.08	17.14	16.00
7.5	36	4.00E+05	3.99E+04	22.00	20.43	18.38	17.09
15	36	4.00E+05	3.82E+04	22.80	21.13	19.03	17.66
20	36	4.00E+05	3.64E+04	23.28	21.54	19.41	17.98
25	36	4.00E+05	3.42E+04	23.72	21.91	19.76	18.28
25.1	36	4.00E+05	3.42E+04	26.14	24.01	21.77	20.03
30	36	4.00E+05	3.24E+04	26.65	24.44	22.18	20.36
35	36	4.00E+05	3.05E+04	27.20	25.03	22.61	20.84
40	36	4.00E+05	2.86E+04	27.73	25.61	23.03	21.30
45	36	4.00E+05	2.69E+04	28.26	26.19	23.45	21.76
45.1	36	2.94E+05	2.69E+04	23.92	22.44	19.94	18.73
50	36	2.94E+05	2.53E+04	24.40	22.94	20.33	19.13
55	36	2.94E+05	2.38E+04	24.92	23.47	20.73	19.55
60	36	2.94E+05	2.23E+04	25.47	24.03	21.18	20.00
65	36	2.94E+05	2.11E+04	26.08	24.64	21.66	20.49
65.1	36	1.87E+05	2.11E+04	22.90	21.80	19.17	18.26
70	36	1.87E+05	1.99E+04	23.49	22.38	19.63	18.73
75	36	1.87E+05	1.87E+04	24.12	23.01	20.13	19.22
80	36	1.87E+05	1.78E+04	24.81	23.69	20.69	19.78
85	36	1.87E+05	1.68E+04	25.55	24.42	21.28	20.36
85.1	36	1.87E+05	1.68E+04	27.24	26.06	22.70	21.73
90	36	1.87E+05	1.59E+04	28.05	26.86	23.35	22.37
95	36	1.87E+05	1.51E+04	28.95	27.74	24.08	23.09
100	36	1.87E+05	1.43E+04	29.91	28.69	24.86	23.86
105	36	1.87E+05	1.36E+04	30.74	29.51	25.53	24.52
110	36	1.87E+05	1.29E+04	31.50	30.27	26.14	25.14
115	36	1.87E+05	1.22E+04	32.32	31.09	26.81	25.80
120	36	1.87E+05	1.15E+04	33.19	31.95	27.51	26.50
125	36	1.87E+05	1.07E+04	34.11	32.86	28.25	27.23
129.50	36	1.87E+05	9.08E+03	34.83	33.57	28.80	27.77

## 5. Verification of bending moment in ULS

Z (m)	M (kN·m)	Med (kN·m)	N (kN)	Ned (kN)	Ac (m2)	yc (m)	Mrd (kN·m)
-155	0	0	4.05E+05	5.46E+05	28.43	7.47	4.04E+06
-150.35	4.20E+03	5.68E+03	3.84E+05	5.19E+05	28.43	7.60	3.96E+06
-145.7	1.68E+04	2.26E+04	3.18E+05	4.29E+05	28.43	7.99	3.63E+06
-128.74	1.59E+05	2.14E+05	2.01E+05	2.71E+05	28.43	8.56	2.89E+06
-111.78	4.73E+05	6.39E+05	1.35E+05	1.82E+05	28.43	8.82	2.39E+06
-94.81	8.28E+05	1.12E+06	1.24E+05	1.68E+05	28.43	8.85	2.31E+06
-77.85	1.11E+06	1.49E+06	1.01E+05	1.36E+05	28.43	8.93	2.12E+06
-60.89	1.27E+06	1.72E+06	8.90E+04	1.20E+05	28.43	8.96	2.02E+06
-43.93	1.35E+06	1.82E+06	7.75E+04	1.05E+05	28.43	8.50	2.98E+06
-26.96	1.40E+06	1.89E+06	6.64E+04	8.97E+04	28.43	8.55	2.90E+06
-10	1.35E+06	1.83E+06	5.61E+04	7.58E+04	28.43	8.60	2.83E+06
-6.67	1.32E+06	1.78E+06	5.06E+04	6.83E+04	25.61	6.23	3.52E+06
-3.33	1.28E+06	1.73E+06	4.70E+04	6.34E+04	22.78	5.13	2.88E+06
0	1.23E+06	1.66E+06	4.35E+04	5.87E+04	19.95	4.00	2.23E+06
7.5	1.12E+06	1.51E+06	3.99E+04	5.39E+04	19.32	3.76	2.08E+06
15	1.01E+06	1.36E+06	3.82E+04	5.16E+04	18.69	3.51	1.94E+06
20	9.66E+05	1.30E+06	3.64E+04	4.91E+04	18.29	3.35	1.85E+06
25	9.02E+05	1.22E+06	3.42E+04	4.62E+04	17.88	3.20	1.75E+06
25.1	9.01E+05	1.22E+06	3.42E+04	4.62E+04	16.16	2.70	1.48E+06
30	8.43E+05	1.14E+06	3.24E+04	4.37E+04	15.80	2.55	1.39E+06
35	7.85E+05	1.06E+06	3.05E+04	4.11E+04	15.44	2.39	1.30E+06
40	7.26E+05	9.80E+05	2.86E+04	3.86E+04	15.07	2.23	1.21E+06
45	6.72E+05	9.07E+05	2.69E+04	3.63E+04	14.71	2.07	1.12E+06
45.1	6.71E+05	9.06E+05	2.69E+04	3.63E+04	13.13	2.90	1.17E+06
50	6.21E+05	8.38E+05	2.53E+04	3.42E+04	12.81	2.75	1.11E+06
55	5.69E+05	7.68E+05	2.38E+04	3.21E+04	12.49	2.59	1.04E+06
60	5.20E+05	7.02E+05	2.23E+04	3.02E+04	12.17	2.43	9.72E+05
65	4.75E+05	6.41E+05	2.11E+04	2.85E+04	11.84	2.27	9.04E+05
65.1	4.74E+05	6.40E+05	2.11E+04	2.85E+04	8.97	2.82	7.39E+05
70	4.30E+05	5.81E+05	1.99E+04	2.69E+04	8.73	2.67	6.96E+05
75	3.86E+05	5.21E+05	1.87E+04	2.53E+04	8.49	2.51	6.53E+05
80	3.47E+05	4.69E+05	1.78E+04	2.40E+04	8.25	2.35	6.09E+05
85	3.09E+05	4.17E+05	1.68E+04	2.27E+04	8.00	2.19	5.66E+05
85.1	3.08E+05	4.16E+05	1.68E+04	2.27E+04	7.48	1.94	5.01E+05
90	2.70E+05	3.65E+05	1.59E+04	2.14E+04	7.26	1.78	4.58E+05
95	2.39E+05	3.23E+05	1.51E+04	2.04E+04	7.04	1.62	4.15E+05
100	2.10E+05	2.84E+05	1.43E+04	1.93E+04	6.81	1.46	3.72E+05
105	1.81E+05	2.44E+05	1.36E+04	1.83E+04	6.58	1.29	3.29E+05
110	1.56E+05	2.10E+05	1.29E+04	1.74E+04	6.36	1.13	2.87E+05
115	1.33E+05	1.80E+05	1.22E+04	1.65E+04	6.13	0.97	2.45E+05
120	1.12E+05	1.51E+05	1.15E+04	1.56E+04	5.90	0.81	2.04E+05
125	9.49E+04	1.28E+05	1.07E+04	1.45E+04	5.68	0.65	1.63E+05
129.50	8.19E+04	1.11E+05	9.08E+03	1.23E+04	5.47	0.52	1.31E+05

## 6. Verification of shear force in ULS

Z (m)	Q (kN)	N (kN)	Vu1 (kN)	Vsu (kN)	Vcu (kN)	Vcu min (kN)	Vu2 (kN)
-155	1.59E+03	4.05E+05	1.70E+05	3.65E+04	2.38E+04	2.99E+04	6.64E+04
-150.35	4.77E+03	3.84E+05	1.70E+05	3.65E+04	2.33E+04	2.92E+04	6.57E+04
-145.7	1.50E+04	3.18E+05	1.65E+05	3.66E+04	1.98E+04	2.48E+04	6.14E+04
-128.74	3.36E+04	2.02E+05	1.55E+05	3.81E+04	1.38E+04	1.71E+04	5.53E+04
-111.78	4.49E+04	1.37E+05	1.49E+05	4.39E+04	1.04E+04	1.29E+04	5.68E+04
-94.81	4.71E+04	1.26E+05	1.48E+05	5.07E+04	9.93E+03	1.22E+04	6.30E+04
-77.85	2.53E+04	1.00E+05	1.46E+05	6.04E+04	8.69E+03	1.07E+04	7.10E+04
-60.89	2.35E+04	8.72E+04	1.45E+05	6.81E+04	8.10E+03	9.91E+03	7.80E+04
-43.93	2.14E+04	7.56E+04	1.51E+05	7.52E+04	1.22E+04	1.45E+04	8.97E+04
-26.96	1.85E+04	6.44E+04	1.51E+05	8.35E+04	1.18E+04	1.40E+04	9.75E+04
-10	1.50E+04	5.72E+04	1.50E+05	8.77E+04	1.16E+04	1.37E+04	1.01E+05
-6.67	1.47E+04	5.01E+04	1.50E+05	9.00E+04	1.95E+04	2.29E+04	1.13E+05
-3.33	1.60E+04	4.66E+04	1.37E+05	8.90E+04	1.94E+04	2.28E+04	1.12E+05
0	1.60E+04	4.33E+04	1.20E+05	8.76E+04	1.92E+04	2.27E+04	1.10E+05
7.5	1.51E+04	3.98E+04	1.17E+05	8.60E+04	1.99E+04	2.36E+04	1.10E+05
15	1.46E+04	3.81E+04	1.13E+05	8.16E+04	2.00E+04	2.37E+04	1.05E+05
20	1.30E+04	3.64E+04	1.11E+05	8.13E+04	1.99E+04	2.36E+04	1.05E+05
25	1.25E+04	3.42E+04	1.08E+05	8.03E+04	1.99E+04	2.35E+04	1.04E+05
25.1	1.25E+04	3.42E+04	9.41E+04	8.03E+04	1.87E+04	2.22E+04	1.02E+05
30	1.21E+04	3.24E+04	9.21E+04	7.92E+04	1.87E+04	2.21E+04	1.01E+05
35	1.16E+04	3.05E+04	9.00E+04	7.79E+04	1.87E+04	2.22E+04	1.00E+05
40	1.12E+04	2.86E+04	8.80E+04	7.66E+04	1.87E+04	2.22E+04	9.88E+04
45	1.08E+04	2.69E+04	8.60E+04	7.52E+04	1.87E+04	2.22E+04	9.74E+04
45.1	1.08E+04	2.69E+04	7.29E+04	7.52E+04	1.34E+04	1.58E+04	9.10E+04
50	1.04E+04	2.53E+04	7.12E+04	7.36E+04	1.34E+04	1.58E+04	8.94E+04
55	9.97E+03	2.38E+04	6.95E+04	7.18E+04	1.34E+04	1.58E+04	8.76E+04
60	9.57E+03	2.23E+04	6.77E+04	6.99E+04	1.34E+04	1.58E+04	8.57E+04
65	9.19E+03	2.11E+04	6.60E+04	6.76E+04	1.34E+04	1.58E+04	8.34E+04
65.1	9.18E+03	2.11E+04	4.24E+04	6.76E+04	7.32E+03	8.51E+03	7.61E+04
70	8.81E+03	1.99E+04	4.13E+04	6.51E+04	7.33E+03	8.53E+03	7.37E+04
75	8.44E+03	1.87E+04	4.02E+04	6.24E+04	7.35E+03	8.55E+03	7.10E+04
80	8.09E+03	1.78E+04	3.91E+04	5.96E+04	7.37E+03	8.59E+03	6.82E+04
85	7.73E+03	1.68E+04	3.80E+04	5.64E+04	7.39E+03	8.62E+03	6.51E+04
85.1	7.73E+03	1.68E+04	3.37E+04	6.00E+04	6.90E+03	8.03E+03	6.81E+04
90	7.38E+03	1.59E+04	3.28E+04	5.64E+04	6.92E+03	8.07E+03	6.45E+04
95	7.05E+03	1.50E+04	3.18E+04	5.34E+04	6.95E+03	8.11E+03	6.15E+04
100	6.73E+03	1.42E+04	3.08E+04	5.01E+04	6.97E+03	8.14E+03	5.83E+04
105	6.40E+03	1.33E+04	2.98E+04	4.66E+04	6.95E+03	8.13E+03	5.47E+04
110	6.08E+03	1.26E+04	2.88E+04	4.33E+04	6.90E+03	8.07E+03	5.14E+04
115	5.76E+03	1.18E+04	2.78E+04	4.01E+04	6.85E+03	8.02E+03	4.82E+04
120	5.45E+03	1.11E+04	2.68E+04	3.67E+04	6.81E+03	7.97E+03	4.47E+04
125	5.16E+03	1.06E+04	2.58E+04	3.36E+04	6.77E+03	7.93E+03	4.15E+04
129.50	4.71E+03	4.71E+03	2.50E+04	5.12E+04	6.51E+03	7.61E+03	5.88E+04

## 7. Verification of torsion in ULS

Z (m)	Mz (kNm)	e (m)	he (m)	Ae (m <sup>2</sup> )	Tu1 (kNm)	Tu2 (kNm)	Tu3 (kNm)
-155	0	0.5	0.49	257.30	3.34E+06	6.90E+06	4.06E+05
-150.35	1.89E-13	0.5	0.49	257.30	3.34E+06	6.90E+06	4.06E+05
-145.7	8.11E-13	0.5	0.49	257.30	3.25E+06	6.90E+06	4.06E+05
-128.74	5.91E-12	0.5	0.49	257.30	3.05E+06	6.90E+06	4.06E+05
-111.78	1.48E-11	0.5	0.49	257.30	2.93E+06	6.90E+06	4.06E+05
-94.81	2.04E-11	0.5	0.49	257.30	2.92E+06	6.90E+06	4.06E+05
-77.85	5.14E+04	0.5	0.49	257.30	2.87E+06	6.90E+06	4.06E+05
-60.89	5.14E+04	0.5	0.49	257.30	2.86E+06	6.90E+06	4.06E+05
-43.93	5.14E+04	0.5	0.49	257.30	2.98E+06	6.90E+06	5.54E+05
-26.96	5.14E+04	0.5	0.49	257.30	2.96E+06	6.90E+06	5.54E+05
-10	5.14E+04	0.5	0.49	257.30	2.96E+06	6.90E+06	5.54E+05
-6.67	5.14E+04	0.5	0.49	208.71	2.64E+06	5.60E+06	7.11E+05
-3.33	5.14E+04	0.5	0.48	165.13	2.13E+06	4.43E+06	6.11E+05
0	5.14E+04	0.5	0.48	126.68	1.63E+06	3.40E+06	5.18E+05
7.5	5.14E+04	0.5	0.48	118.82	1.52E+06	3.19E+06	4.97E+05
15	5.14E+04	0.5	0.48	111.22	1.42E+06	2.98E+06	4.77E+05
20	4.17E+04	0.5	0.48	106.46	1.36E+06	2.85E+06	4.65E+05
25	4.17E+04	0.5	0.48	101.80	1.30E+06	2.73E+06	4.52E+05
25.1	4.17E+04	0.45	0.43	102.60	1.18E+06	2.75E+06	4.54E+05
30	4.17E+04	0.45	0.43	98.12	1.13E+06	2.63E+06	4.42E+05
35	4.18E+04	0.45	0.43	93.65	1.08E+06	2.51E+06	4.30E+05
40	4.18E+04	0.45	0.43	89.28	1.03E+06	2.39E+06	4.17E+05
45	4.18E+04	0.45	0.43	85.02	9.78E+05	2.28E+06	4.05E+05
45.1	4.18E+04	0.4	0.39	85.75	8.81E+05	2.30E+06	3.22E+05
50	4.18E+04	0.4	0.38	81.66	8.38E+05	2.19E+06	3.12E+05
55	4.17E+04	0.4	0.38	77.58	7.96E+05	2.08E+06	3.02E+05
60	4.17E+04	0.4	0.38	73.61	7.54E+05	1.97E+06	2.92E+05
65	4.17E+04	0.4	0.38	69.74	7.14E+05	1.87E+06	2.83E+05
65.1	4.17E+04	0.3	0.29	71.16	5.52E+05	1.91E+06	2.09E+05
70	4.17E+04	0.3	0.29	67.43	5.23E+05	1.81E+06	2.01E+05
75	4.17E+04	0.3	0.29	63.73	4.93E+05	1.71E+06	1.94E+05
80	4.17E+04	0.3	0.29	60.14	4.65E+05	1.61E+06	1.86E+05
85	4.17E+04	0.3	0.29	56.65	4.38E+05	1.52E+06	1.79E+05
85.1	4.17E+04	0.28	0.27	56.85	4.11E+05	1.63E+06	1.83E+05
90	4.17E+04	0.28	0.27	53.52	3.87E+05	1.53E+06	1.76E+05
95	4.17E+04	0.28	0.27	50.23	3.62E+05	1.44E+06	1.69E+05
100	4.17E+04	0.28	0.27	47.05	3.39E+05	1.35E+06	1.62E+05
105	4.17E+04	0.28	0.27	43.97	3.16E+05	1.26E+06	1.55E+05
110	4.17E+04	0.28	0.27	40.99	2.95E+05	1.17E+06	1.48E+05
115	4.17E+04	0.28	0.27	38.12	2.74E+05	1.09E+06	1.41E+05
120	4.17E+04	0.28	0.27	35.35	2.53E+05	1.01E+06	1.35E+05
125	4.17E+04	0.28	0.27	32.69	2.34E+05	9.35E+05	1.28E+05
129.495	4.17E+04	0.28	0.27	30.39	2.17E+05	8.69E+05	1.22E+05

## 8. Interaction of forces

Z	T (kNm)	N (kN)	M (kNm)	Pinf (kN)	$\tau$	$\rho * f_{yd} < 0$	T+V < 1
-155	0	4.05E+05	0	6.24E+04	0	-18.59	0.01
-150.35	1.89E-13	3.84E+05	4.20E+03	7.19E+04	7.56E-19	-19.27	0.03
-145.7	8.11E-13	3.18E+05	1.68E+04	7.22E+04	3.24E-18	-22.52	0.12
-128.74	5.91E-12	2.02E+05	1.59E+05	7.40E+04	2.36E-17	-29.50	0.28
-111.78	1.48E-11	1.35E+05	4.73E+05	7.59E+04	5.90E-17	-36.00	0.40
-94.81	2.04E-11	1.25E+05	8.28E+05	7.77E+04	8.15E-17	-40.25	0.42
-77.85	5.14E+04	9.87E+04	1.11E+06	7.95E+04	0.21	-44.43	0.25
-60.89	5.14E+04	8.69E+04	1.27E+06	8.13E+04	0.21	-46.74	0.23
-43.93	5.14E+04	7.52E+04	1.35E+06	1.61E+05	0.21	-45.32	0.20
-26.96	5.14E+04	6.37E+04	1.40E+06	1.65E+05	0.21	-46.24	0.18
-10	5.14E+04	5.47E+04	1.35E+06	1.68E+05	0.21	-46.06	0.15
-6.67	5.14E+04	4.98E+04	1.32E+06	3.09E+05	0.25	-42.88	0.15
-3.33	5.14E+04	4.68E+04	1.28E+06	3.08E+05	0.32	-45.35	0.18
0	5.14E+04	4.33E+04	1.23E+06	3.05E+05	0.42	-49.01	0.21
7.5	5.14E+04	3.98E+04	1.12E+06	3.21E+05	0.45	-46.95	0.20
15	5.14E+04	3.81E+04	1.01E+06	3.23E+05	0.59	-45.37	0.18
20	4.17E+04	3.64E+04	9.66E+05	3.24E+05	0.62	-45.10	0.18
25	4.17E+04	3.42E+04	9.02E+05	3.24E+05	0.65	-44.22	0.18
25.1	4.17E+04	3.42E+04	9.01E+05	3.20E+05	0.71	-44.64	0.21
30	4.17E+04	3.23E+04	8.43E+05	3.20E+05	0.75	-43.73	0.21
35	4.18E+04	3.04E+04	7.85E+05	3.22E+05	0.78	-42.57	0.20
40	4.18E+04	2.86E+04	7.26E+05	3.24E+05	0.82	-41.33	0.20
45	4.18E+04	2.69E+04	6.72E+05	3.25E+05	0.87	-40.15	0.21
45.1	4.18E+04	2.69E+04	6.71E+05	2.43E+05	0.96	-46.11	0.24
50	4.18E+04	2.53E+04	6.21E+05	2.44E+05	1.01	-44.92	0.24
55	4.17E+04	2.37E+04	5.69E+05	2.44E+05	1.06	-43.56	0.24
60	4.17E+04	2.23E+04	5.20E+05	2.45E+05	1.12	-42.15	0.24
65	4.17E+04	2.11E+04	4.75E+05	2.45E+05	1.19	-40.76	0.24
65.1	4.17E+04	2.11E+04	4.74E+05	1.58E+05	1.53	-50.03	0.36
70	4.17E+04	1.99E+04	4.30E+05	1.59E+05	1.62	-48.23	0.37
75	4.17E+04	1.87E+04	3.86E+05	1.60E+05	1.72	-46.22	0.37
80	4.17E+04	1.77E+04	3.47E+05	1.61E+05	1.82	-44.33	0.38
85	4.17E+04	1.68E+04	3.09E+05	1.62E+05	1.93	-42.19	0.38
85.1	4.17E+04	1.68E+04	3.08E+05	1.62E+05	2.06	-42.22	0.42
90	4.17E+04	1.58E+04	2.70E+05	1.63E+05	2.19	-39.68	0.43
95	4.17E+04	1.50E+04	2.39E+05	1.63E+05	2.34	-37.53	0.44
100	4.17E+04	1.41E+04	2.10E+05	1.64E+05	2.50	-35.21	0.45
105	4.17E+04	1.33E+04	1.81E+05	1.64E+05	2.68	-32.73	0.47
110	4.17E+04	1.25E+04	1.56E+05	1.63E+05	2.87	-30.49	0.48
115	4.17E+04	1.18E+04	1.33E+05	1.62E+05	3.09	-28.28	0.50
120	4.17E+04	1.10E+04	1.12E+05	1.61E+05	3.34	-25.83	0.52
125	4.17E+04	1.03E+04	9.49E+04	1.59E+05	3.62	-23.70	0.55
129.50	4.17E+04	8.76E+03	8.19E+04	1.58E+05	3.90	-22.08	0.57



## APPENDIX 2. NUMERICAL RESULTS FOR CIRCUMFERENTIAL STRUCTURE

### 1. Post-tensioning steel and losses in the floater

x (m)	P0max (kN)	$\Delta P1$ (kN)	$\Delta P2$ (kN)	$\Delta P3$ (kN)	Po (kN)	$\Delta Pinf$ (kN)	Pinf (kN)
-9.05	4356	0	8	68	4280	203	4077
-9.02	4356	25	30	67	4233	200	4033
-8.94	4356	50	53	67	4187	197	3990
-8.80	4356	75	0	67	4214	199	4015
-8.61	4356	100	0	67	4190	197	3992
-8.61	4356	124	0	66	4165	196	3970
-8.06	4356	149	0	66	4141	194	3947
-7.72	4356	173	0	65	4117	192	3925
-7.32	4356	197	0	65	4094	191	3903
-6.88	4356	221	0	65	4070	189	3881
-6.40	4356	245	0	64	4046	188	3859
-5.88	4356	269	0	64	4023	186	3837
-5.32	4356	293	0	64	4000	185	3815
-4.73	4356	316	0	63	3977	183	3793
-4.11	4356	340	0	63	3954	182	3772
-3.46	4356	363	0	63	3931	180	3751
-2.80	4356	386	0	62	3908	179	3729
-2.11	4356	409	0	62	3885	177	3708
-1.42	4356	432	0	61	3863	176	3687
-0.71	4356	454	0	61	3841	174	3666
0	4356	477	0	61	3818	173	3646
0.71	4356	499	0	60	3796	171	3625
1.42	4356	522	0	60	3774	170	3605
2.11	4356	544	0	60	3753	168	3584
2.80	4356	566	0	59	3731	167	3564
3.46	4356	588	0	59	3709	166	3544
4.11	4356	609	0	59	3688	164	3524
4.73	4356	631	0	58	3667	163	3504
5.32	4356	653	0	58	3645	161	3484
5.88	4356	674	0	58	3624	160	3464
6.40	4356	695	0	57	3603	159	3445
6.88	4356	716	0	57	3583	157	3425
7.32	4356	737	0	57	3562	156	3406
7.72	4356	758	0	56	3541	155	3387
8.06	4356	779	0	56	3521	153	3368
8.36	4356	800	0	56	3500	152	3349
8.61	4356	820	0	55	3480	150	3330
8.80	4356	841	0	55	3460	149	3311
8.94	4356	861	0	55	3440	148	3292
9.02	4356	881	0	54	3420	147	3274
9.05	4356	901	0	54	3400	145	3255

## 2. Post-tensioning steel losses in section of 0.3 metres thickness

x (m)	P0max (kN)	$\Delta P1$ (kN)	$\Delta P2$ (kN)	$\Delta P3$ (kN)	Po (kN)	$\Delta Pinf$ (kN)	Pinf (kN)
-4.82	396	0	1	0.49	395	12	383
-4.81	396	2	3	0.49	390	11	379
-4.76	396	4	5	0.48	386	11	375
-4.69	396	7	0	0.48	389	11	377
-4.58	396	9	0	0.48	387	11	375
-4.45	396	11	0	0.48	384	11	373
-4.29	396	13	0	0.48	382	11	371
-4.11	396	15	0	0.47	380	11	369
-3.90	396	18	0	0.47	378	11	367
-3.67	396	20	0	0.47	376	11	365
-3.41	396	22	0	0.47	374	11	363
-3.13	396	24	0	0.46	372	11	361
-2.83	396	26	0	0.46	370	10	359
-2.52	396	28	0	0.46	367	10	357
-2.19	396	30	0	0.45	365	10	355
-1.84	396	32	0	0.45	363	10	353
-1.49	396	34	0	0.45	361	10	351
-1.13	396	36	0	0.45	359	10	349
-0.75	396	38	0	0.44	357	10	347
-0.38	396	40	0	0.44	355	10	345
0.00	396	42	0	0.44	353	10	344
0.38	396	44	0	0.44	351	10	342
0.75	396	46	0	0.43	349	9	340
1.13	396	48	0	0.43	347	9	338
1.49	396	50	0	0.43	345	9	336
1.84	396	52	0	0.43	343	9	334
2.19	396	54	0	0.42	341	9	332
2.52	396	56	0	0.42	339	9	331
2.83	396	58	0	0.42	338	9	329
3.13	396	60	0	0.42	336	9	327
3.41	396	62	0	0.42	334	9	325
3.67	396	64	0	0.41	332	9	323
3.90	396	66	0	0.41	330	9	322
4.11	396	67	0	0.41	328	8	320
4.29	396	69	0	0.41	326	8	318
4.45	396	71	0	0.40	324	8	316
4.58	396	73	0	0.40	323	8	314
4.69	396	75	0	0.40	321	8	313
4.76	396	77	0	0.40	319	8	311
4.81	396	78	0	0.39	317	8	309
4.82	396	80	0	0.39	315	8	308

### 3. Post-tensioning steel losses in section of 0.4 metres thickness

x (m)	P0max (kN)	$\Delta P1$ (kN)	$\Delta P2$ (kN)	$\Delta P3$ (kN)	Po (kN)	$\Delta Pinf$ (kN)	Pinf (kN)
-5.34	396	0	1	0.37	395	11	383
-5.32	396	2	3	0.36	391	11	379
-5.27	396	4	5	0.36	386	11	375
-5.19	396	7	0	0.36	389	11	378
-5.07	396	9	0	0.36	387	11	376
-4.93	396	11	0	0.36	385	11	374
-4.75	396	13	0	0.36	382	11	372
-4.55	396	15	0	0.35	380	11	369
-4.32	396	18	0	0.35	378	11	367
-4.06	396	20	0	0.35	376	11	365
-3.77	396	22	0	0.35	374	10	363
-3.46	396	24	0	0.35	372	10	361
-3.14	396	26	0	0.34	370	10	359
-2.79	396	28	0	0.34	367	10	357
-2.42	396	30	0	0.34	365	10	355
-2.04	396	32	0	0.34	363	10	353
-1.65	396	34	0	0.34	361	10	351
-1.25	396	36	0	0.34	359	10	350
-0.83	396	38	0	0.33	357	10	348
-0.42	396	40	0	0.33	355	10	346
0.00	396	42	0	0.33	353	9	344
0.42	396	44	0	0.33	351	9	342
0.83	396	46	0	0.33	349	9	340
1.25	396	48	0	0.32	347	9	338
1.65	396	50	0	0.32	345	9	336
2.04	396	52	0	0.32	343	9	334
2.42	396	54	0	0.32	341	9	332
2.79	396	56	0	0.32	339	9	331
3.14	396	58	0	0.31	338	9	329
3.46	396	60	0	0.31	336	9	327
3.77	396	62	0	0.31	334	8	325
4.06	396	64	0	0.31	332	8	323
4.32	396	66	0	0.31	330	8	322
4.55	396	68	0	0.31	328	8	320
4.75	396	69	0	0.30	326	8	318
4.93	396	71	0	0.30	324	8	316
5.07	396	73	0	0.30	323	8	315
5.19	396	75	0	0.30	321	8	313
5.27	396	77	0	0.30	319	8	311
5.32	396	79	0	0.30	317	8	309
5.34	396	80	0	0.29	315	8	308

#### 4. Post-tensioning steel losses in section of 0.45 metres thickness

x (m)	P0max (kN)	$\Delta P1$ (kN)	$\Delta P2$ (kN)	$\Delta P3$ (kN)	Po (kN)	$\Delta Pinf$ (kN)	Pinf (kN)
-5.85	396	0	1	0.33	395	11	384
-5.83	396	2	3	0.32	391	11	379
-5.78	396	4	5	0.32	386	11	375
-5.69	396	7	0	0.32	389	11	378
-5.56	396	9	0	0.32	387	11	376
-5.40	396	11	0	0.32	385	11	374
-5.21	396	13	0	0.32	382	11	372
-4.99	396	15	0	0.32	380	11	370
-4.73	396	18	0	0.31	378	11	367
-4.45	396	20	0	0.31	376	10	365
-4.14	396	22	0	0.31	374	10	363
-3.80	396	24	0	0.31	372	10	361
-3.44	396	26	0	0.31	370	10	359
-3.06	396	28	0	0.30	367	10	357
-2.66	396	30	0	0.30	365	10	355
-2.24	396	32	0	0.30	363	10	353
-1.81	396	34	0	0.30	361	10	351
-1.37	396	37	0	0.30	359	10	350
-0.92	396	39	0	0.30	357	10	348
-0.46	396	41	0	0.29	355	9	346
0.00	396	43	0	0.29	353	9	344
0.46	396	45	0	0.29	351	9	342
0.92	396	47	0	0.29	349	9	340
1.37	396	49	0	0.29	347	9	338
1.81	396	51	0	0.29	345	9	336
2.24	396	53	0	0.28	343	9	334
2.66	396	54	0	0.28	341	9	332
3.06	396	56	0	0.28	339	9	331
3.44	396	58	0	0.28	337	9	329
3.80	396	60	0	0.28	335	9	327
4.14	396	62	0	0.28	334	8	325
4.45	396	64	0	0.28	332	8	323
4.73	396	66	0	0.27	330	8	322
4.99	396	68	0	0.27	328	8	320
5.21	396	70	0	0.27	326	8	318
5.40	396	72	0	0.27	324	8	316
5.56	396	73	0	0.27	322	8	315
5.69	396	75	0	0.27	321	8	313
5.78	396	77	0	0.26	319	8	311
5.83	396	79	0	0.26	317	8	309
5.85	396	81	0	0.26	315	8	308

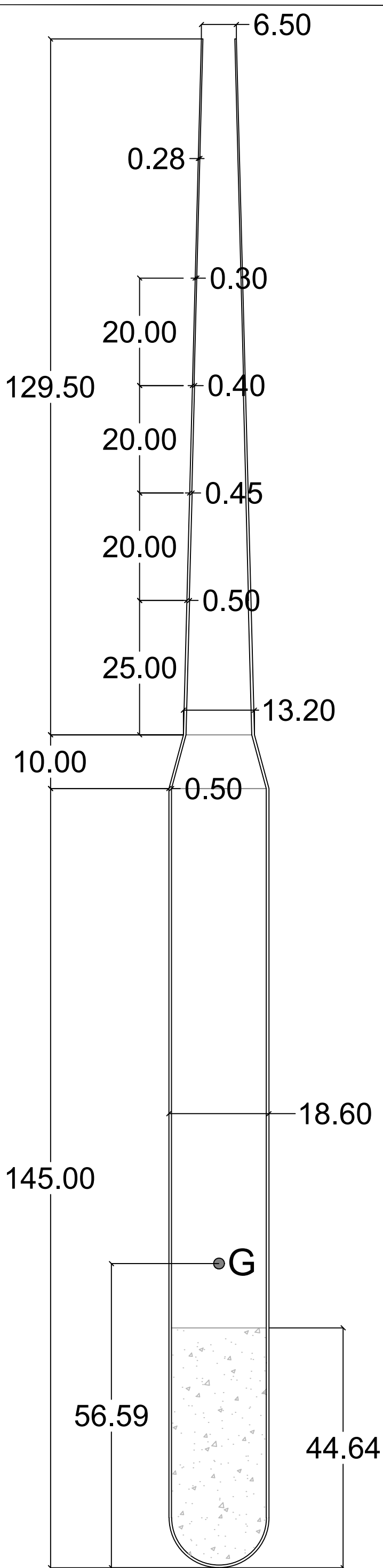
## 5. Post-tensioning steel losses in section of 0.5 metres thickness

x (m)	P0max (kN)	$\Delta P1$ (kN)	$\Delta P2$ (kN)	$\Delta P3$ (kN)	Po (kN)	$\Delta Pinf$ (kN)	Pinf (kN)
-6.60	792	0	1	1.77	789	24	765
-6.58	792	5	6	1.75	780	24	756
-6.52	792	9	10	1.73	772	23	748
-6.42	792	13	0	1.74	777	24	753
-6.28	792	18	0	1.73	772	23	749
-6.10	792	22	0	1.72	768	23	745
-5.88	792	27	0	1.71	764	23	741
-5.63	792	31	0	1.70	759	23	736
-5.34	792	35	0	1.69	755	23	732
-5.02	792	40	0	1.68	751	22	728
-4.67	792	44	0	1.67	746	22	724
-4.29	792	48	0	1.66	742	22	720
-3.88	792	52	0	1.65	738	22	716
-3.45	792	57	0	1.64	734	21	712
-3.00	792	61	0	1.64	729	21	708
-2.53	792	65	0	1.63	725	21	704
-2.04	792	69	0	1.62	721	21	700
-1.54	792	73	0	1.61	717	21	696
-1.03	792	77	0	1.60	713	20	693
-0.52	792	82	0	1.59	709	20	689
0.00	792	86	0	1.58	705	20	685
0.52	792	90	0	1.57	701	20	681
1.03	792	94	0	1.56	697	20	677
1.54	792	98	0	1.55	693	19	673
2.04	792	102	0	1.54	689	19	670
2.53	792	105	0	1.54	685	19	666
3.00	792	109	0	1.53	681	19	662
3.45	792	113	0	1.52	677	19	659
3.88	792	117	0	1.51	673	18	655
4.29	792	121	0	1.50	670	18	651
4.67	792	125	0	1.49	666	18	648
5.02	792	129	0	1.48	662	18	644
5.34	792	132	0	1.48	658	18	641
5.63	792	136	0	1.47	654	17	637
5.88	792	140	0	1.46	651	17	633
6.10	792	144	0	1.45	647	17	630
6.28	792	147	0	1.44	643	17	626
6.42	792	151	0	1.43	640	17	623
6.52	792	155	0	1.43	636	17	619
6.58	792	158	0	1.42	632	16	616
6.60	792	162	0	1.41	629	16	613

## 6. Post-tensioning steel losses along the transition piece

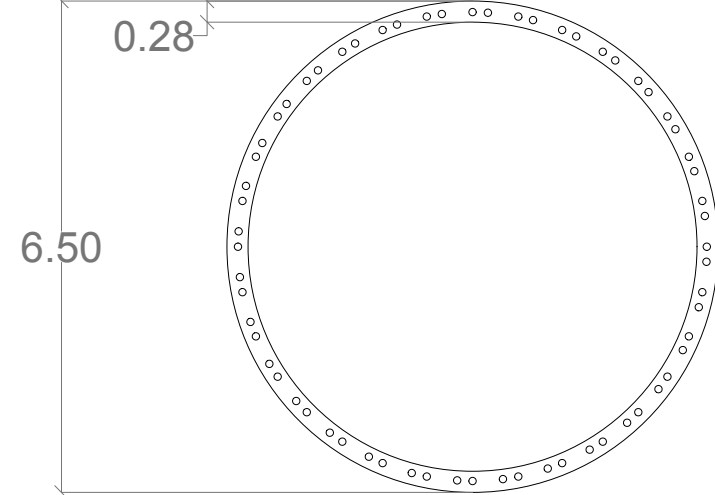
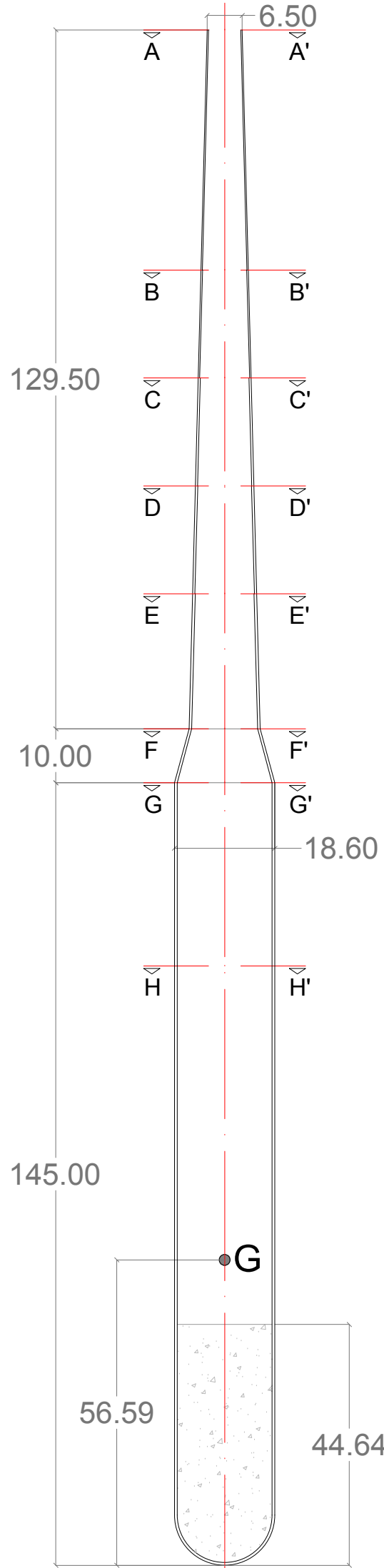
z (m)	P0max (kN)	$\Delta P1$ (kN)	$\Delta P2$ (kN)	$\Delta P3$ (kN)	Po (kN)	$\Delta Pinf$ (kN)	Pinf (kN)
0	1584	324	0	7	1254	37	1216
-1	1584	324	0	7	1253	37	1216
-2	1584	325	0	7	1253	37	1216
-3	3168	650	0	28	2490	93	2397
-4	3168	651	0	28	2489	93	2396
-5	3168	652	0	28	2488	93	2395
-6	3168	653	0	28	2487	93	2394
-7	4356	899	0	54	3403	145	3258
-8	4356	900	0	54	3402	145	3256
-9	4356	901	0	54	3401	145	3255
-10	4356	903	0	54	3399	145	3254

## **APPENDIX 3: DRAWINGS**



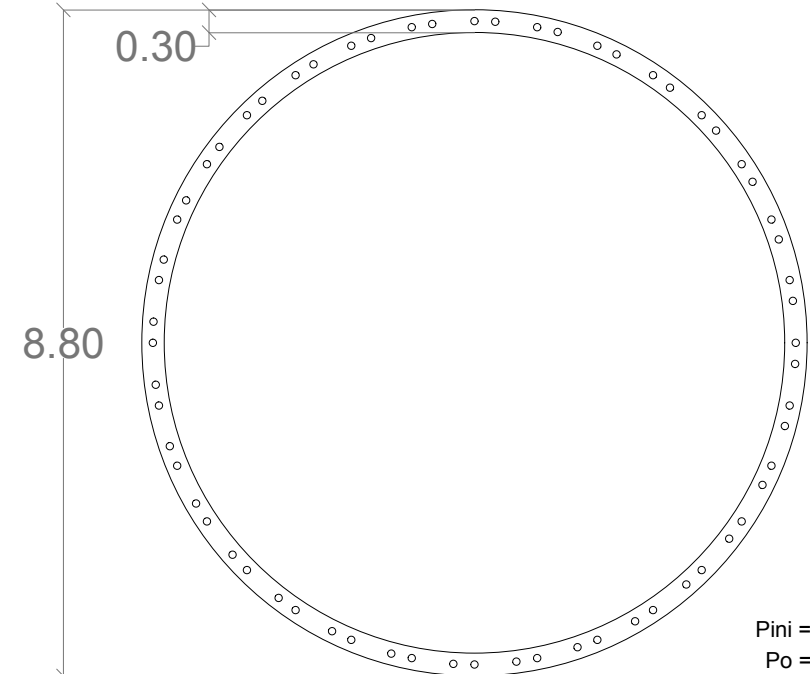
-  16 tendons
-  32 tendons
-  64 tendons
-  80 tendons
-  96 tendons





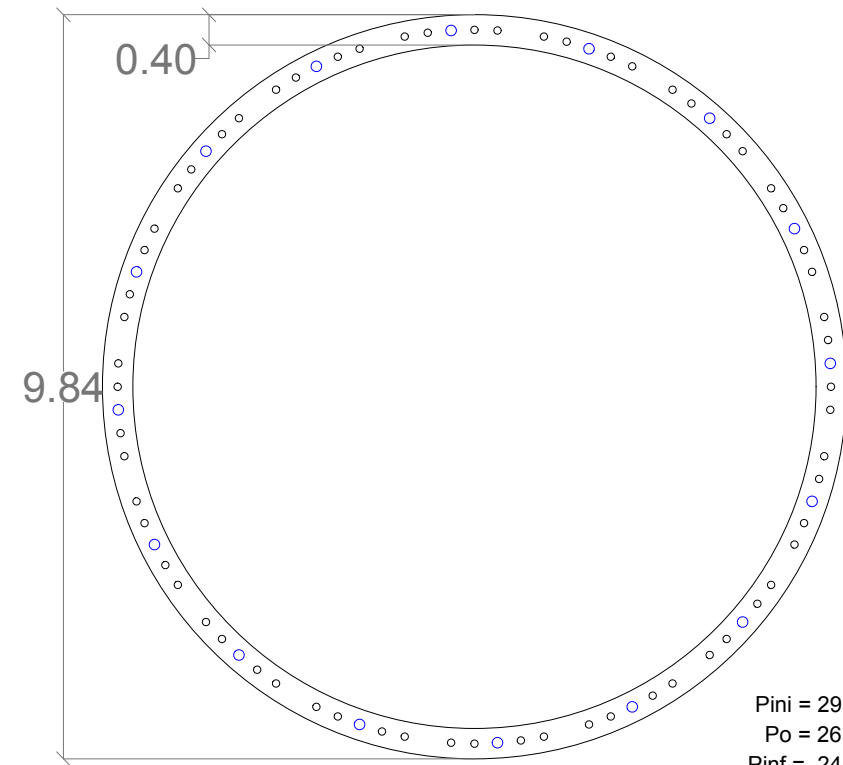
**SECTION A-A'**

Pini = 187448 kN  
 Po = 164557 kN  
 Pinf = 158311 kN  
 E. 1:100



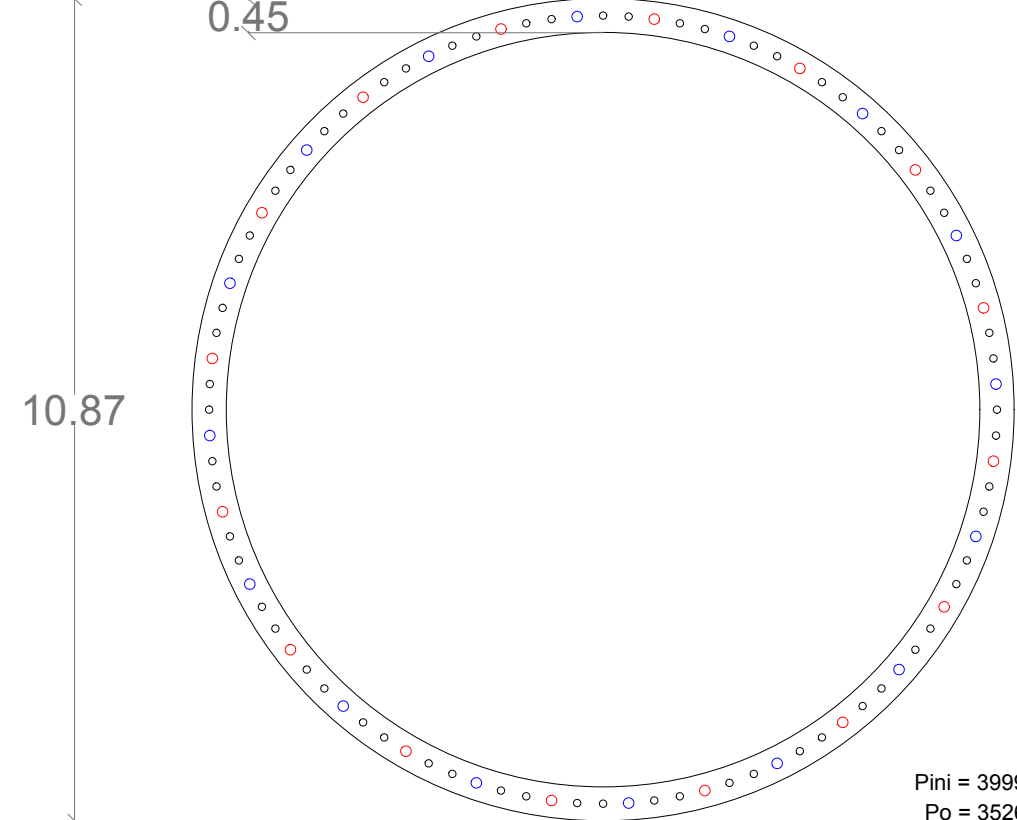
**SECTION B-B'**

Pini = 187448 kN  
 Po = 170327 kN  
 Pinf = 162031 kN  
 E. 1:100



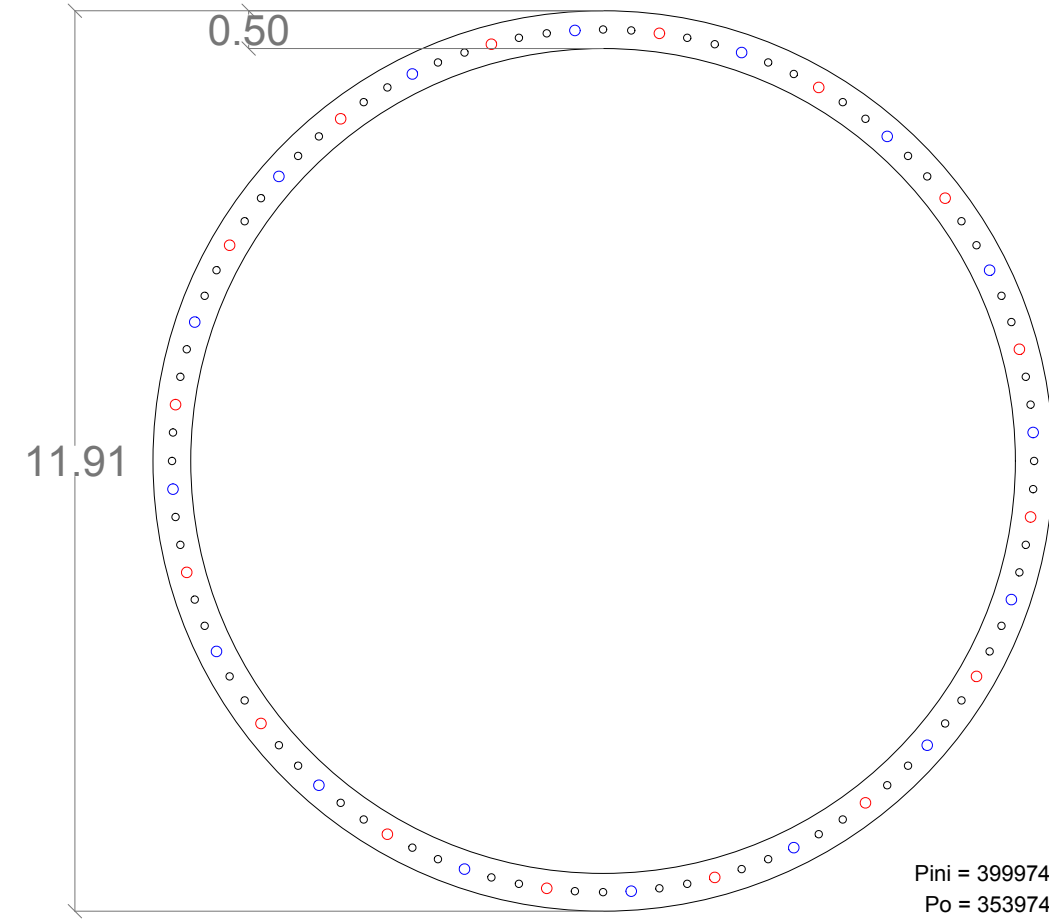
**SECTION C-C'**

Pini = 293731 kN  
 Po = 261043 kN  
 Pinf = 245446 kN  
 E. 1:100



**SECTION D-D'**

Pini = 399974 kN  
 Po = 352669 kN  
 Pinf = 324554 kN  
 E. 1:100



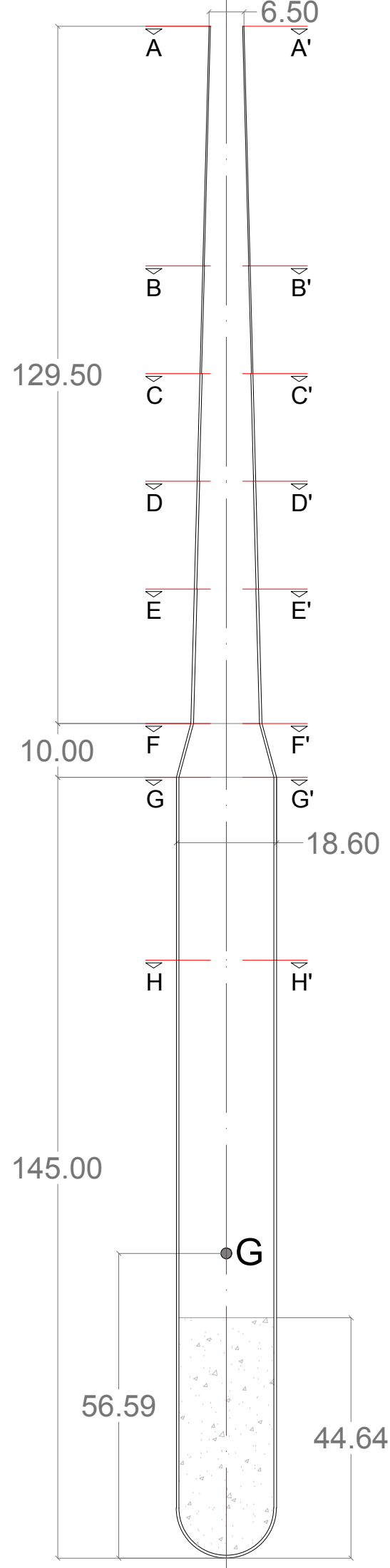
**SECTION E-E'**

Pini = 399974 kN  
 Po = 353974 kN  
 Pinf = 323896 kN  
 E. 1:100

- 15 strands post-tensioning tendons. D=95 mm. Po=2940 kN/tendon.
- 34 strands post-tensioning tendons. D=137 mm. Po=6640 kN/tendon.
- 34 strands post-tensioning tendons. D=137 mm. Po=6640 kN/tendon.

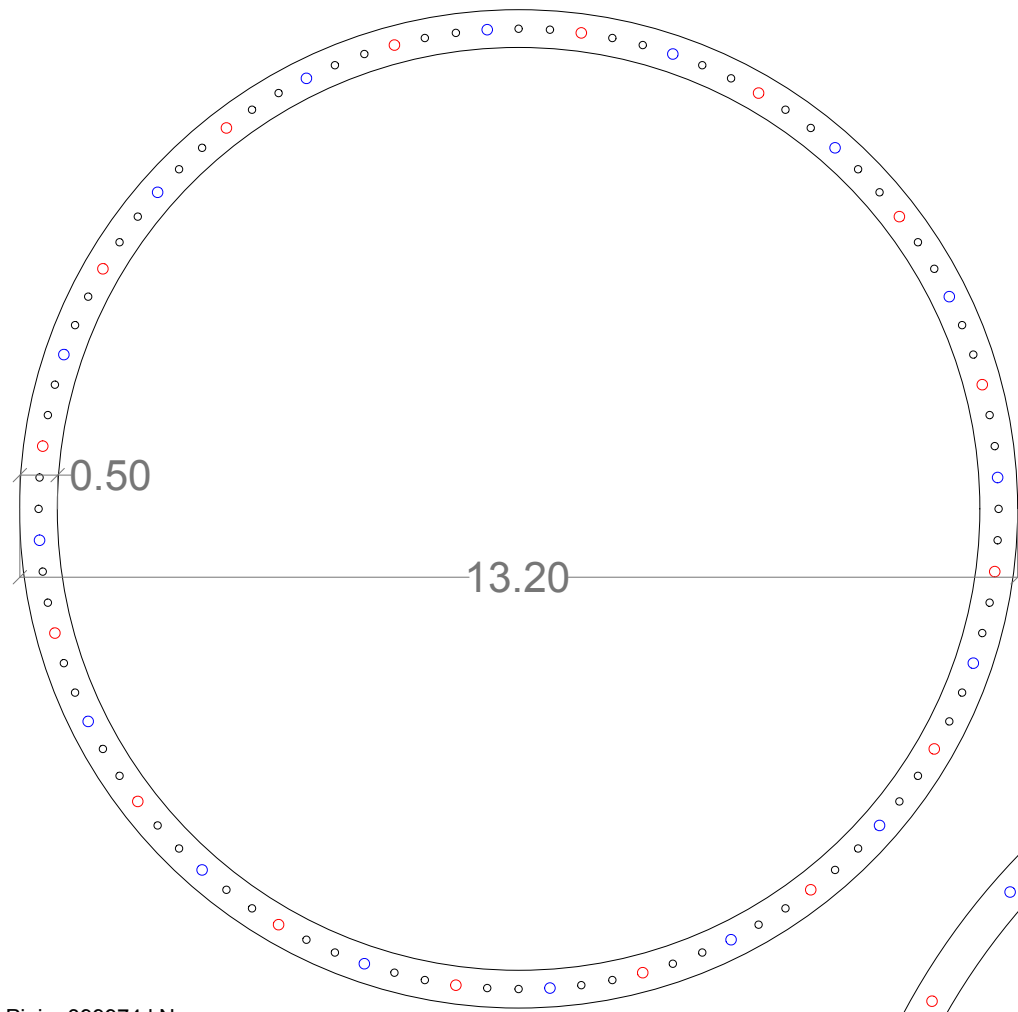
Concrete HP-80/B/20/IIIb-Qb	Reduction factor = 1.5
Active reinforcement Y-1860-S7	Reduction factor = 1.15

Drawing: Post-tensioning steel definition.	Date: JUNE 2020	Number: 2
Project: Design and structural verification of a concrete spar type platform for a 15 MW wind turbine.		
Author: IAGO LORENZO GARCIA		
 <small>Escola Tècnica Superior d'Enginyeria de Camins, Canals i Ports          UPC BARCELONATECH</small>	Page: 1/3	

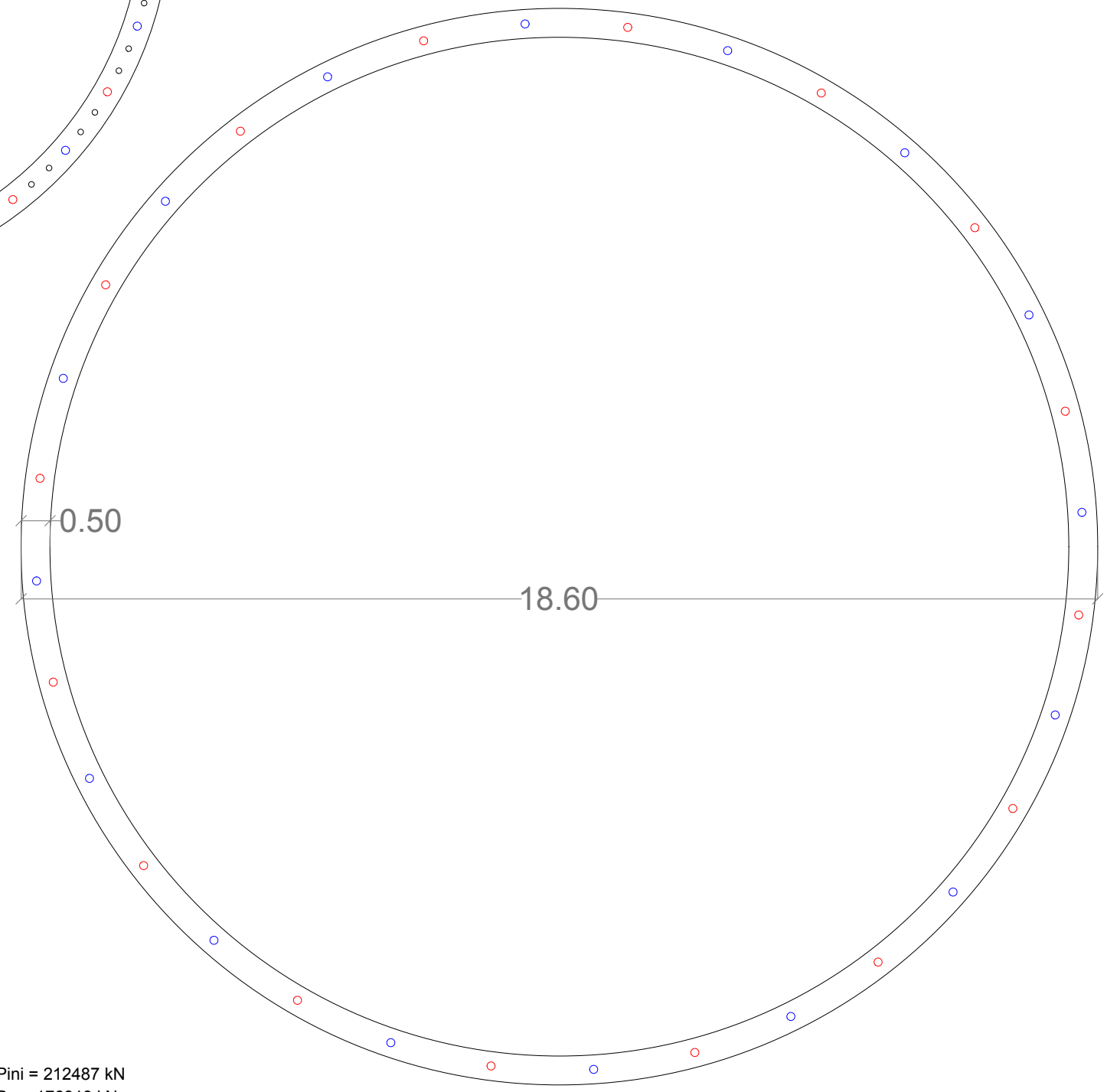


Pini = 399974 kN  
 Po = 331247 kN  
 Pinf = 305432 kN  
 E. 1:100

E. 1:1000



SECTION F-F'



SECTION G-G'

Pini = 212487 kN  
 Po = 176313 kN  
 Pinf = 168373 kN  
 E. 1:100

- 15 strands post-tensioning tendons. D=95 mm. Po=2940 kN/tendon.
- 34 strands post-tensioning tendons. D=137 mm. Po=6640 kN/tendon.
- 34 strands post-tensioning tendons. D=137 mm. Po=6640 kN/tendon.

Concrete HP-80/B/20/IIIb-Qb	Reduction factor = 1.5
Active reinforcement Y-1860-S7	Reduction factor = 1.15

Number:	2	Page:	2/3
---------	---	-------	-----

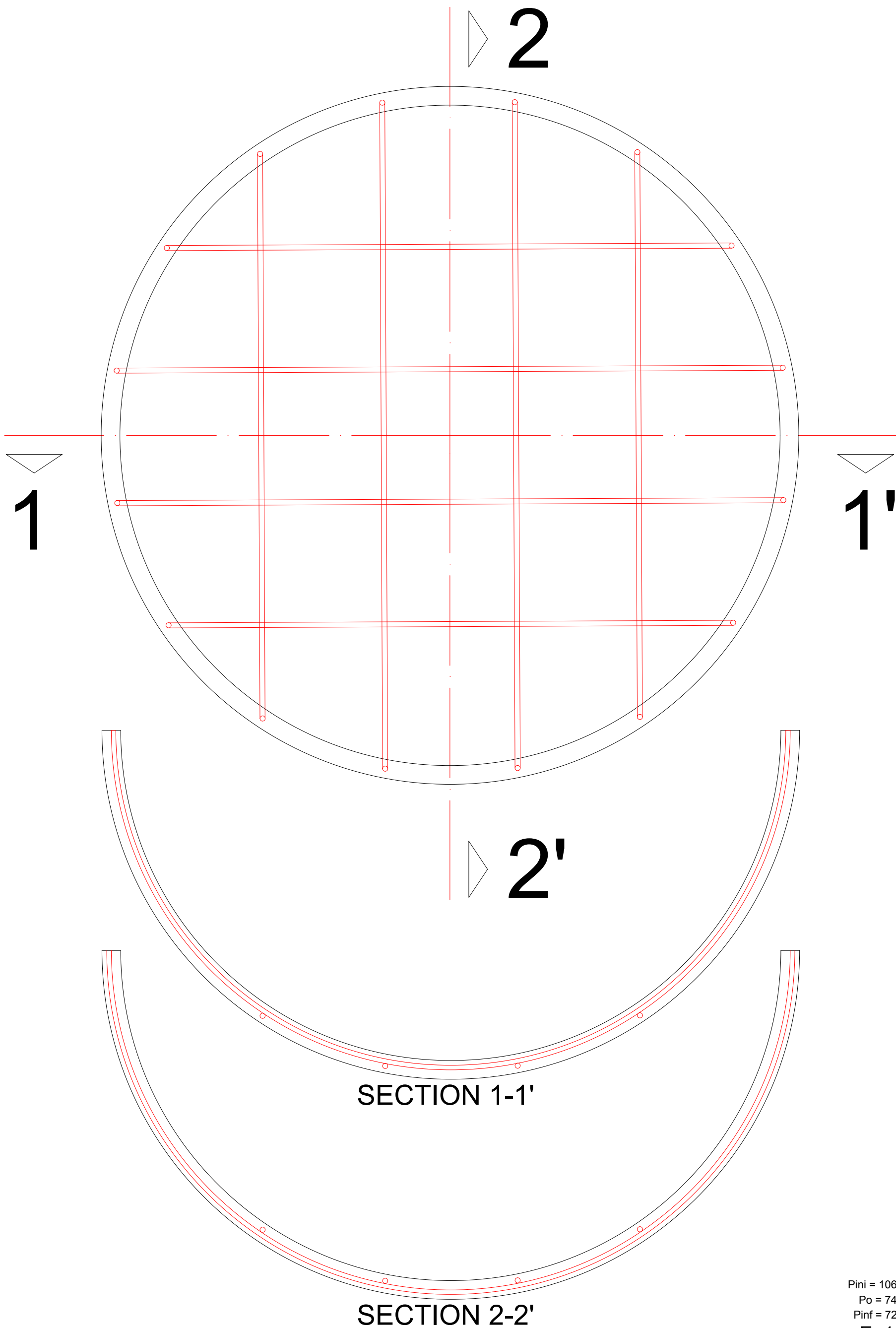
Date:	JUNE 2020
-------	-----------

Scale:	
--------	--

Drawing:	Post-tensioning steel definition.
----------	-----------------------------------


Project:	Design and structural verification of a concrete spar type platform for a 15 MW wind turbine.
----------	---

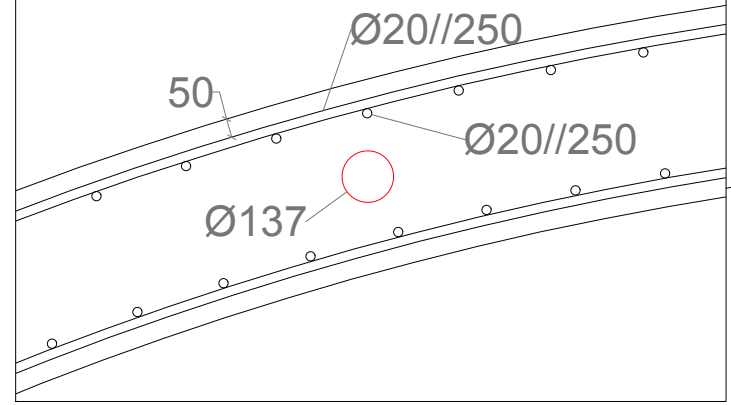
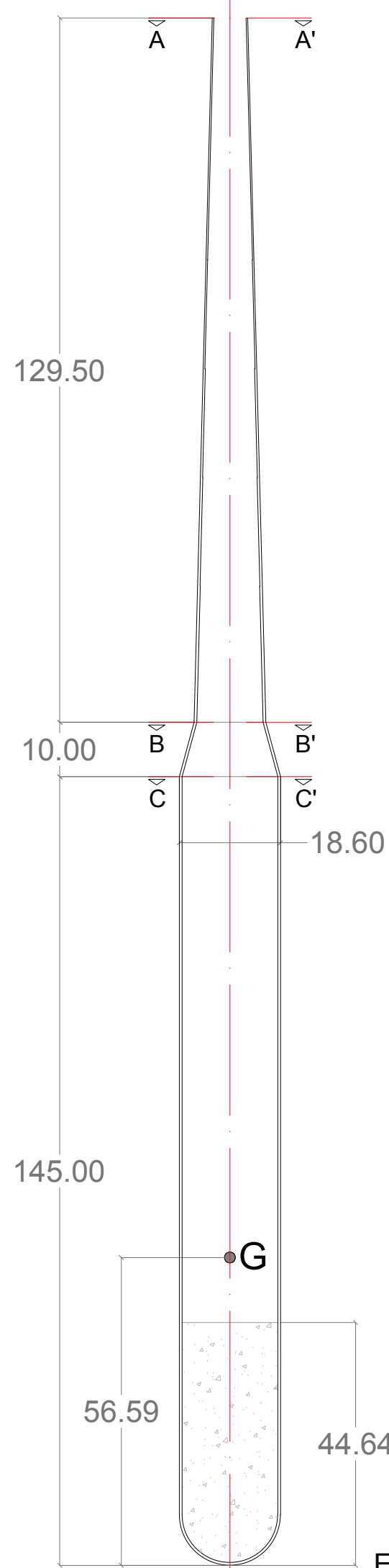
Author:	IAGO LORENZO GARCIA
---------	---------------------



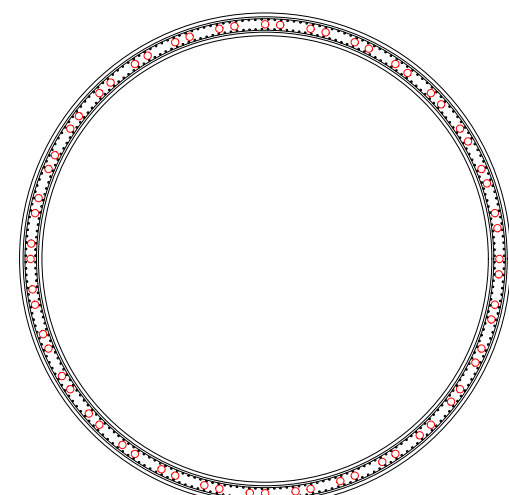
Pini = 106243 kN  
 Po = 74496 kN  
 Pinf = 72219 kN  
 E. 1:100

# SECTION H/H'//BOTTOM OF THE FLOATER

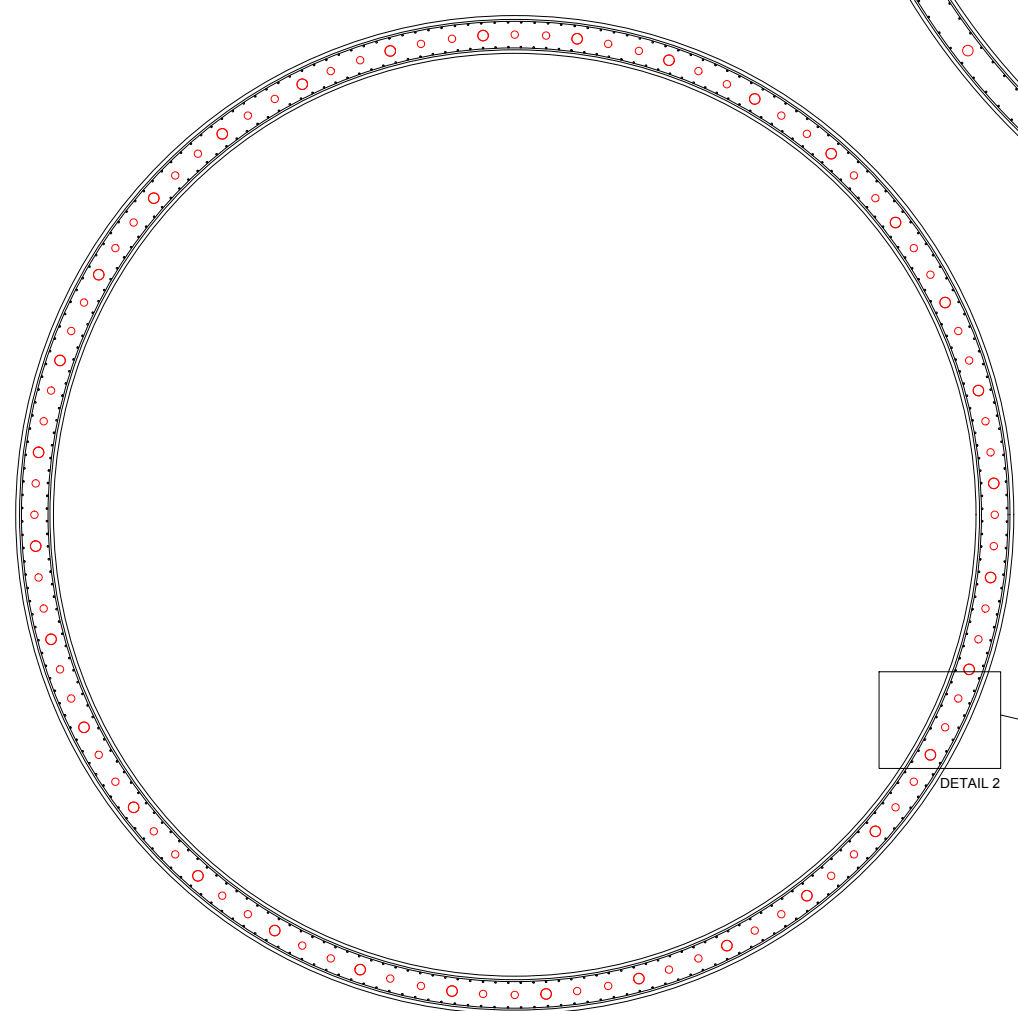
 <b>Escola de Camins</b> <small>Escola Tècnica Superior d'Enginyeria de Camins, Canals i Ports        UPC BARCELONATECH</small>	Author: IAGO LORENZO GARCÍA	Project: Design and structural verification of a concrete spar type platform for a 15 MW wind turbine.	Drawing: Post-tensioning steel definition.	Scale: 1:100	Date: JUNE 2020	Number: 2
						Page: 3/3



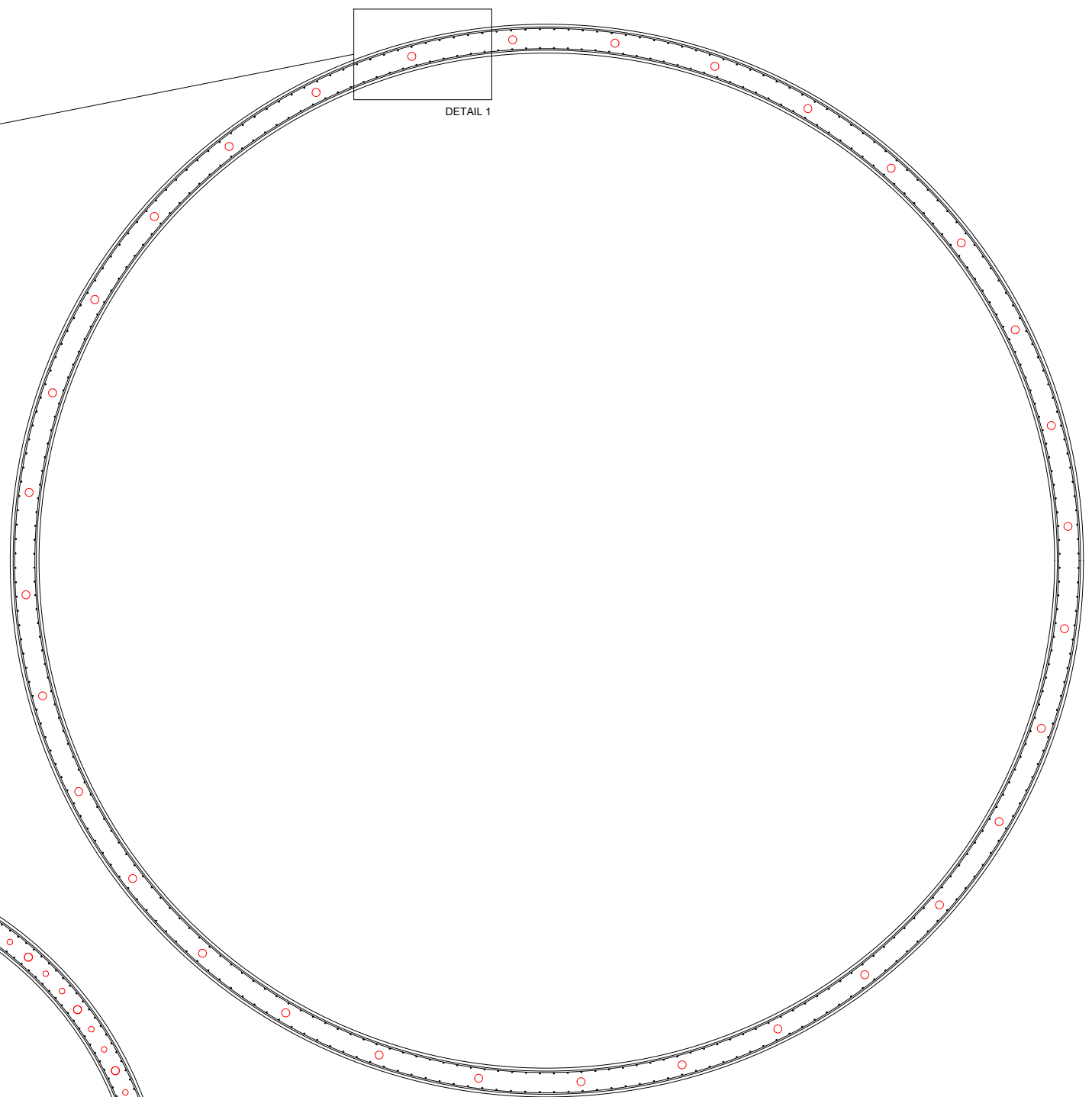
DETAIL 1 E. 1:20



SECTION A-A' E. 1:100



SECTION B-B' E. 1:100



SECTION C-C' E. 1:100

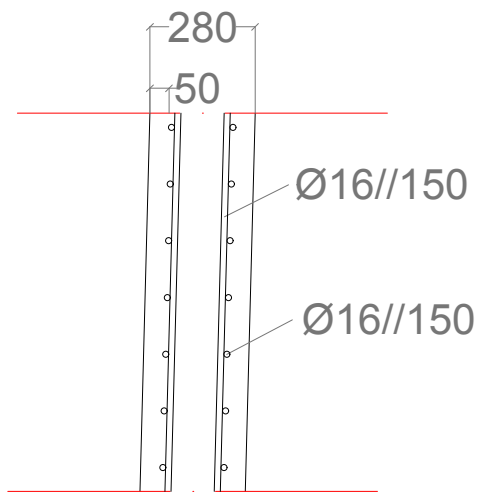
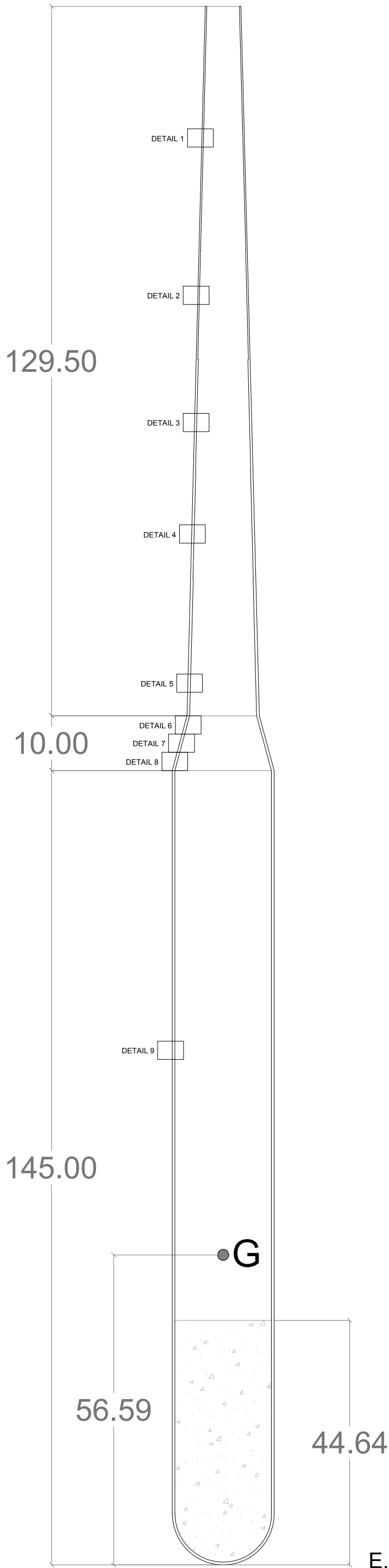


DETAIL 2 E. 1:20

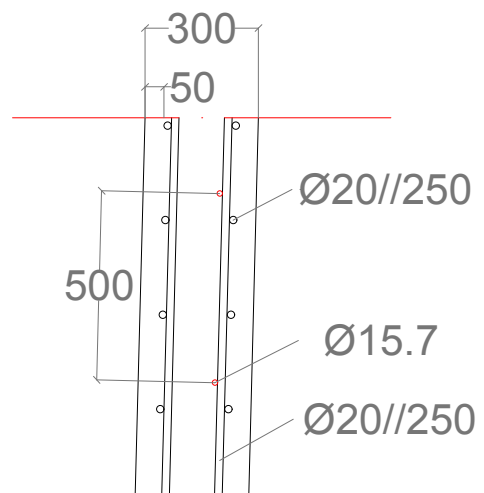
- Passive reinforcement
- Active reinforcement

Concrete HP-80/B/20/IIIb-Qb	Reduction factor = 1.5
Active reinforcement Y-1860-S7	Reduction factor = 1.15
Passive reinforcement B-500-S	Reduction factor = 1.15

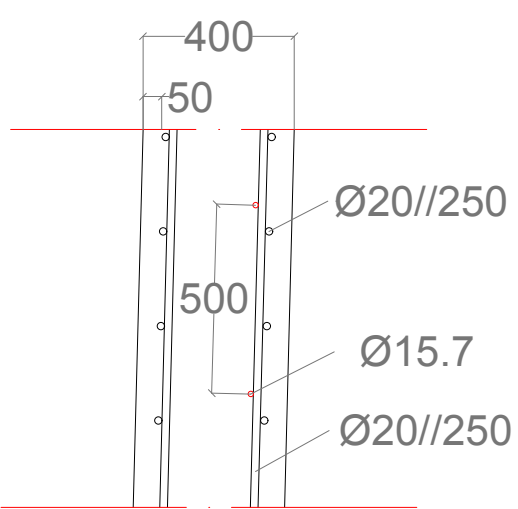
Drawing: Passive reinforcement.	Date: JUNE 2020	Number: 3	Page: 1/2
Project: Design and structural verification of a concrete spar type platform for a 15 MW wind turbine.			
Author: IAGO LORENZO GARCIA			
 Escola Tècnica Superior d'Enginyeria de Camins, Canals i Ports UPC BARCELONATECH			



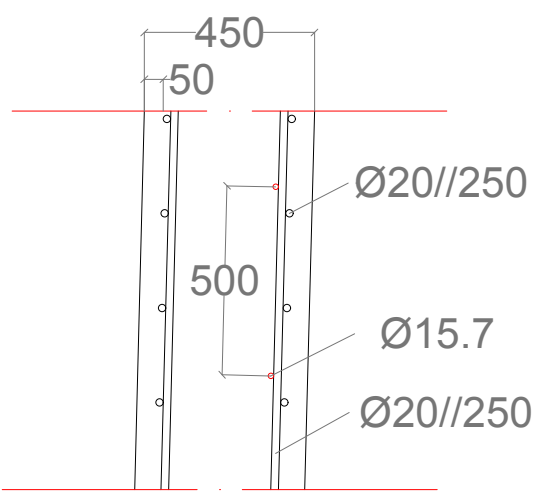
DETAIL 1 E. 1:20



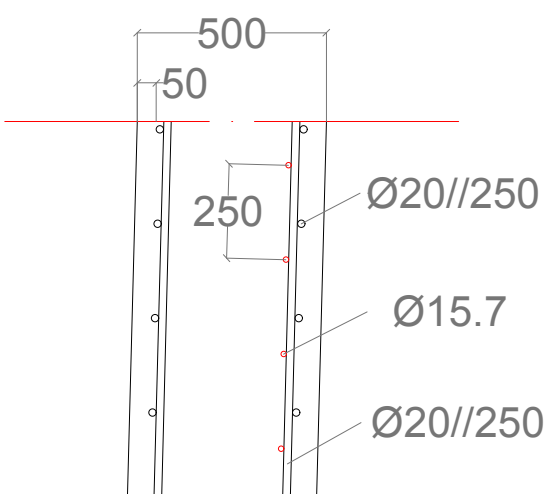
DETAIL 2 E. 1:20



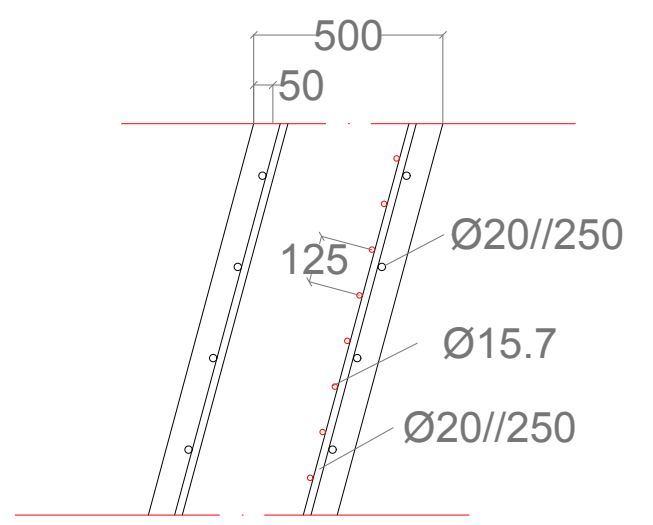
DETAIL 3 E. 1:20



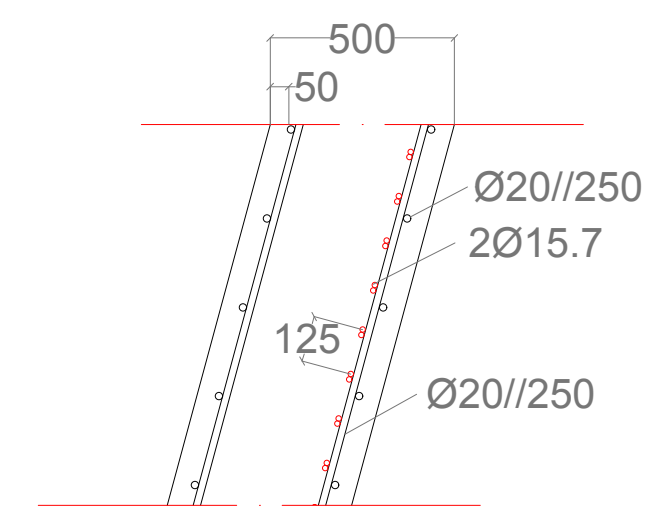
DETAIL 4 E. 1:20



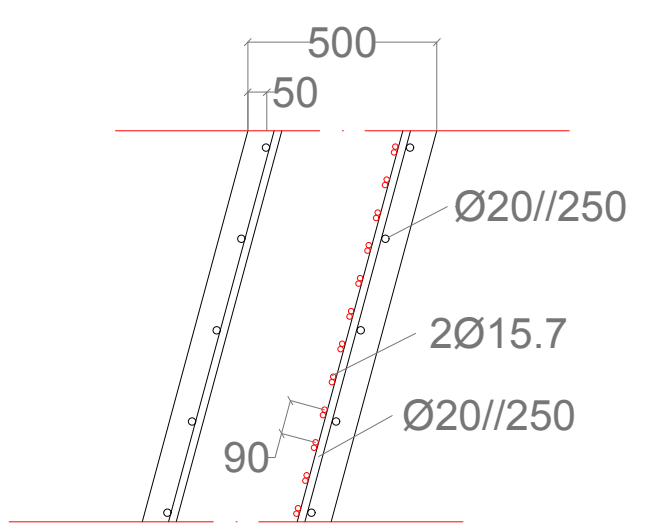
DETAIL 5 E. 1:20



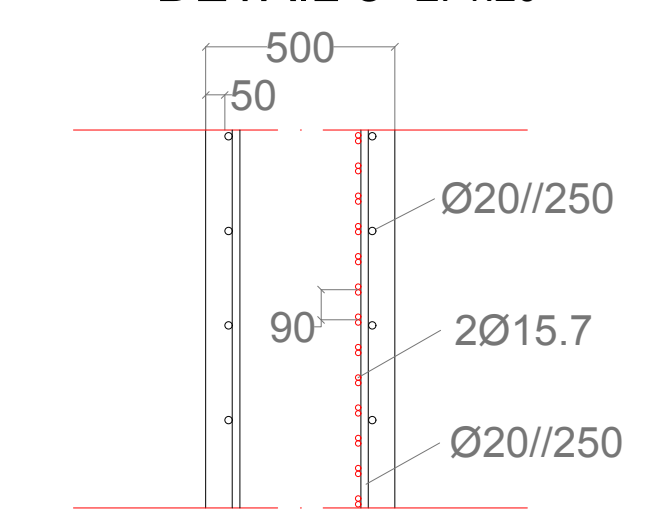
DETAIL 6 E. 1:20



DETAIL 7 E. 1:20



DETAIL 8 E. 1:20



DETAIL 9 E. 1:20

○ Passive reinforcement  
 ○ Active reinforcement

Concrete HP-80/B/20/IIIb-Qb	Reduction factor = 1.5
Active reinforcement Y-1860-S7	Reduction factor = 1.15
Passive reinforcement B-500-S	Reduction factor = 1.15

MATERIAL	SECTION	TENDON	VOLUME (m3)	WEIGHT (kg)	RATIO (kg/m3)
CONCRETE HP-80/B/20/IIIb-Qb	Bottom of the floater		257.37		
	Floater		3858.14		
	Transition piece		241.90		
	Tower		2060.12		
	TOTAL		6417.53		
LONGITUDINAL POST-TENSIONING STEEL Y-1860-S7		15 strands	25.31	198648.39	
		34 strands	32.53	255394.06	
	TOTAL		57.84	454042.45	70.75
CIRCUMFERENTIAL POST-TENSIONING STEEL Y-1860-S7	Floater	Mono-strands	31.95	250855.67	
	Transition piece	Mono-strands	1.25	9794.93	
	Tower	Mono-strands	1.40	10956.46	
	TOTAL		34.60	271607.05	42.32
LONGITUDINAL PASSIVE STEEL B-500-S			20.91	164176.13	25.58
CIRCUMFERENTIAL PASSIVE STEEL B-500-S	Floater		26.59	208703.6	
	Transition piece		1.03	8070.50	
	Tower		13.11	102940.77	
	TOTAL		40.73	319714.87	49.82